# Geostatistical Modeling of Safaniya Reservoir in Safaniya Field

by

Hesham Mohammad Al-Qassab

A Thesis Presented to the

FACULTY OF THE COLLEGE OF GRADUATE STUDIES

KING FAHD UNIVERSITY OF PETROLEUM & MINERALS

DHAHRAN, SAUDI ARABIA

In Partial Fulfillment of the
Requirements for the Degree of

**MASTER OF SCIENCE**

In

**GEOLOGY**

March, 1997

# GEOSTATISTICAL MODELING OF SAFANIYA RESERVOIR IN SAFANIYA FIELD

BY


## HESHAM MOHAMMAD AL-QASSAB


A Thesis Presented to the

FACULTY OF THE COLLEGE OF GRADUATE STUDIES

**KING FAHD UNIVERSITY OF PETROLEUM & MINERALS**

DHAHRAN, SAUDI ARABIA

In Partial Fulfillment of the
Requirements for the Degree of

# MASTER OF SCIENCE
## In
## GEOLOGY

KING FAHD UNIVERSITY OF PETROLEUM AND MINERALS
DHAHRAN 31261, SAUDI ARABIA

COLLEGE OF GRADUATE STUDIES

This thesis, written by Hesham Mohammad Al-Qassab under the direction of his Thesis Advisor and approved by his Thesis Committee, has been presented to and accepted by the Dean of the College of Graduate Studies, in partial fulfillment of the requirements for the degree of MASTER OF SCIENCE in GEOLOGY.

Thesis Committee

Dr. Z. Al-Harari, Thesis Advisor

Dr. A.J. Al-Khalifa, Member

Dr. G. Korvin, Member

Department Chairman

Dean, College of Graduate Studies

30/3/97
Date

## ACKNOWLEDGMENT

Acknowledgment is due to King Fahd University of Petroleum and Minerals for support of this research.

I wish to express my appreciation to Dr. Z. Y. Al-Harari who served as my major advisor. I also wish to thank the other members of my Thesis Committee Dr. A. J. Al-Khalifa and Dr. G. Korvin.

Thanks are also due to Ministry of Petroleum and Minerals for the release of data. Special thanks are due to Saudi Aramco represented in M. Baqi, Vice President of Exploration, A. J. Al-Khalifa, Manager of Geological Department, for their support for the approval to use Safaniya Field data. I would like to thank S. Bader for her review of the manuscript and H. Al-Sabti for his discussion. Last but of course not least, I would like to thank my family for their support.

# TABLE OF CONTENTS

## LIST OF FIGURES

**Figure #** **Page #**

**Figure #** **Page #**

## List of Tables

# موجز الرسالة

الإسم: هشام محمد عبدالمحسن القصاب
عنوان الدراسة: النموذج الجيوإحصائي لمكمن السفانية في حقل السفانية
التخصص: جيولوجيا
تاريخ منح الدرجة: مارس ١٩٩٧ م

تبحث الرسالة عن دور الإحصاء الجيولوجي في صياغة مكامن البترول، حيث تم إختيار خمسة وأربعون بئر للدراسة من منتصف حقل السفانية المغمور الواقع في شمال المملكة العربية السعودية . تم إختيار طبقة واحدة من بين اثني عشر طبقة زمنية جيولوجية من مكمن السفانية للتحليل في هذا البحث . وكان العامل الأساسي في إختيار هذه الطبقة هو طبيعتها الغير المتجانسة والتي تشكل نوع من التحدي في بناء النموذج الثلاثي الأبعاد .

يتناول البحث في مقدمته نبذة عن الجيولوجيا الإقليمية لعضو السفانية في حقل السفانية ، في القسم الثاني من البحث يتم التحليل الإحصائي الأولي للمتغيرات المتاحة لهذا البحث مثل مساميات الصخور والسحنات الجيولوجية والمساميات المصاحبة لهذه السحنات .

إن هذا النوع من التحليل ساعد في إيضاح بعض النتائج في القسم الأخير من البحث والذي إعتنى بصياغة المكمن .

لقد صيغ الإستمرار الحيزي بإستخدام إحدى الأدوات التي تستعمل في هذا المجال والتي تسمى بالفاريوقرام . بعدها ، تم إستخدام الفاريوقرام التأشيري لفحص الفئات الفردية من السحنات المتاحة للبحث .

لقد تم توليد عدة نماذج ثلاثية الأبعاد للمكمن قيد الدراسة بإستخدام النتائج المستخلصة من التحليل الحيزي الوارد الذكر ، أول هذه النماذج نموذج النفاذية والذي طبق نظام كريجد في إيجاده . وللتغلب على نتائجة المتجانسة تم إستخدام نظام س . ج . س . كما تم إنتاج نموذج ثماني السحنات بإستخدام نظام س .أ . س .

وأخيرا وبعد البناء الهندسي لهذا النموذج ، تم توزيع النفاذية لكل سحنة على حدة بإستخدام نظام س . ج . س .

درجة الماجستير في العلوم
جامعة الملك فهد للبترول والمعادن
الظهران - المملكة العربية السعودية
مارس ١٩٩٧ م

# THESIS ABSTRACT


| | |
|---|---|
| Name: | Hesham Mohammad Al-Qassab |
| Thesis Title: | Geostatistical Modeling of Safaniya Reservoir in Safaniya Field |
| Major Field | Geology |
| Date: | March 1997 |



The thesis investigates the role of geostatistics in reservoir modeling. Fourty five wells from the central part of the Safaniya Oil Field in Saudi Arabia were chosen for this study. Out of twelve geological time sequences, SFNC Sequence was selected to be analyzed. This sequence was chosen due to its heterogeneous characteristics as it presents a challenge when building 3D geocellular models.

The regional geology of the Safaniya Member in Safaniya Field was first discussed. Statistical analysis of the physical properties of SFNC Sequence such as porosity and facies based porosity was done. Such analysis helped in explaining some results in the modeling step. Spatial continuity was then modeled using variograms which is the basic tool for identifying the patterns of spatial continuity of a variable. Furthermore, Indicator variograms were calculated to provide additional flexibility to examine individual classes of the variables under study.

Several three dimensional reservoir models were generated using the results obtained from the spatial analysis. Kriged porosity volume was generated using the porosity variograms calculated from the fourty five wells available to this study. The smoothed results of kriged porosity was overcomed by using Sequential Gaussian Simulation. The non parameteric Sequential Indicator Simulation was then used to build geological architecture of lithofacies using the results obtained from indicator kriging of lithofacies. Once the geological

architecture was built up by eight facies, porosity was finally distributed among each facies using Sequential Gaussian Simulation.

Master of Science Degree
King Fahd University of Petroleum and Minerals
Dhahran, Saudi Arabia
March, 1997

# CHAPTER 1

# GEOLOGY OF SAFANIYA FIELD

## 1.1 INTRODUCTION

Reservoir characterization can yield major improvements in reservoir performance prediction and reservoir development and management. In order to fulfill the objective of modeling a petroleum reservoir, a detailed geological description should be done and understood first. However, the only sources of interpreting the geology of an area are from discrete point sources namely drilled oil wells. These wells are far away in most cases and represent only scattered samples of the population, in this case the whole reservoir. These samples can be correlated with each other, but there are a lot of uncertainties about this correlation. For example, if two wells show a channel sand on the same level, one would tend to connect them with each other. The risk of

mismatching these channels can be of great influence in reservoir simulation and hence production.

Geostatistics has been introduced to the oil industry in the mid nineteen eighties to help in characterizing the petroleum reservoirs. It basically deals with variables called regionalized variables which occupy certain locations within the space (or reservoir). Regionalized variables can include continuous and discrete variables such as physical properties (porosity & permeability) and lithology respectively.

However, Geostatistics is considered as a double-edged knife. This is due to the fact that if it is misused it can be extremely destructive. On the other hand, if it is used properly it can help in highly optimizing the characteristics of a given reservoir. Unfortunately, most of the geostatistical work in the petroleum industry has been handled by non-geologists. Understanding the geological processes that led to the deposition of the reservoir and thus the distribution of the facies that resulted from a particular system or process is crucial. Models that have been derived without any geological constraints are of questionable value.

The principal objective of this study is to investigate the rule of geostatistics and then present a proper geostatistically derived model utilizing the spatial continuity of physical properties of the rocks within the reservoir. However, the study is based on the understanding and then utilizing the geological processes which led to the deposition of the reservoir.

The Safaniya Field is located in the northwestern part of Saudi Arabia within the Arabian Gulf. It is the largest offshore oil field in the world. The Safaniya structure is a low-relief anticline with NE-SW axial trend produced by uplift movements of deep seated basement faults. Its productive area is about 65 Km. long and 15 Km wide. Figure 1-1 shows the location of the Safaniya Field.

The Safaniya Reservoir in the central part of the Safaniya Field has been chosen for this study. However, in this chapter, the Safaniya Member will be presented in the whole Safaniya Field and sometimes within the Northern Offshore Area of the Arabian Gulf. This will be very helpful in understanding the regional geological variations of Safaniya Member within the Safaniya Field. Having understood the regional geological variations, the central portion of Safaniya Field will be utilized to apply certain statistical geostatistical methods.

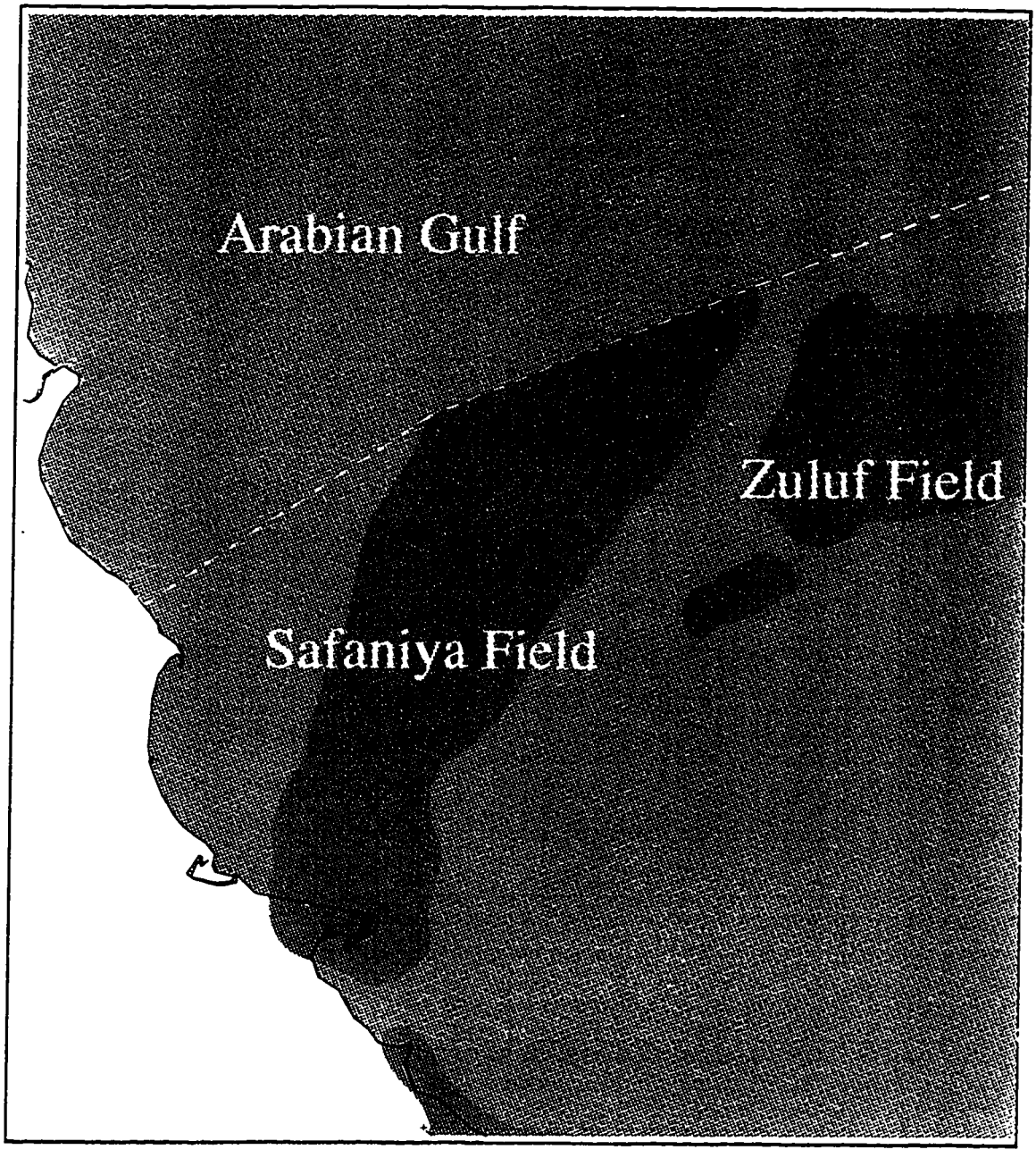


Figure 1-1: Location map of Safaniya Field

Numerous studies have been made on Safaniya Field. These studies focused mostly on the geology of the field. The studies were done mostly by Saudi Aramco and Chevron Oil Company. However, besides these studies other studies from nearby fields such as Zuluf and Marjan were also utilized in this thesis.

## 1.2 GEOLOGICAL SETTING OF SAFANIYA MEMBER

Safaniya Member is Albian to Cenomanian in age and lies within the lower part of the Middle Cretaceous Wasia Formation. It overlies the Khafji Member and is underlain by Mauddud Member.

The Wasia Formation in the Arabian peninsula was deposited during the Middle Cretaceous from the Albian through the Toronian time. In the Northern Arabian Gulf Area, Wasia Formation has been subdivided into seven distinguished members that were deposited during transgressive carbonates and regressive clastic episodes. These are (from old to young); Khafji, Safaniya, Mauddud, Wara, Ahmadi, Rumaila, and Mishrif. As shown in Figure 1-2, the Wasia Formation overlies the Shua'iba Formation of Aptian age. The Shua'iba Formation consists of carbonates and is considered as stable shelf in the

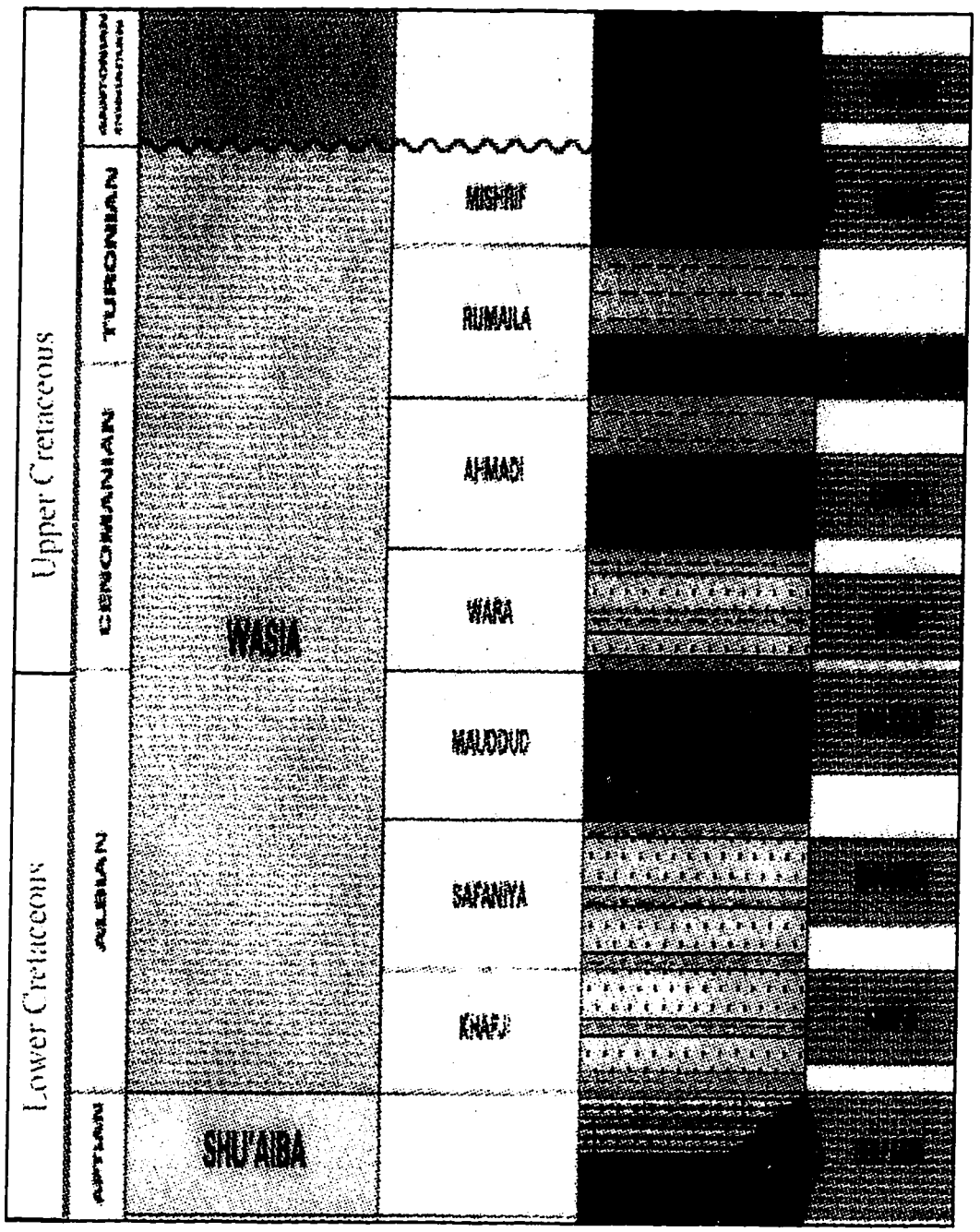


Figure 1-2: Composite stratigraphic column of the Wasia Formation In the Northern Offshore Area. After Aramco staff

Northern Area of the Arabian Gulf. It was deposited during a major transgressive of the sea followed by a major unconformity marking the end of the Lower Cretaceous time.

However during the Middle Cretaceous time, a major drop in sea level caused the progradation of the clastic sediments, from landward side allowing the Khafji Member to be deposited. This progradation was disrupted by a major transgressive cycle which deposited the Dair Limestone over the Khafji Member. The Dair Limestone consists of Argillaceous limestone in the east, where it is consider as a basin depocenter, and shale in the west in Safaniya field near the shelf.

Another major drop in sea level brought about a cycle of progradation resulting in the deposition of the Safaniya Member. Such progradation was in the form of fluvial to fluvial dominated delta which extended from the source area at the Arabian Shield to basin depocenters near the Iranian border. However, this sedimentary cycle was not as extensive as the previous one. This is evidenced by the fact that the Safaniya Member pinches out quicker than Khafji Member moving away from the source area toward the basin. On the other hand, Khafji and Safaniya members are lithologically quite similar

and dominated by siliciclastic sediments. These members decrease in their sand content toward the Iranian border.

The Mauddud Member overlies the Safaniya Member which was deposited during a major rise in sea level and relatively low subsidence in the area. Other members of the Wasia Formation were deposited by similar depositional cycles. For instances Wara Member overlaying the Mauddud Member was similarly deposited by progradation of sand after a major sea level drop.

The Safaniya Member is characterized by the absence of major conglomeratic facies except at channel lags. Clean sandstone units are abundant within the Safaniya Member. These clean sandstone units constitute the Safaniya Reservoir. The Safaniya Reservoir is characterized by the a presence of clean, medium to coarse grained porous, and permeable sandstone. However, reservoir quality deteriorates moving upward toward the top of Safaniya Member.

## 1.3 STRUCTURAL INFLUENCE

The paleostructure can be of great influence on the stratigraphy and therefore on the sedimentation of an area. In order to study the stratigraphy of a particular area, its paleostructural configuration which proceeded the sedimentation has to be outlined.

Kashifi discussed the plate tectonics and structural evolution of the Zagros Geosyncline in south western Iran. In his model he proposed a Geosynclinal basin resulting from the collision of the Arabian plate with the Iranian plate. His model shows that the paleogeomorphological configuration of the Arabian Gulf area and the Arabian Peninsula remained stable. A similar model was also illustrated by R. W. Powers and others. In their models, the shield rocks on the plateau of Western Arabia remained stable and positive since Precambrian.

The Arabian foreland shelf east of the Arabian shield has been subdivided into three tectonic provinces; the Stable Interior Homocline adjacent to the Arabian Shield, the Unstable Interior Platform next to the Homocline, and the basinal areas. The basinal areas include the Sirhan-Turayf

Basin in the north, the Dibdibah Basin in the northeast which is marginal to the Arabian Gulf, the Northern Arabian Gulf Basin, and the Rub al-Khali Basin.

The Safaniya Field along with adjacent fields such as Zuluf and Marjan Fields are located in the northern offshore of the Arabian Peninsula. It is located between two basins; the Northern Arabian Gulf Basin and the Dibdibha Basin. Similar to other fields in Eastern Arabia, the structure of the Safaniya Field was formed as a result of the continued structural growth of the present day structures and local highs since the Cretaceous period due to basement uplift. The uplift was caused by the deep-seated basement faults which are parallel to the present day structural alignments. This structural configuration (Figure 1-3) was then modified by the continuous reactivation of movements along the basement fault planes which resulted in the growth of structures.

It is thought that the configuration of the paleostructure influenced the distribution of facies during the deposition of Wasia Formation. The Wasia Formation was deposited after a major sharp sea level drop after the Shua'iba Formation was deposited. The sea level drop was probably due to regional tectonic events which resulted from plate tectonic movements of the Arabian plate and its collision with the Iranian plate along the Zagros suture zone. This

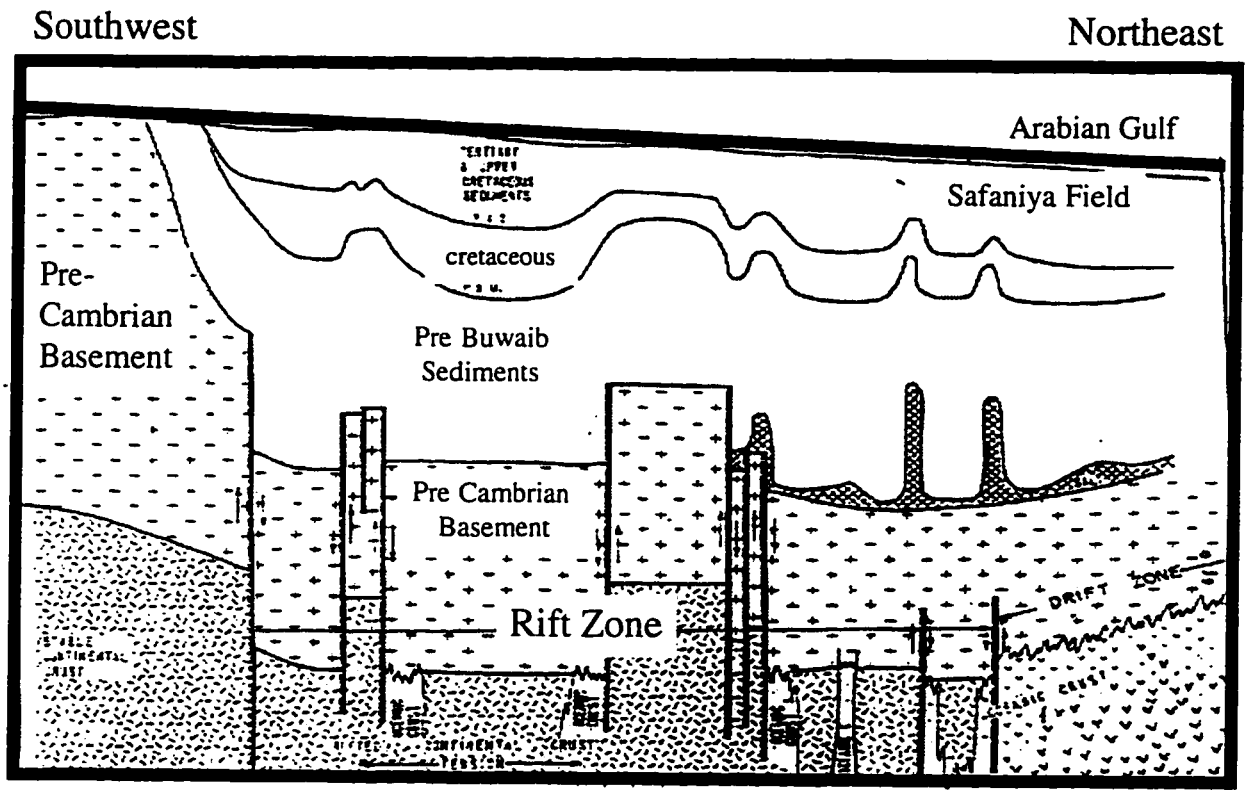


Figure 1-3: Structural configuration of Safaniya Field. (After Mahmoud 1979)

drop of sea level was followed by progradation of clastic sediments from the Arabian shield toward basin depocenters. Thus, basins were formed as direct results of structural growth due to the reactivation of deep seated faults. This is clearly seen in the lithologic changes that resulted from the transgressive phase which was interrupted by the Oman Orogeny and hence represented by alternating clastics and carbonates in what is called the Middle Cretaceous Oscillatory Phase.

## 1.4 STRATIGRAPHY OF THE SAFANIYA MEMBER

In the Safaniya Field, the Safaniya Member consists of alternating quartz sandstone, siltstone, shale, argillaceous limestone, and minor amounts of siderite and carbonaceous sediments. The Safaniya Member can be subdivided into five units based on the dominant lithological content (Figure 1-4). These are as follows:

1. Lower Safaniya Shale/Silt
2. Lower Safaniya Stringers
3. Main Sand
4. Upper Safaniya Stringers
5. Upper Safaniya Shale

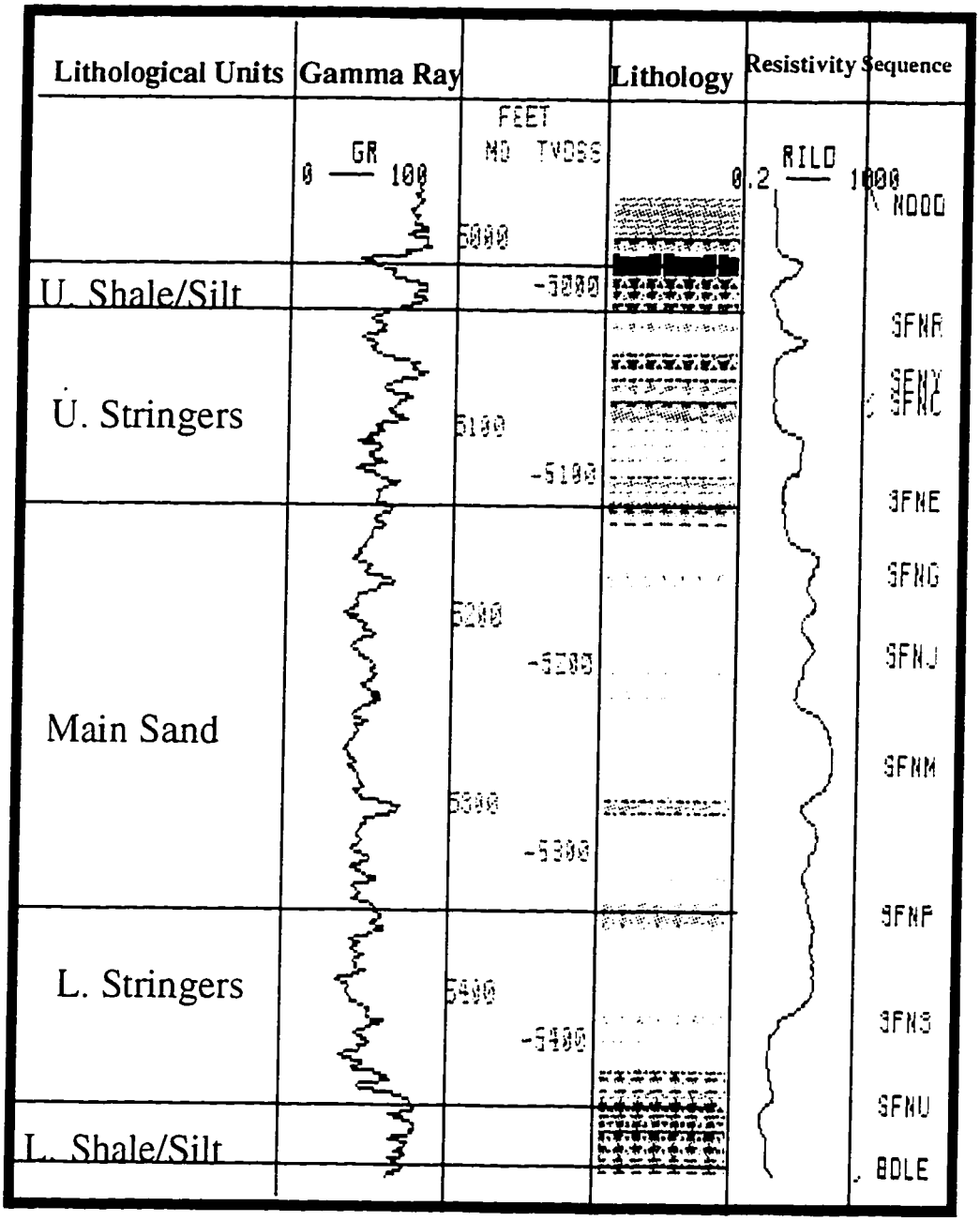


Figure 1-4: Type log representing the Safaniya Member units

1. **Lower Safaniya Shale/Silt**

This interval consists mainly of a dark gray homogeneous shale section interbedded with siltstone and shaly to silty sandstone. The top of this interval is defined as the base of the Safaniya Reservoir. (Due to the lack of reliable and clear stratigraphic correlation through this part of the interval, the base of Safaniya Reservoir is considered as the top of the Khafji Member). The sand/shale ratio of this interval increases moving to the south where this interval is composed mainly of sandstone interbedded with shale.

2. **Lower Safaniya Stringers:**

This interval overlies the Lower Safaniya Shale/Silt. It is composed of interbedded siltstone, sandstone and shale and shows discontinuous facies distribution. However, sand bodies are laterally continuous and have communication with the above Safaniya Main Sand.

3. **Main Sand:**

The Main Sand Interval of Safaniya Member consists of mainly thick, homogeneous, clean sandstone with occasional shale stringers. This

interval forms the most productive portion of Safaniya Reservoir. The Main Sand consists of stacked channels and/or mouth bars. The sandstone is coarse at the channel lags and medium at the middle grading into fine to very fine grains at the top of the channel. The clean sandstone lithofacies are generally friable, well sorted to poorly sorted, subrounded to rounded with abundant cross-bedding. The sand/shale ratio decreases to the north of Safaniya Field as well as to the east and pinches out into the Iranian border.

**4. Upper Safaniya Stringers**

This interval consists of interbedded sandstone, shale, and siltstone. It unconformably overlies the Main Sand Interval. The top of this interval is considered as the top of the Safaniya Reservoir in areas which show no Upper Sand development. The sand exhibits a channel fill where the shale represents the facies between the channels.

**5. The Upper Safaniya Shale**

This is an interval composed of uniform shale and argillaceous limestone. Isolated sand bodies are also found in the southern part of Safaniya Field. However, a gradual facies change from sandy to silty

and to shale toward the north and east toward the Iranian border. The top of this interval is considered as the top of Safaniya member. However, this interval has gradation lithological contact with the overlying Mauddud Member. In some instances, there is no obvious lithological marker which distinguishes it from the Mauddud Member. The abundance of shaly facies indicates the gradual transgression of the sea prior to Mauddud deposition.

In general, these five intervals are more sandy in the south which are nearer to the source area. As a result, the Main Sand becomes thicker at the expense of other shaly intervals. However, the opposite is seen in the north of Safaniya Field. In other words, the Main Sand becomes thinner and other shaly intervals get thicker.

## 1.5 RESERVOIR ZONATION OF SAFANIYA MEMBER

Safaniya Reservoir is part of the Safaniya Member. Since the Safaniya Member consists of several deltaic progradation and retrogradation one might expect to have the same type of system repeated

vertically. However, the only way to distinguish these cycles is to subdivide the Safaniya Member into chronostratigraphic time horizons.

The Safaniya Member has been subdivided by SAUDI ARAMCO geologists into eleven sequences (also called layers) based on time stratigraphy (chronostratigraphy). Geological and engineering data were also studied and integrated in order to establish such layering. Some of these data include core studies, paleontological studies, open hole logs, formation analysis logs and reservoir engineering data such as pressure and drill stem tests.

It should also be emphasized that the designation of the sequences was not based on lithological criteria. As a result, one sequence might hold several lithologies such as clean sandstone, shaly sandstone, siltstone and homogeneous shale. In fact, these sequences correspond to sequence of progradation and retrogradation of the delta. In other words, time lines (sequences) are represented by transgressive surfaces that bound the progradational sequences. Recognition of these progradational sequences is very important because they are considered to be the building blocks of

reservoirs. Their recognition and interpretation are an essential first step in understanding reservoir distribution and reservoir behavior.

## 1.6 DEPOSITIONAL ENVIRONMENT

In order to characterize a given reservoir, several geological descriptions should take place. Beside those which have been already described, one vital geological criterion that should be emphasized is the system under which all these sediments were brought from the source to the basin; the depositional environment. If the depositional environment is well understood in a given area, all remaining geological descriptions can be used in a process of fine tuning the required geological model. For instance, if one knows the depositional environment in a given area, then the expected lateral and vertical variations will be better defined. Having understood the gross lateral variations, the rest of the geological descriptions such as zonation of the reservoir, or the application of geostatistics for reservoir characterization will constitute finer details of the required model.

The depositional environment of Safaniya Member should be considered along with that of other members of the Wasia Formation. This is due the fact

that Safaniya Member is considered as one of the cyclical depositional systems within the Wasia Formation. It is also believed that the depositional environment of other members should be consistent with the general characteristics of the Safaniya Member in the entire Northern Arabian Gulf Area. Moreover, other factors influencing the depositional environment such as the drop in sea level, regional and local tectonic movements, distance from the source area, and the configuration of the depositional slope should be taken into account. Each of these factors will have its own influence on the depositional system.

The Safaniya Member in Safaniya Field was mainly deposited by relatively large cratonic delta systems which occupied the top of the transgressive shale of the Khafji Member. The delta systems were associated with fluvial systems and less significantly with marine systems. The abundance of fining upward sequences which are associated with some coal beds and root structures indicates that this delta was fluvial dominated. The fluvial systems were closer to the source area than the main delta systems, whereas, the marine systems were near the carbonate shelf (Base Lower Dair Limestone). The entire system of fluvial dominated delta was prograding eastward toward the basin

depocenters. As a result, the highly gradient meandering sandy streams were cutting older deltaic sediments of older rocks.

The Lower Stringers and part of the Main Sand section were generally deposited by the prograding fluvial dominated shallow marine delta. The Main Sand was deposited by the marginal marine environment . The marginal marine environments would include crevasse splays, marsh and swamps.

After considering core descriptions and analyzing electrical logs, the following depositional environments can be identified:

**I) Subaqueous Delta Plain**

**a- Prodelta**

**b- Delta Front (Distributary Mouth Bar)**

*1) Distal*

*2) Proximal*

**II) Lower Delta Plain**

**a- Active /Abandoned distributary channels**

**b- Bay-fill deposits**

*1-Interdistributary Bay*

*2-Marsh & Swamps*

*3- Subaqueous Levees*

**III) Upper Delta Plain**

**a-Fluvial channels**

*Meandering Streams*

**b-Flood plain deposits**

**VI)Shallow-Marginal Environment.**

# CHAPTER 2

# CLASSICAL AND SPATIAL ANALYSIS

## 2.1 Introduction

The goal of this chapter is to give an introduction to some basic geostatistical methods dealing with the spatial modeling which can be applied to petroleum geology. These methods represent the basic concepts of spatial correlation such as variograms and correlograms. Data available will be first reviewed and then basic univariate and bivariate statistical methods are introduced and examined by the data set available to this study. This analysis will provide an initial statistical snapshot of the data set available.

## 2.2 Data Available:

Data available to this study include:

The following data for fourty five wells with one foot sample rate:

1- Locations of 45 wells (see Figure 2-1).

2- Volume of Shale (VSH) curve.

3- Porosity logs.

4- Lithofacies (lithology) derived from a suite of logs such as VSH, Density and Gamma ray logs.

Only data related to the target sequence SFNC were retrieved. Analysis of the data files revealed that the Top and Base of SFNC were marked in all the fourty five wells.

## 2.3 Statistical Analysis

The position of Top and Base of SFNC are known, for forty five wells basic statistics of the following variables are analyzed.

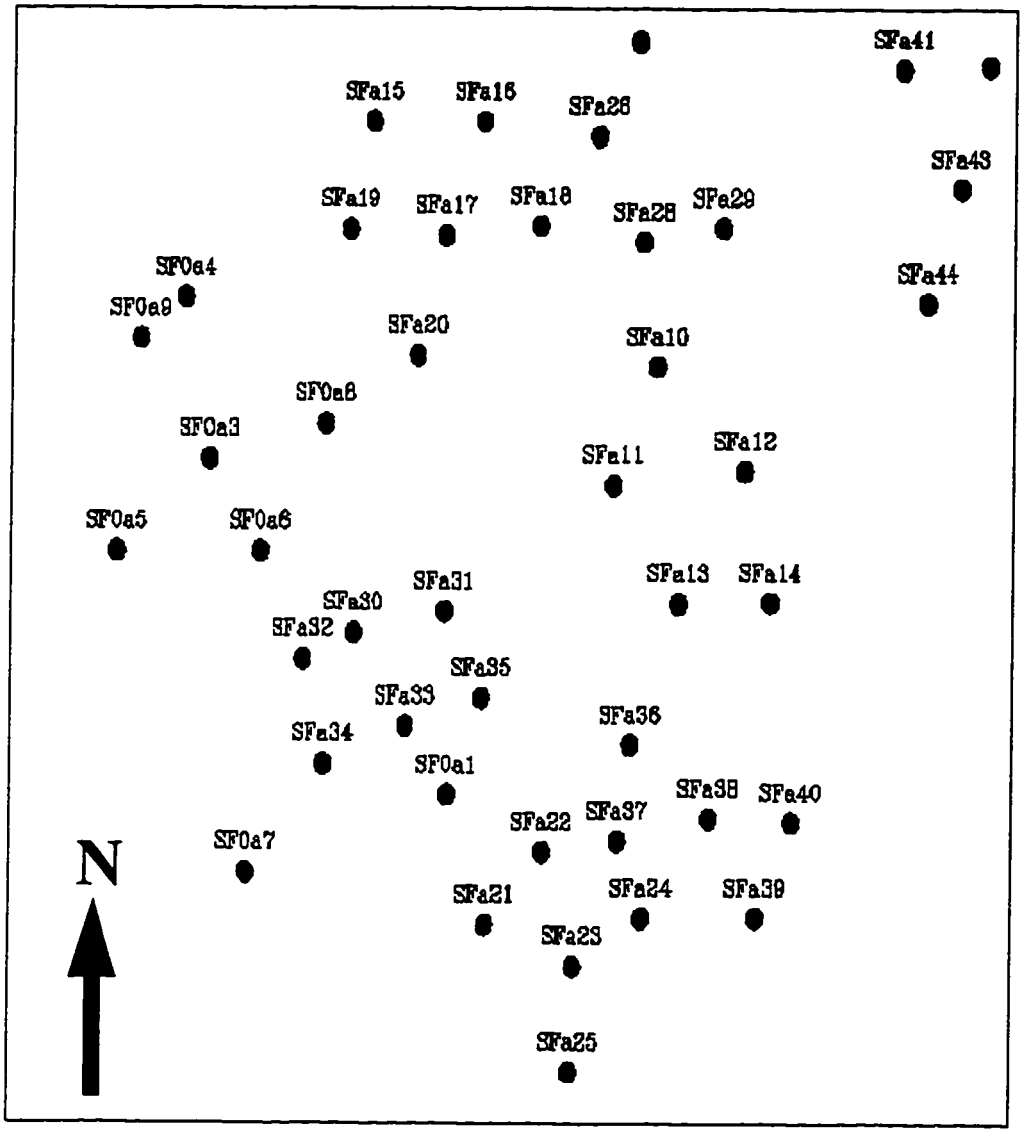


Figure 2-1: Location map of the study area

**A) Univariate Histograms:**

One of the most common and useful presentation of the data sets is the histogram. This is done by forming a frequency table which shows how often observed values fall within certain intervals or class. The information of the frequency table is then plotted on its corresponding graph; the histogram. It is very common to use a constant class width for the histogram so that the height of each bar is proportional to the number of values within that class.

Univariate histogram of the following variables are presented as follows:

**1- Depth to Top and Base of SFNC**:

Figure 2-2a and Figure 2-2b show structural configurations of the Top and Base of SFNC respectively. The histograms of both Top and Base of SFNC show similar distribution in shape which are not considered as normal distributions( Figure 2-2c and B-2d).

**2-Thickness of SFNC:**

The thickness of SFNC is close to the shape of a normal distribution with the exception of two outliers which don't fall within the main distribution (Figure 2-3).

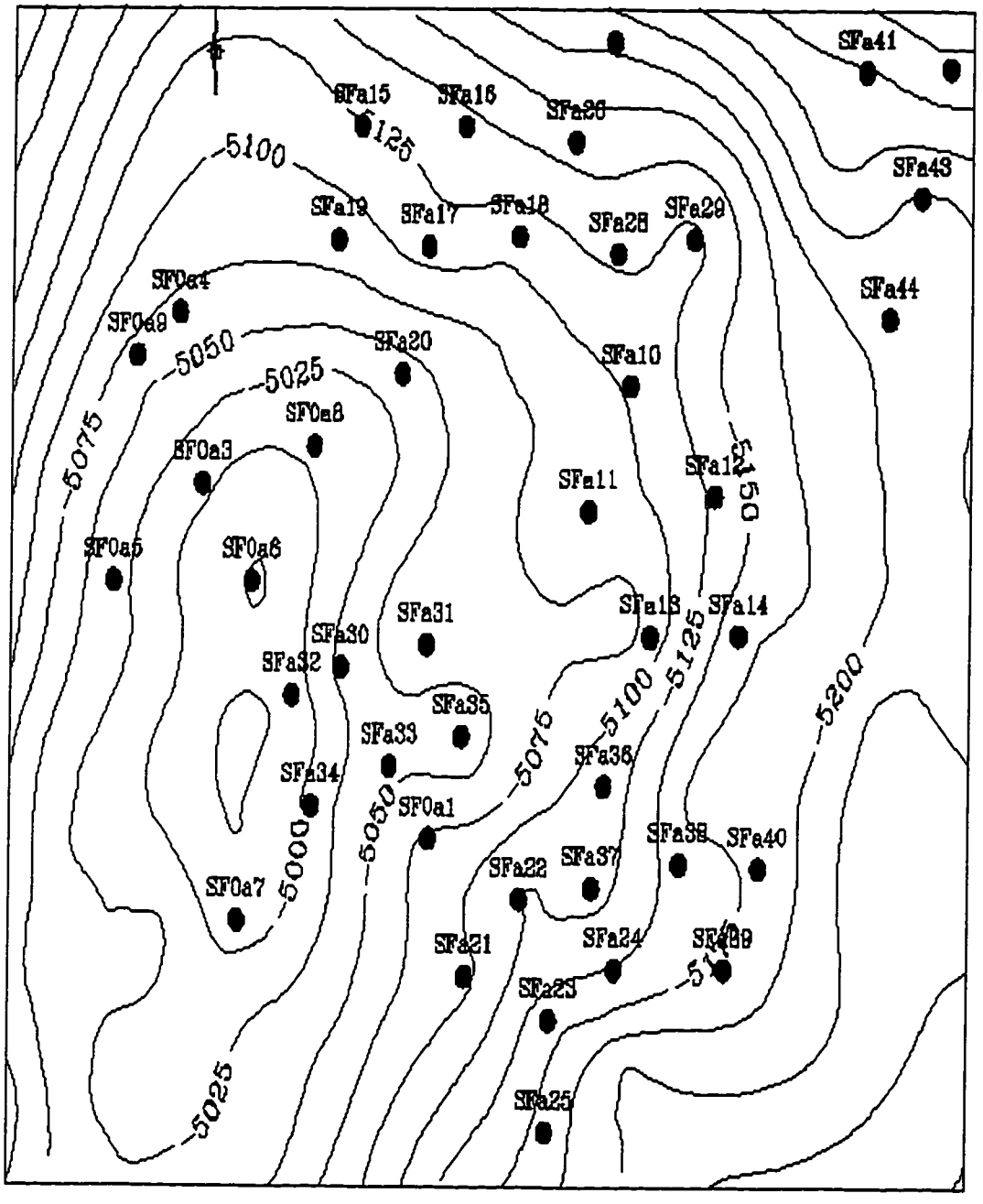


Figure 2-2a:Structure map to the top of SFNC Sequence

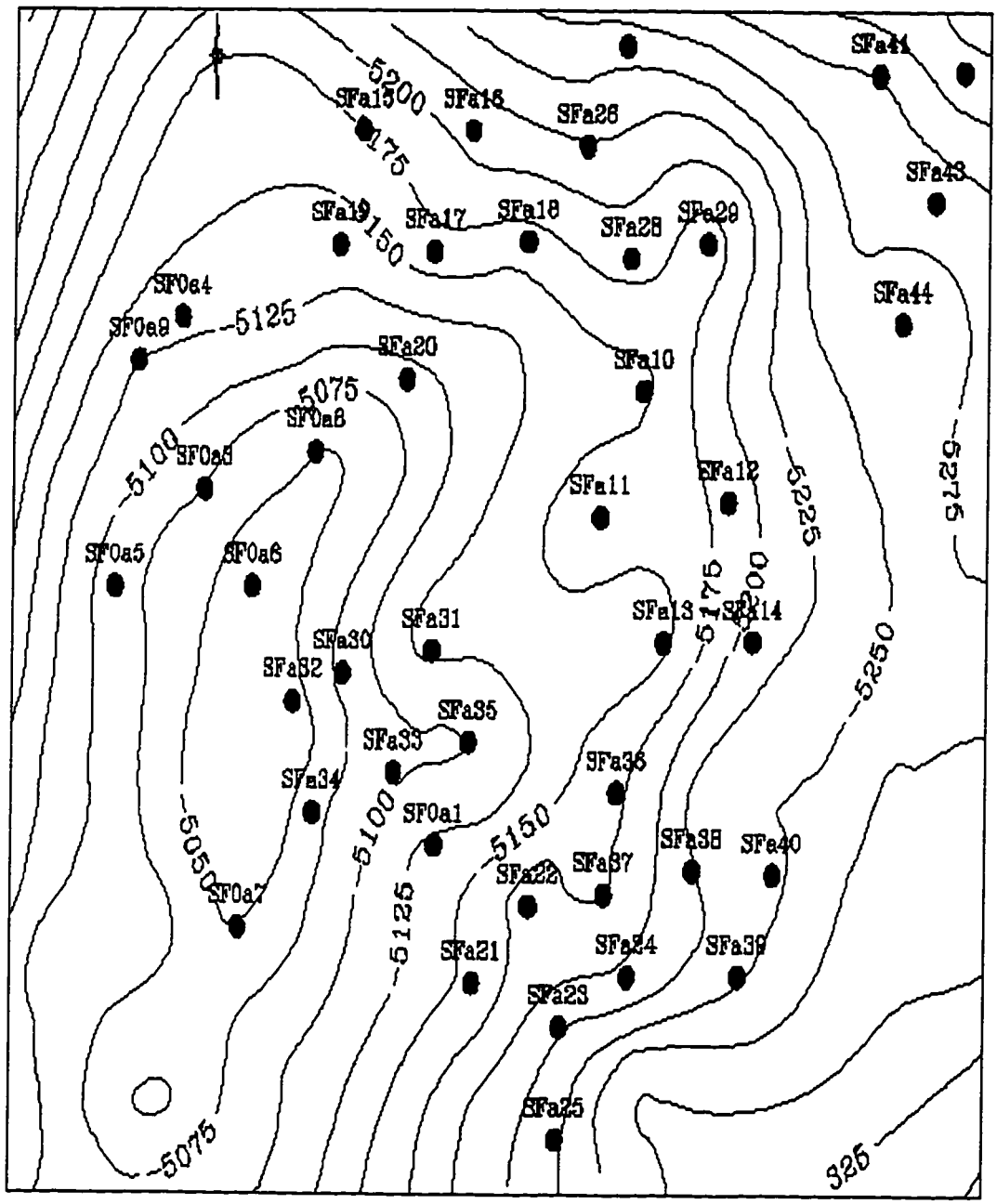


Figure 2-2b:Structure map to the base of SFNC Sequence

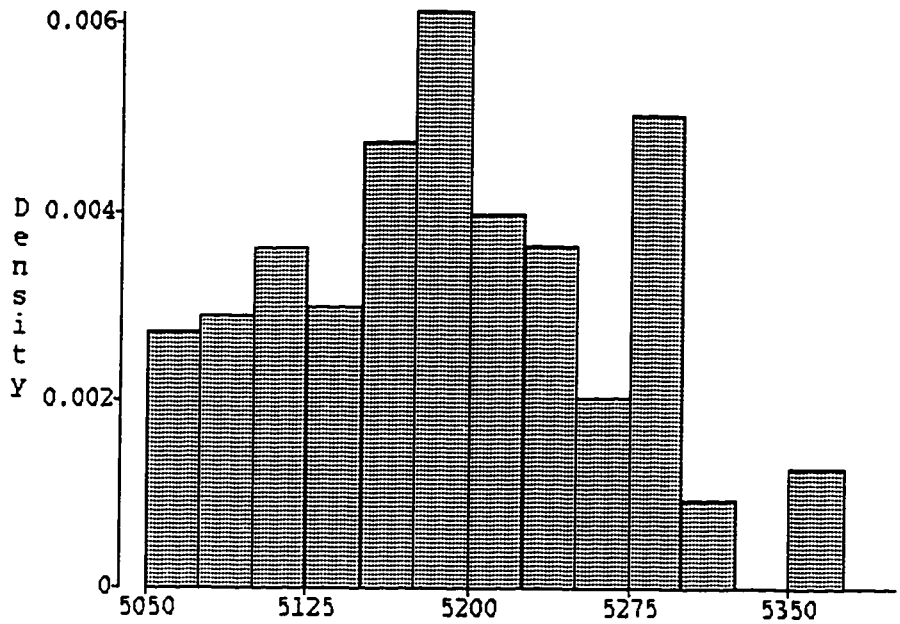


N=45
Mean=5188.86
Std Dev=75.55

Quantiles

| | | | | | |
|---|---|---|---|---|---|
| 100% Max | 5373.0000 | 99% | 5373.0000 | Range | 318.0000 |
| 75% Q3 | 5240.0000 | 95% | 5307.0000 | Q3-Q1 | 109.0000 |
| 50% Med | 5194.0000 | 90% | 5285.0000 | Mode | 5152.0000 |
| 25% Q1 | 5131.0000 | 10% | 5076.0000 | | |
| 0% Min | 5055.0000 | 5% | 5073.0000 | | |
| | | 1% | 5055.0000 | | |

**Figure 2-2c:Depth distribution of SFNC top**

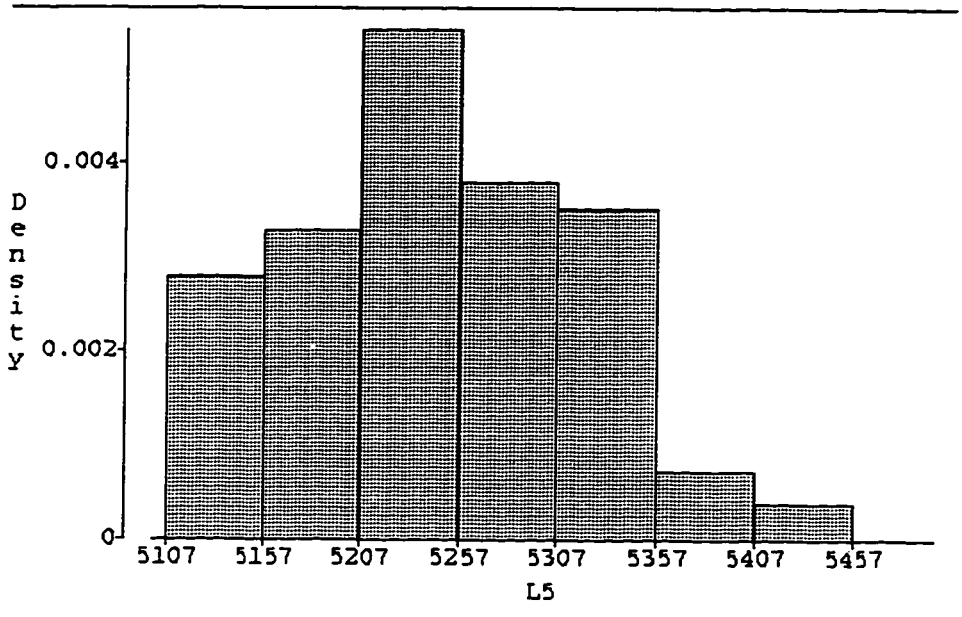


N=45
Mean=5246.25
Std Dev=75.34

| Quantiles | | | | | |
|---|---|---|---|---|---|
| 100% Max | 5421.0000 | 99% | 5421.0000 | Range | 311.0000 |
| 75% Q3 | 5297.0000 | 95% | 5365.0000 | Q3-Q1 | 109.0000 |
| 50% Med | 5246.0000 | 90% | 5347.0000 | Mode | 5347.0000 |
| 25% Q1 | 5188.0000 | 10% | 5143.0000 | | |
| 0% Min | 5110.0000 | 5% | 5133.0000 | | |
| | | 1% | 5110.0000 | | |

**Figure 2-2d:Depth distribution of SFNC base**

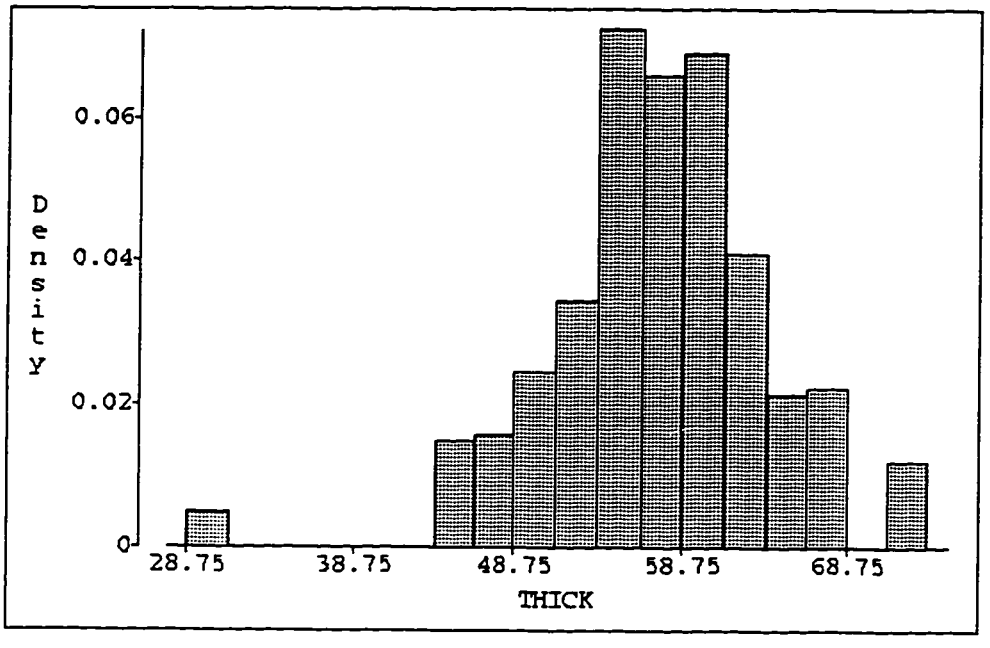


N=45
Mean=57.39
Std Dev=6.77

| Quantiles | | | | | |
|---|---|---|---|---|---|
| 100% Max | 73.0000 | 99% | 73.0000 | Range | 43.0000 |
| 75% Q3 | 61.0000 | 95% | 68.0000 | Q3-Q1 | 7.0000 |
| 50% Med | 57.0000 | 90% | 65.0000 | Mode | 60.0000 |
| 25% Q1 | 54.0000 | 10% | 49.0000 | | |
| 0% Min | 30.0000 | 5% | 48.0000 | | |
| | | 1% | 30.0000 | | |

**Figure 2-3:Thickness distribution of SFNC**

**3-Volume of Shale:**

Volume of Shale (Vsh) is derived from Gamma ray log by the following:

$$Vsh = \frac{(gr) - (gr\_cl.ss)}{(gr\_sh) - (gr\_cl.ss)}$$

gr= Gamma Ray value

gr_cl.ss= Gamma Ray value of a clean sandstone.

gr_sh= Gamma Ray value of shale.

Figure 2-4 Shows the distribution of Vsh within SFNC sequence. It shows that there is more than one subclasses of Vsh is present. For example the histogram shows at least four classes of Vsh; one which is close to zero indicating very clean sands and another one at upper end of Vsh at 100% Vsh indicating a pure shale. The other two classes are between these two end members.

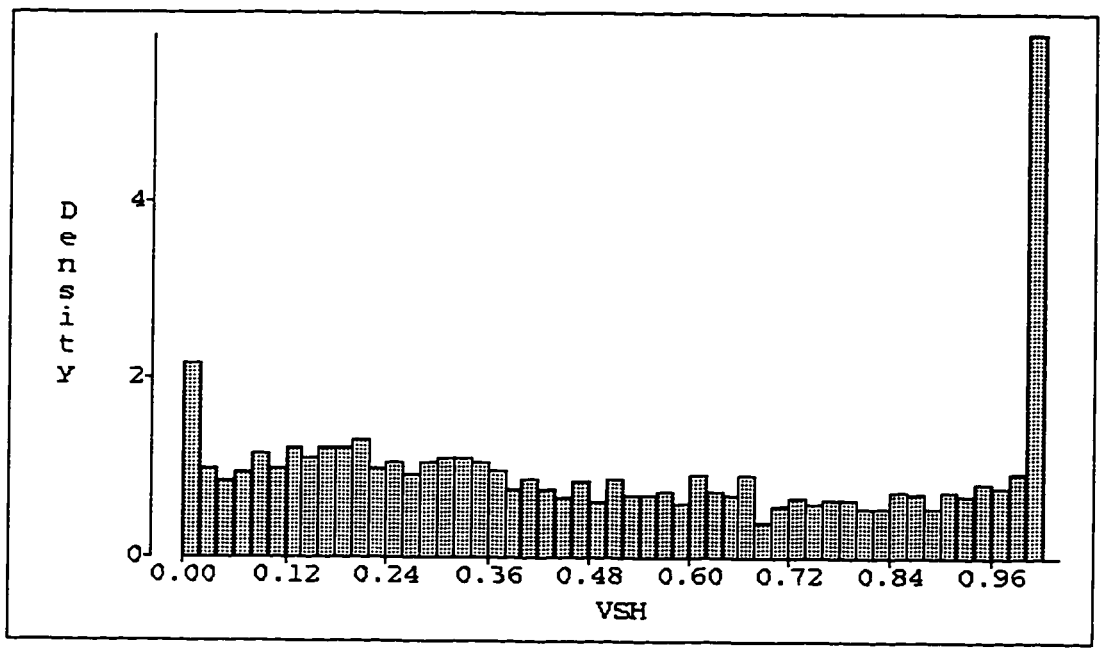


N=2448
Mean=0.5037
Std Dev=0.3316

| Quantiles | | | | | |
|---|---|---|---|---|---|
| 100% Max | 1.0000 | 99% | 1.0000 | Range | 1.0000 |
| 75% Q3 | 0.8200 | 95% | 1.0000 | Q3-Q1 | 0.6140 |
| 50% Med | 0.4630 | 90% | 1.0000 | Mode | 1.0000 |
| 25% Q1 | 0.2060 | 10% | 0.0790 | | |
| 0% Min | 0 | 5% | 0.0260 | | |
| | | 1% | 0 | | |

Figure 2-4: Volume of shale distribution

### 4-Lithofacies

Lithofacies are derived from a suite of electric logs such as Density, Neutron and Gamma ray using certain thresholds. For example; Density log is used to distinguish Iron (Density>2.35) from non-Iron facies. Once this criteria is established, another cutoff is applied using Gamma ray and Vsh to subdivide Iron rich facies to Iron rich Shale and Iron rich Sandstone, and Non-Iron class to Very Clean Sandstone, Clean Sandstone, Shaly Sandstone, Very Shaly Sandstone. Table 1 shows a detailed description of these cutoffs.

### 5- Porosities

The porosity logs are derived from a suite of logs which include Neutron, Density, and Sonic. Similar to Vsh, the distribution of porosity (Figure 2-5) shows more than one subclass is present. One way to separate these classes is to analyze these properties (Vsh and Porosity) by facies (conditional distribution). The porosity distribution of the following reservoir facies will be analyzed:

| LOG / FACIES | GR API | VSH (%) | DENSITY (gm/cc) | Neutron ( $\phi$ ) |
|---|---|---|---|---|
| V. Clean SANDSTONE | <30 | <1 | <2.35 | |
| Clean SANDSTONE | <30 | 1-20 | <2.35 | |
| Shaly SANDSTONE | 30-40 | 20-30 | <2.35 | |
| V. Shaly SANDSTONE | 40-60 | 30-70 | <2.35 | |
| SHALE | >60 | >70 | <2.35 | |
| IRONSTONE | | | >2.5 | >24 |
| IRON-RICH SANDSTONE | <60 | <70 | 2.35-2.5 | |
| IRON-RICH SHALE | >60 | >70 | 2.35-2.5 | |

Table 1-1: Facies determination using log cutoffs

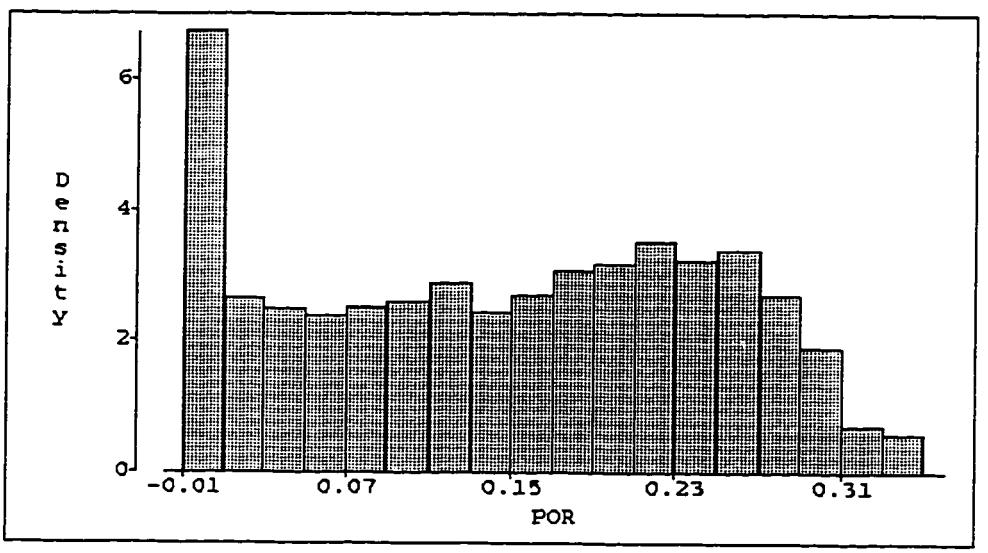


N=2448
Mean=0.1417
Std Dev=0.0986

| Quantiles | | | | | | |
|---|---|---|---|---|---|---|
| 100% | Max | 0.3400 | 99% | 0.3300 | Range | 0.3400 |
| 75% | Q3 | 0.2300 | 95% | 0.2900 | Q3-Q1 | 0.1800 |
| 50% | Med | 0.1500 | 90% | 0.2700 | Mode | 0 |
| 25% | Q1 | 0.0500 | 10% | 0 | | |
| 0% | Min | 0 | 5% | 0 | | |
| | | | 1% | 0 | | |

Figure 2-5:Porosity distribution

***I- Porosity of Very Clean Sandstone Facies:***

The distribution of porosity within this facies shows a normal distribution in shape (Figure 2-6) and occupies the highest range of porosities. This indicate that this facies is the best reservoir quality rock.

***II-Porosity of Clean Sandstone Facies***

The range of porosity of this facies overlaps with the porosity of Very Clean Sandstone facies (Figure 2-7).The porosity ranges from around 18 to 34% representing a good quality reservoir rock. Similar to Very Clean Sandstone facies, porosity of this facies has a shape which looks similar to the normal distribution shape.

***III-Porosity of Shaly Sandstone Facies***

The shape of the distribution of porosity of this facies is close to that of normal (Figure 2-8). Porosity ranges from about 16-28%.

***IV-Porosity of Very Shaly Sandstone Facies***

Figure 2-9 shows the distribution of porosity within the very shaly sandstone facies. The shape of the distribution is close to normal shape.

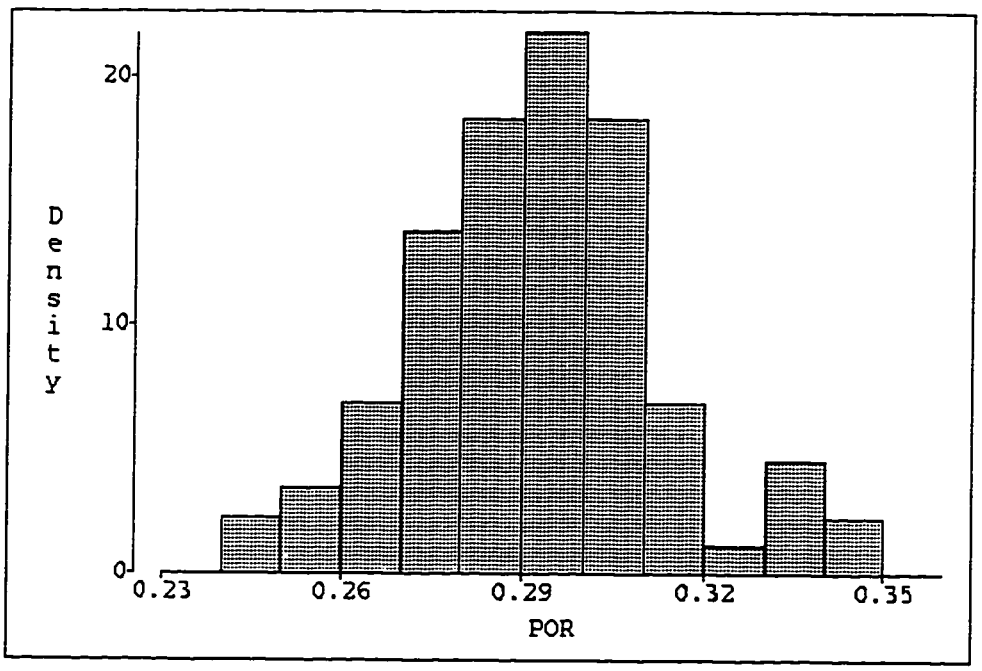


N=87
Mean=0.2874
Std Dev=0.0208

Figure 2-6: Porosity distribution of very clean sandstone

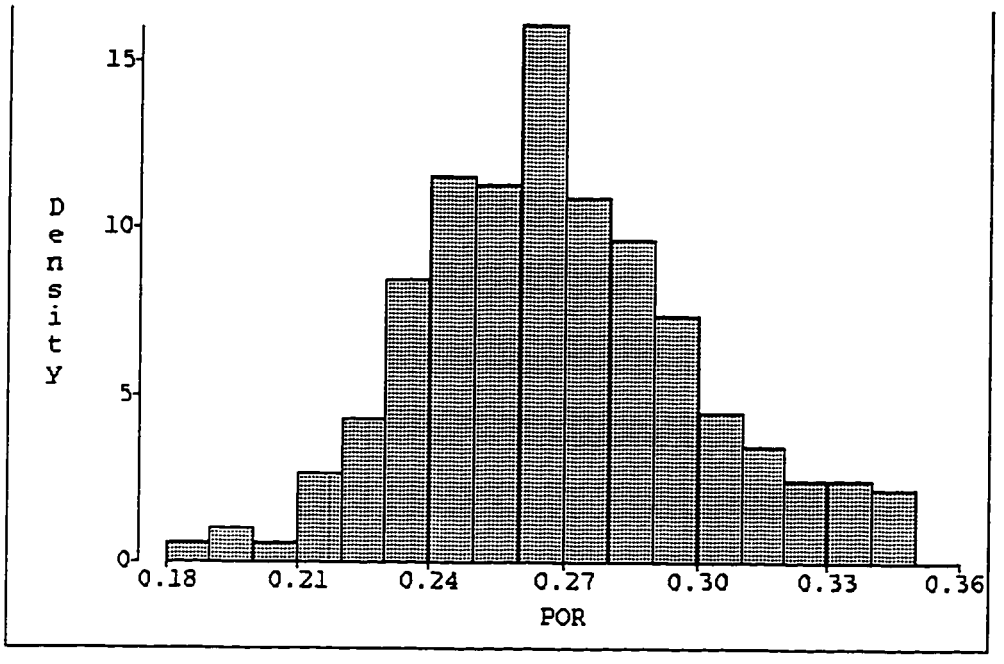


N=485
Mean=0.2632
Std Dev=0.0317

Figure 2-7: Porosity distribution of clean sandstone

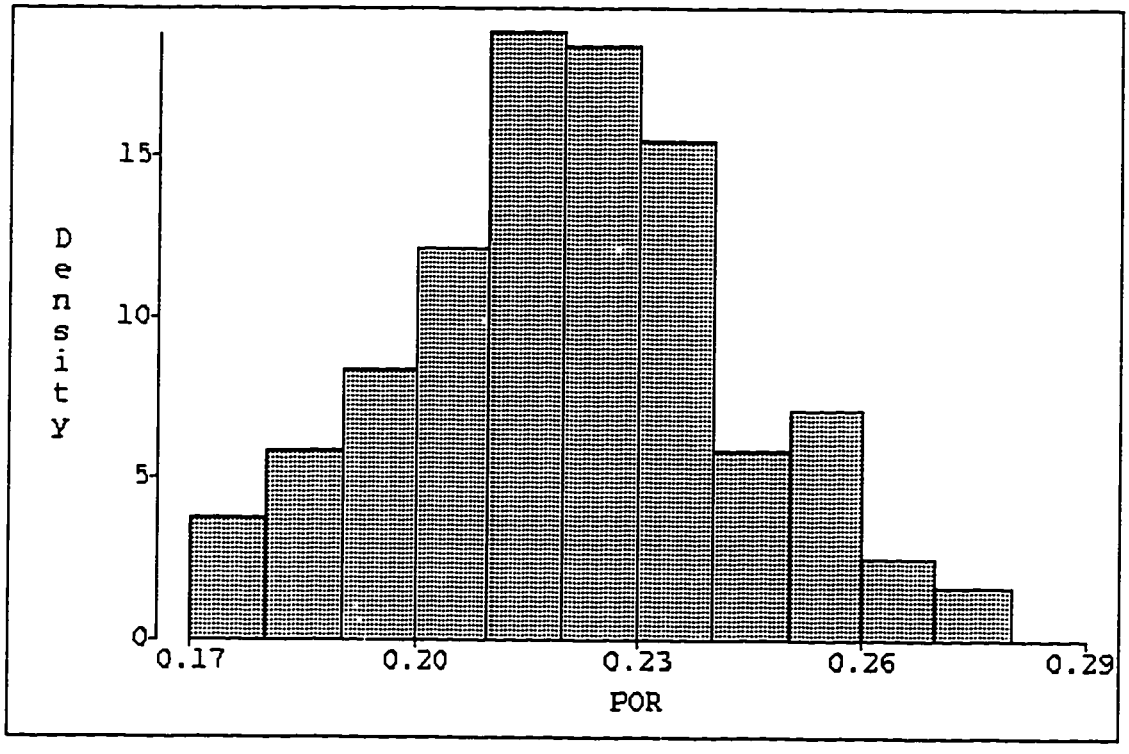


N=239
Mean=0.2156
Std Dev=0.0223

Figure 2-8: Porosity distribution of shaly sandstone

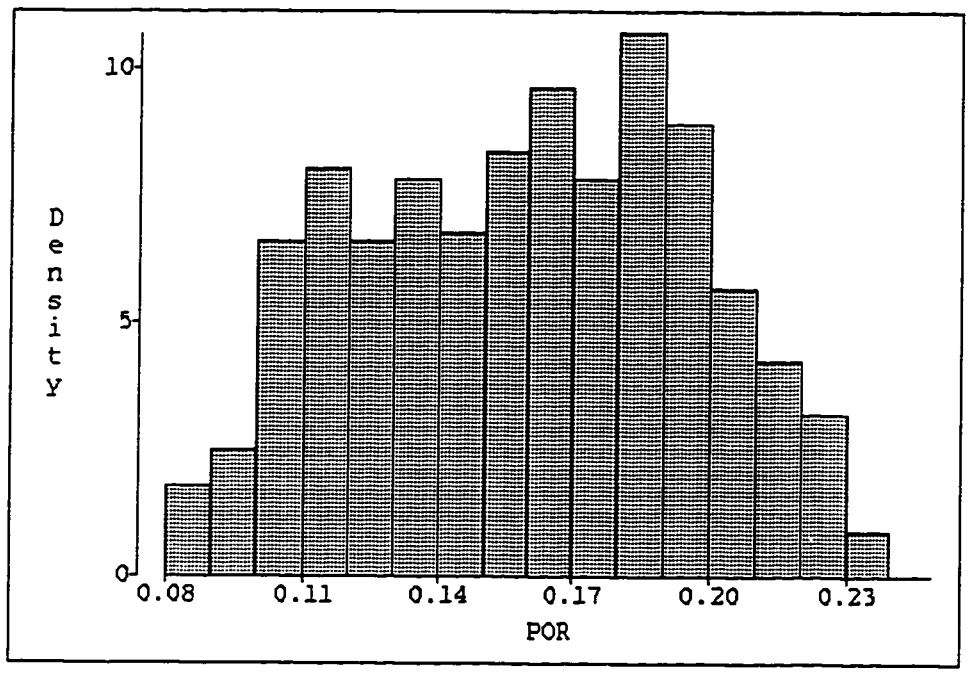


N=559
Mean=0.1542
Std Dev=0.0367

Figure 2-9: Porosity distribution of very shaly sandstone

***V-Porosity of Iron Rich Sandstone Facies***

The distribution of this facies (Figure 2-10) shows a shape which can not be considered as normal. In fact, it shows that it occupies more than one population.

The rest of the facies which include Shale, Ironstone, and Iron Rich Shale are considered to be non reservoir facies and are considered as non porous units.

**B) Scattergrams:**

The univariate tool discussed previously, the histograms, can be used to describe the distributions of individual variables. However, we get a very limited view if we analyze a multivariate data set one variable at a time. One of the important and most interesting feature of earth science is the relationships and dependencies between variables. Scattergrams offer a display tool of bivariate data.

In addition to providing a good qualitative tool for how two variables are related, a scattergram is a useful tool for drawing our attention to erratic values. It is important to check and clean the data in the early stages of the study of a

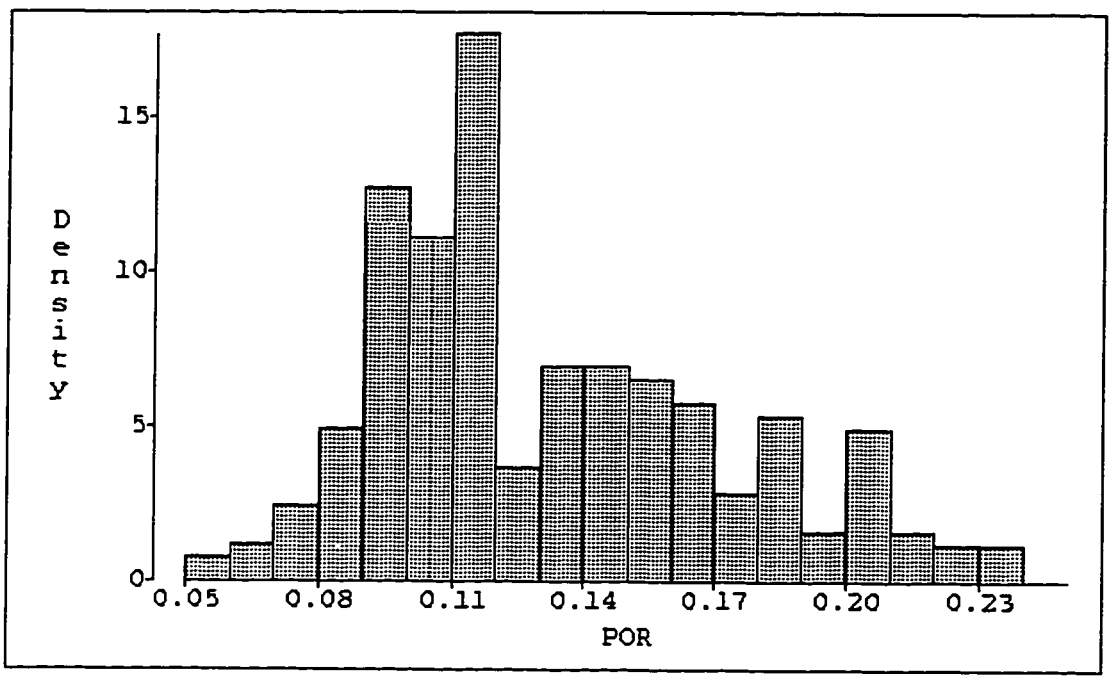


N=243
Mean=0.1279
Std Dev=0.0400

Figure 2-10: Porosity distribution of iron rich sandstone

spatial continuous data because the success of any estimation method depends on how reliable the data is. Thus, scattergram can provide a tool to validate the initial data and help in understanding later results.

Scattergram is plotted between Vsh, porosity, and water saturation (water saturation is derived from resistivity logs). The data for each variable are taken from forty five wells with total number of data for each variable is 2448 samples.

Figure 2-11 shows a scattergram between Vshale and porosity logs. Facies are color coded in the scattergram. The scattergram shows that porosity decreases as the volume of shale increases. It also shows that Very Clean Sandstone facies is the best quality rock since it has the highest porosity and almost no shale.

A scattergram of water saturation and porosity is shown in Figure 2-12 colored by facies. As expected, since SFNC is in the oil zone, water saturation decreases as porosity increase. Again the Very Clean Sandstone facies shows that it is the best quality reservoir rock since it has the least water saturation and the highest porosity.

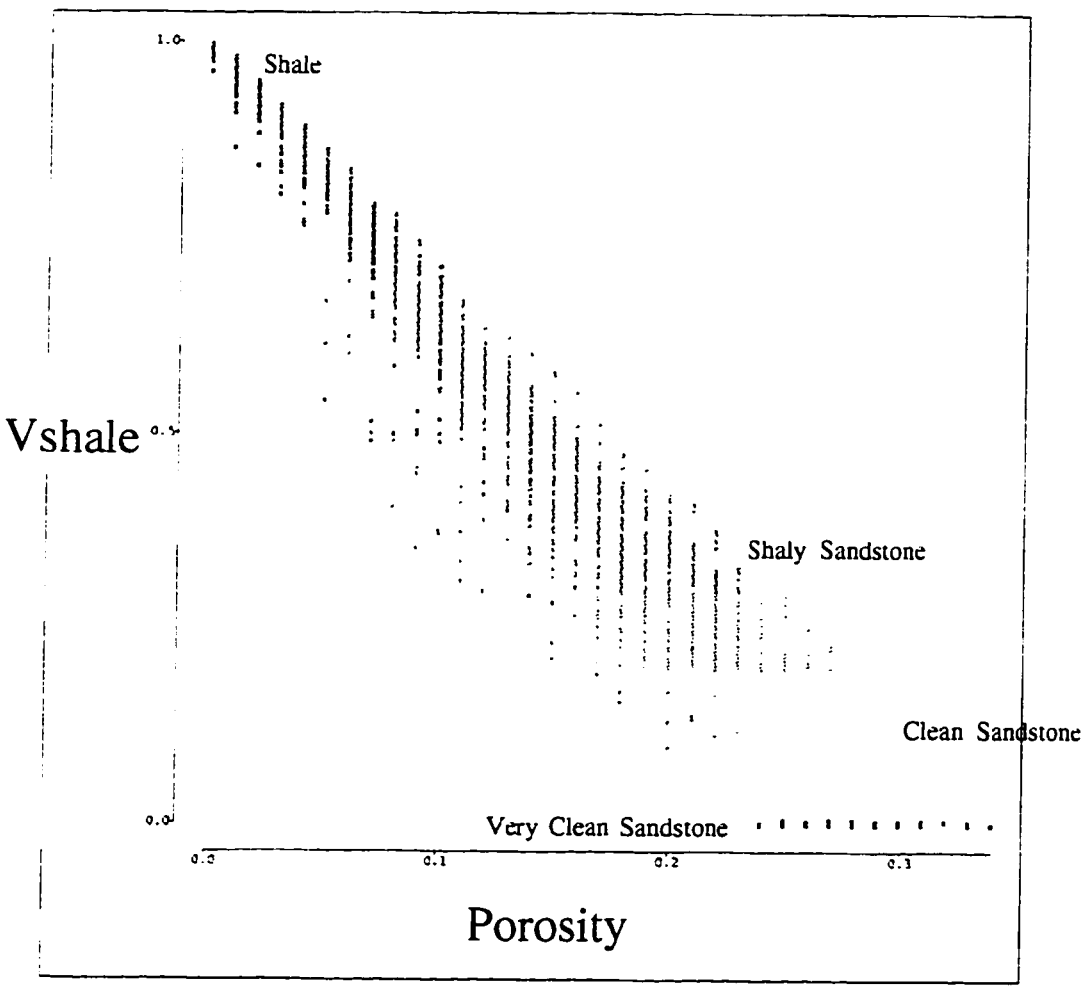


Figure 2-11: Scattergram of Porosity and Volume of Shale; Colors indicate different Lithology

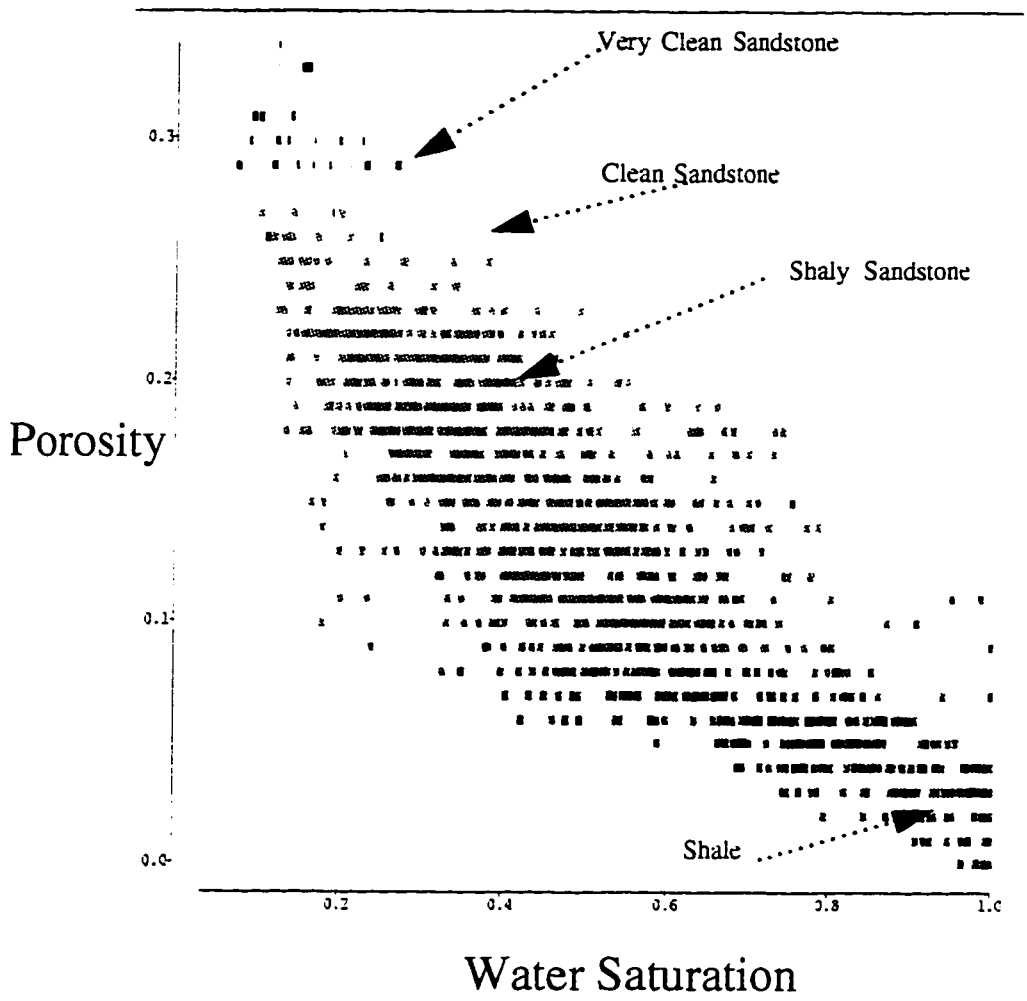


Figure 2-12: Scattergram of Porosity and Water Saturation; Colors indicate different Lithology

## 2.4 The Random Variable Concept

A major feature of geostatistics is the use of the random variable concept. For example, although the distribution of porosity within the reservoir is the results of deterministic processes such as grain configuration, compaction, and other factors such as diagenesis in the case of both carbonates and clastics, those processes are based on some geological and physical mechanisms that are extremely complex. However, this complexity implies that knowledge of porosity at a drilled location does not allow us to predict with full confidence the value of porosity at undrilled location.

Geosatistics recognizes this uncertainty by treating the value at each location as a random variable given that we made some assumptions about the statistical characteristics of the phenomena under study. For example, if the random variable say Z(x) was the value of porosity, then the possible outcomes of this random variable Z(x) would be continuous taking all possible values between zero and some physical maximum value. As a result the probability density function (pdf) of Z(x) called f(x) (see Figure 2-13a) characterizes the probability that porosity falls within an infinitesimal interval (x, x+h). Z(x) can

also be expressed as a cumulative density function. This function which is shown on Figure 2-13b denotes that the random variable Z(x) takes a value that is less or equal to z.

One, however, should not confuse the approaches taken by the non spatial classical statistics and geostatistics. The geostatistical approach always attempts to model the spatial continuity between properties. In fact, geostatistics always assume that the rock properties which are treated as variables result from geological processes that are not independent of one another. This implies that modeling of spatial continuity must be done over a relatively homogeneous area or volume such as a formation within a sedimentary basin.

## 2.5 Spatial Continuity

One striking feature of geostatistics is the use of spatial dependence between data points namely variogram. The spatial continuity is the key to any geostatistical study which is incorporated into any estimation procedures. However, the analysis of spatial continuity in a data set can be very time consuming and frustrating, because it is basically a trial and error procedure

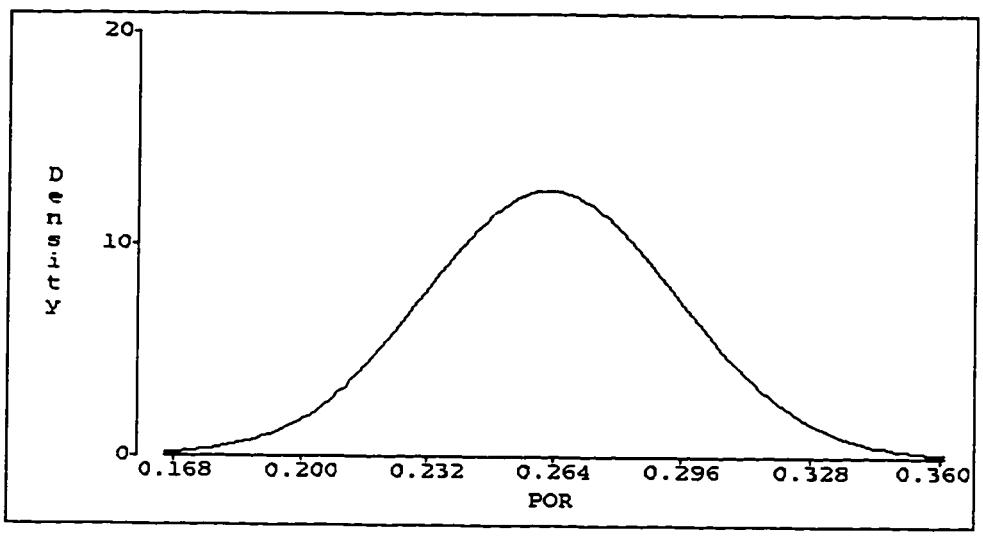


Figure 2-13a: Probability density function (pdf) of porosity

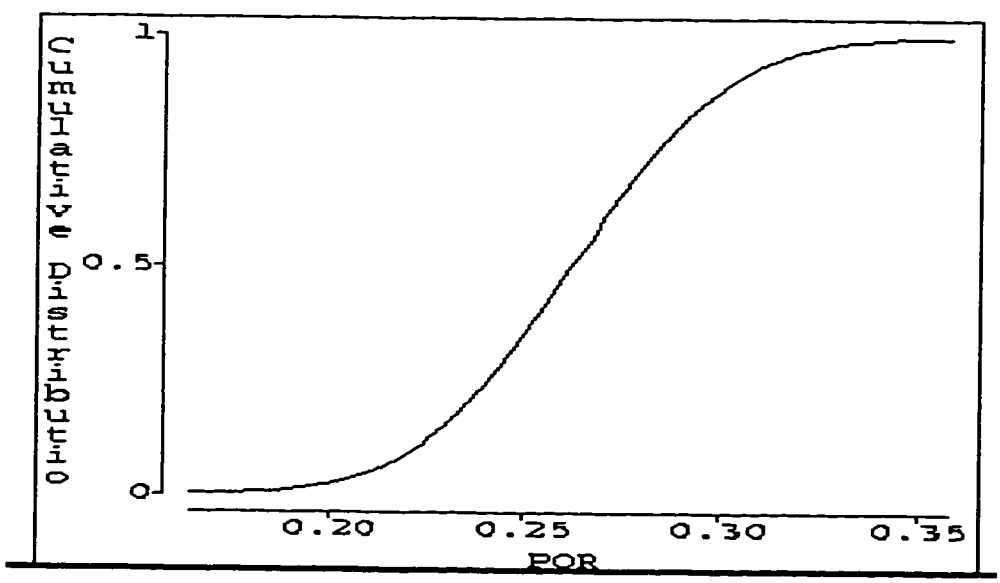


Figure 2-13b: Cumulative density function (cdf) of porosity

which in some cases does not have a solution. Thus obtaining good and representative variograms involves a considerable amount of computations due to the empirical as well as subjective nature of the work.

One simple way to measure spatial continuity is to use h-scattergram. Figure 2-14a shows a schematic cartoon of how four points are plotted on an h-scattergram. For the data configuration shown on Figure 2-14b, an h-scattergram shows all the possible pairs of data value whose locations are separated by a certain direction and lag distance. The shape of the cloud of points on an h-scattergram tells us how continuous the data values are over a certain distance in a particular direction. For example, when the points separated by zero distance are plotted ,we notice that all the points fall on the 45-degrees line meaning that there is no variability at this lag distance. However, as we increase the lag distance to 100 meters in the west to east direction, as shown in Figure 2-15, we notice that the cloud of points gets deviated from the 45-degree line. Looking at the h-scattergrams in Figure 2-15, we notice that the cloud of data points gets fatter as the points spread out away from the 45 degree line to a point where we see a large cloud over the 45-degree line no matter how the distance increases. It is also noticed from the

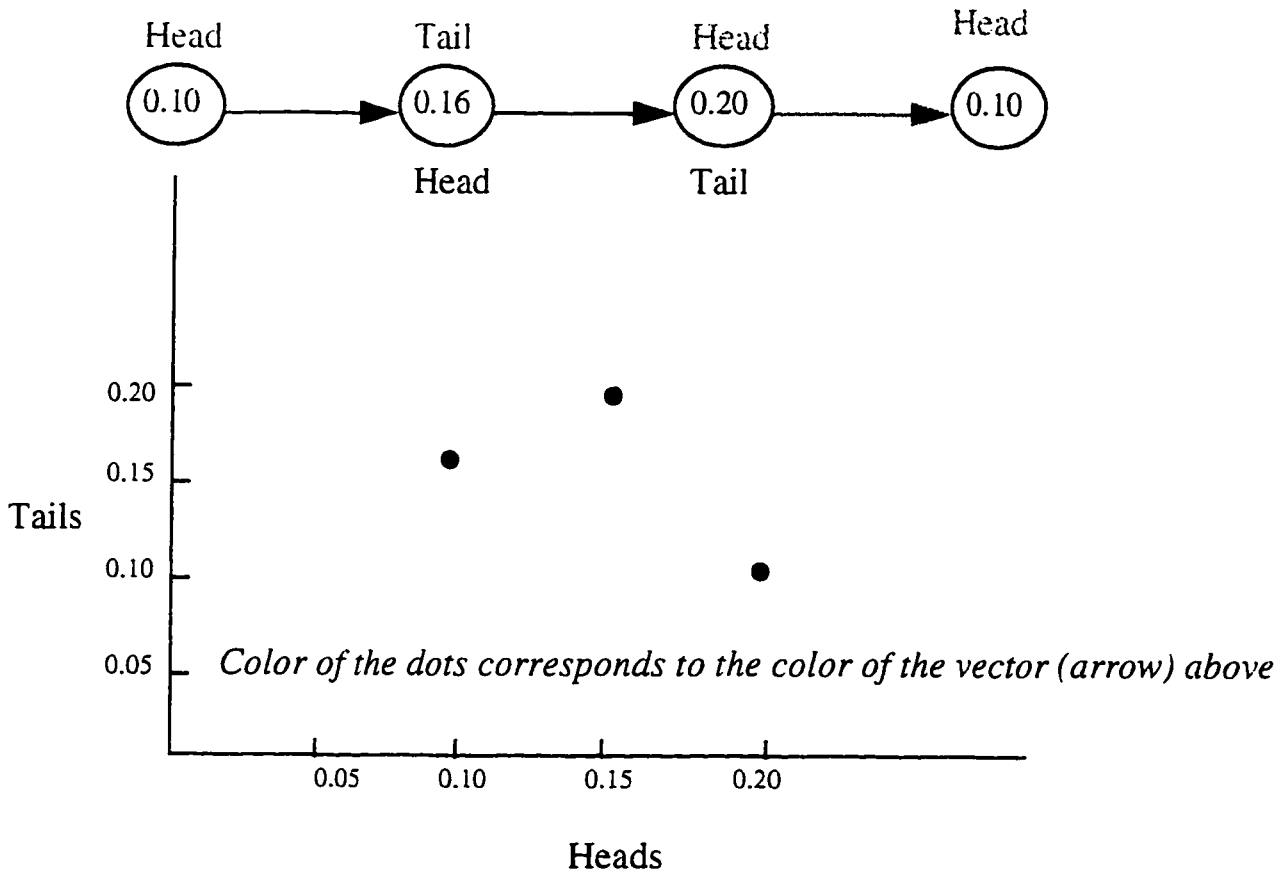


Figure 2-14a: H-scattergram is defined by both distance and direction. The direction is denoted by head and tail; i.e.. vector.

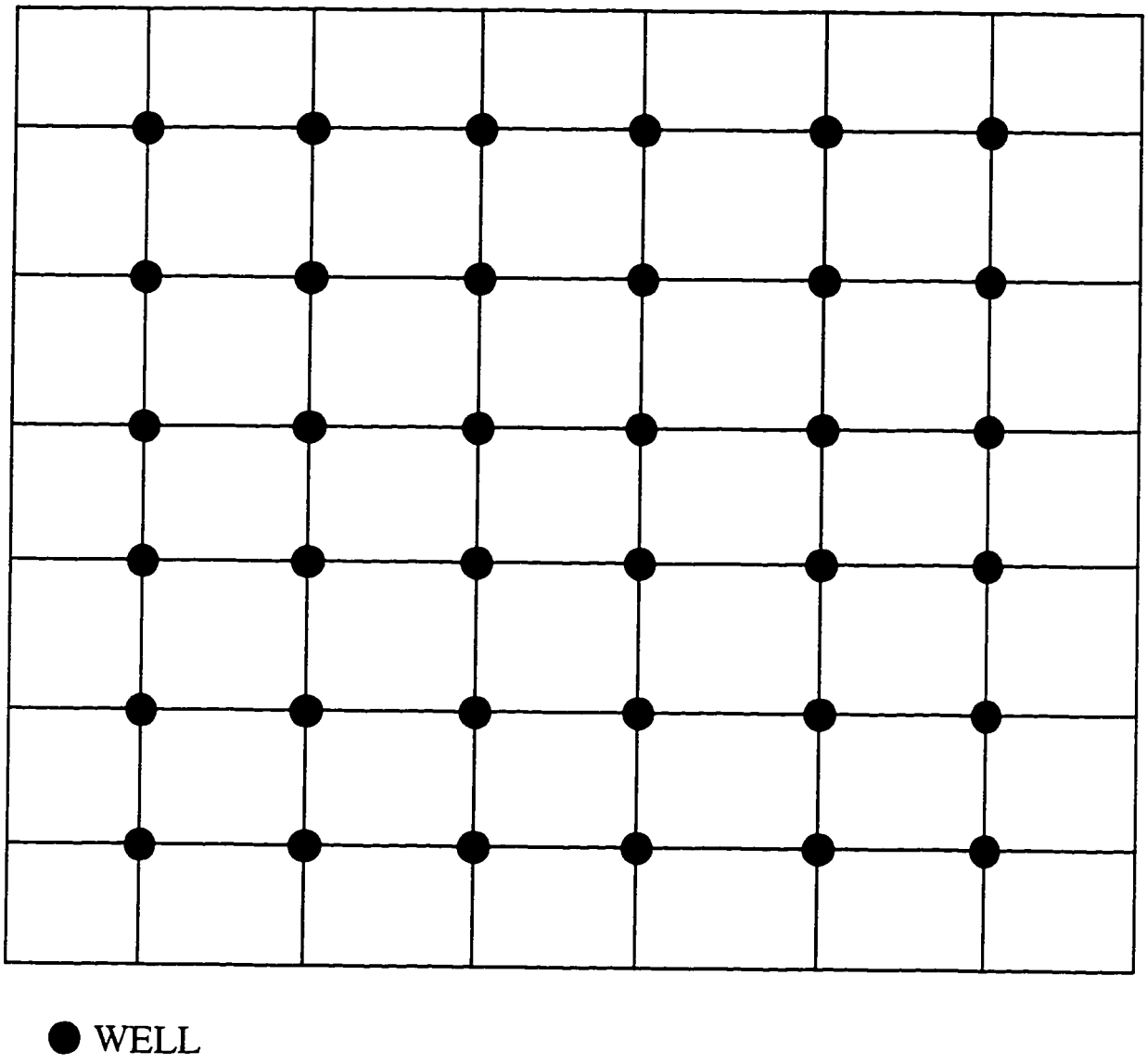


Figure 2-14b: An example of data configuration

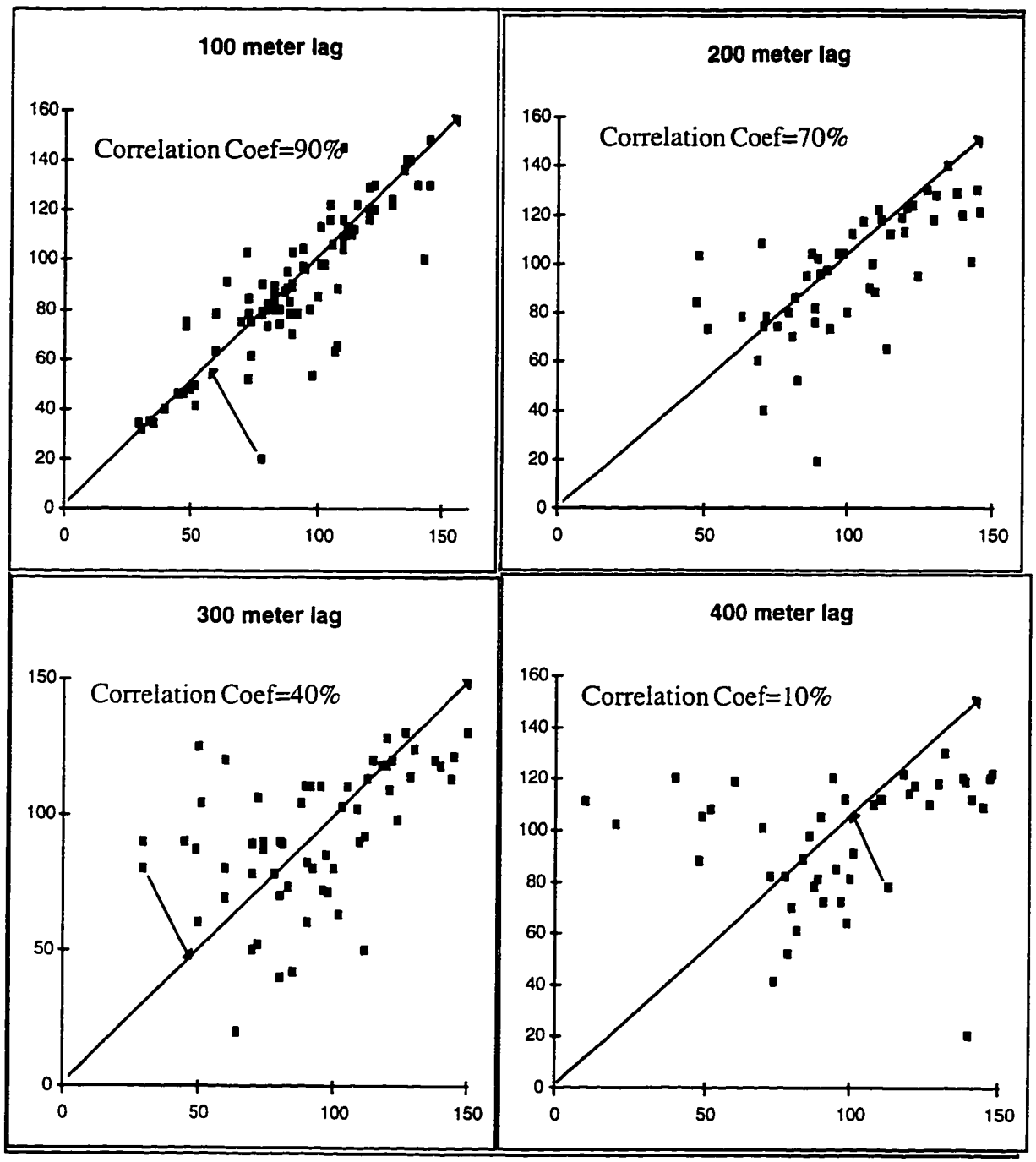


Figure 2-15: Scattergrams showing clouds get bigger as distance increases

statistics of each scattergram that the correlation coefficients decrease as the lag distance increases. As expected, the correlation coefficient decreases and is therefore a useful index for our earlier impression that the cloud of points is getting fatter. If we plot the correlation coefficient of an h-scattergram against its corresponding h value (lag distance) then a correlogram is produced. Correlogram is one measurement of spatial correlation but there are several functions used to measure the spatial correlation including semivariogram, and covariograms. However, in practice, a semivariogram (also called variogram) is calculated instead as a measure of spatial continuity.

**Calculating The Experimental Variogram**

Theoretically, semivariogram, $\gamma(h)$ is defined as half of the expectation of random variable $[Z(x) - Z(x+h)]^2$

$$\gamma(h)= 0.5E[Z(x) - Z(x+h)]^2$$

However, in practice, we compute $\gamma(h)$ from available data by using the following formula:

$$\gamma(h)= \frac{\sum_{i=1}^{N(h)}[Z(x_i+h)-Z(x_i)]^2}{2N(h)}$$

Where Z(x) and Z(x+h) are sample values at points x and x+h respectively. N(h) is the total number of sample pairs separated by h distance.

The following is a simple way to calculate a variogram:

1-Select a value for h (lag distance).

2- Count all pairs separated by h.

3- Calculate sum of squares of differences between the counted pairs.

4- Divide the sum of squares of differences by twice the total number of pairs to get $\gamma(h)$.

5- Select other values of h and repeat the steps from 1 to 4.

6- Plot $\gamma(h)$ against h.

The experimental variogram usually increases as the separation distance between pairs increases. However, after a certain separation distance this is no longer true. The variogram flattens out or at least exhibits a significant change in slope. The distance at which this occurs is referred to as the Range and the value of the variogram at that distance is called the Sill. An ideal shape of the variogram is shown on Figure 2-16.

The previous steps on how to calculate a variogram would produce an isotropic variogram. However, assuming that an acceptable isotropic

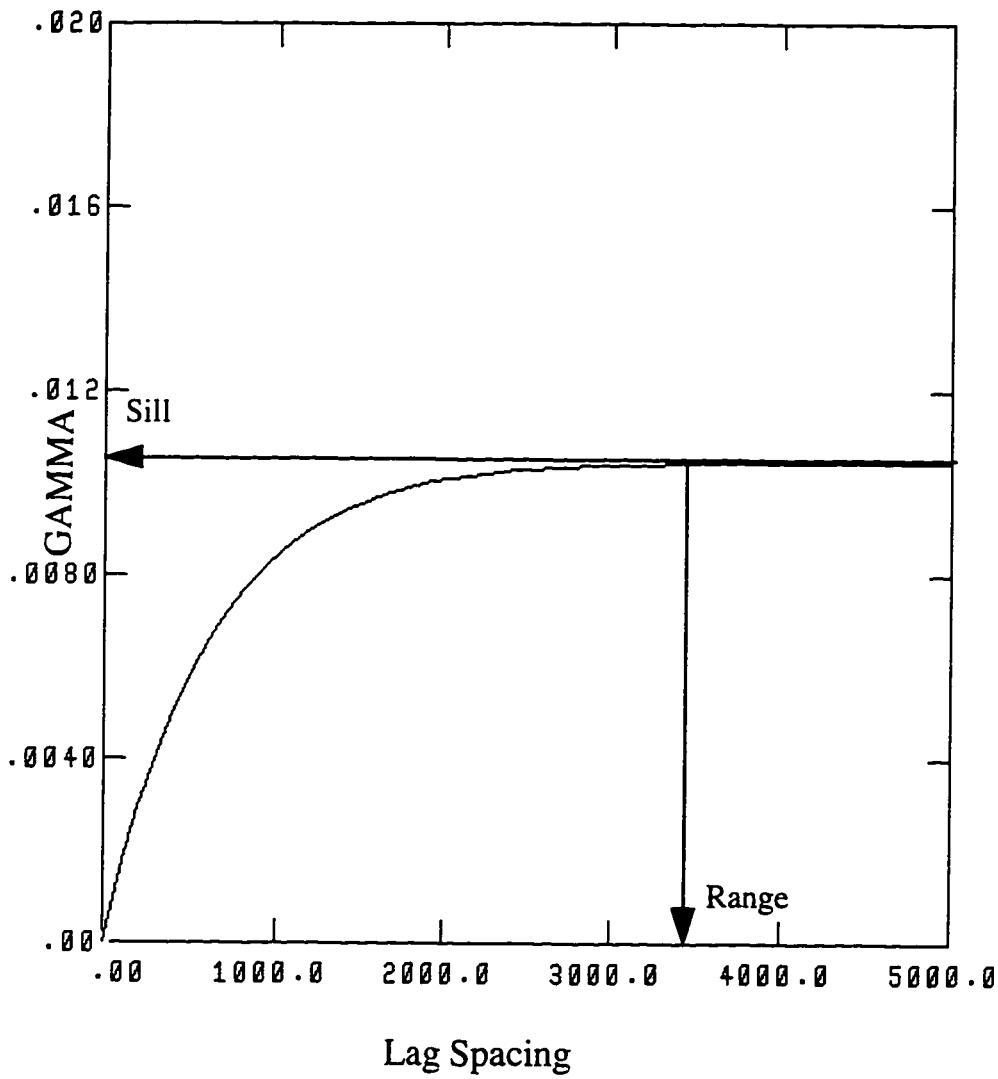


Figure 2-16: An ideal variogram shape.

variogram has been calculated, the final step in the variogram analysis involves determining if any directional anisotropies are present. This is accomplished by calculating variograms in several directions. As a result, the lag distance separation parameter h becomes a vector with magnitude and direction. In addition to direction, an angular tolerance needs to be specified when calculating a directional variogram for non-aligned data. The major advantage of calculating directional variograms is the capturing of any major directional anisotropy.

### Modeling The Experimental Variogram

Experimental variograms provide a discontinuous series of values calculated for a specific set of lag values and directions. However, geostatistical estimation methods such as Kriging, which will be introduced in Chapter 3, require variogram values for any possible separation vector. As a result, if any geostatistical interpolation technique is to be performed as part of a geostatistical analysis of the data, the experimental variogram must be modeled as a continuous vectorial function.

***Variogram Modeling***

A variogram model has two main characteristics; its behavior near the origin and the presence or absence of the sill. Thus, the most commonly used variogram models are divided into two categories:

**A) Models With a Sill (also called Transition models)**

**1-Spherical Variogram Model**

$$\delta\gamma(h)=C[(3h/2a)-0.5(h/a)^3] \qquad 0<=h<a$$

**Or** $\delta\gamma(h)=C$ $\qquad a<=h$

C=sill ,a=range

This variogram model is close to a line in shape near the origin (Figure 2-17). The model is said to be transitive because it reaches a finite sill at a finite range. The tangent of this variogram model at the origin intersects the sill at Two-thirds of the range.

**2-Exponential Variogram Model**

$$\delta\gamma(h)=C[1-\exp(-h/a)]$$

This model approaches the sill asymptotically(Figure 2-17). A practical definition of the range is the distance a, where the variogram is

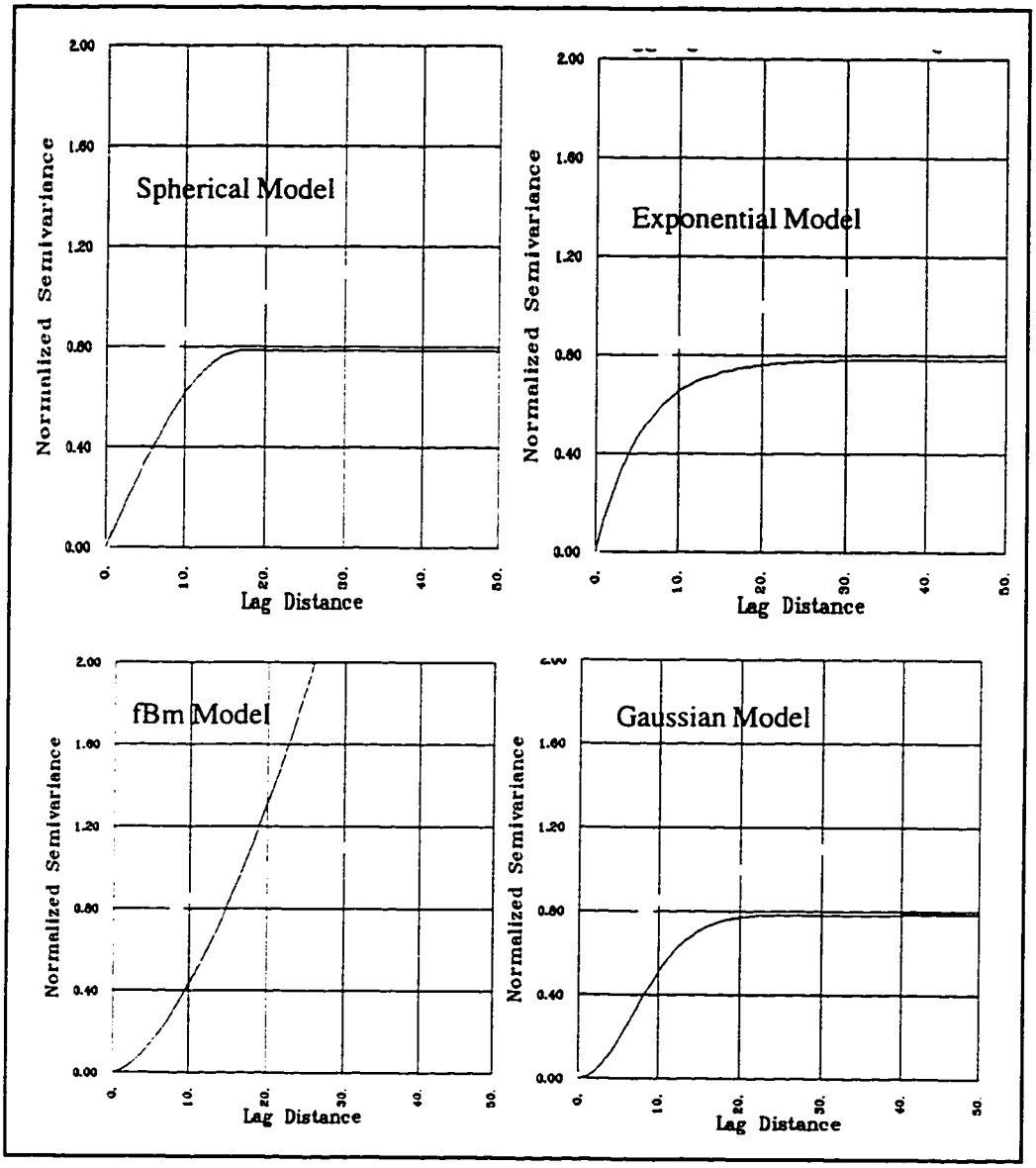


Figure 2-17: Four types of variogram models

0.95C. Geometrically, a tangent at the origin intersects the asymptotic C at lag a/3.

The difference between the spherical and the exponential models is the distance, r, at which their tangents at the origin intersect the sill.

r=2a/3, two third of the range for spherical model

r=a/3, one third of the range for the exponential model

Thus the spherical model reaches its sill faster than the exponential model.

**3-Gaussian Variogram Model**

ðγ(h)=1-exp(-3h2/a2)

The Gaussian model is considered as a transition model for those phenomena which are extremely continuous. The range is considered to be the distance **a**, for which the variogram value is 95% of the sill. The sill is reached asymptotically and the model has a parabolic shape near the origin as shown in Figure 2-17.

### B) Models Without a Sill (also called Non-Transition models)

These models are power function-like in shape because they don't reach a sill and they are considered as non transition.

$\delta(h)=|h|$

Most topographical surfaces such as structure of a marker is well approximated by a class of functions called "fractional Brownian motion", or fBm which has a power law variogram. Measurements of horizontal distributions of variety of soil, outlines of islands and continental coastlines show that they have variograms of this type.

### Fitting The Model

Once a specific model has been chosen, all what remains is fitting it through the experimental variogram. The criteria of choosing the theoretical variogram to fit the experimental variogram is based on few factors such as, for example, the overall shape of the experimental variogram and the phenomena under study ( for example transition variogram models would fit lithology and porosity, where non-transitional variogram would fit structural surfaces). Once

the model is chosen, all what remains is fine tuning of the model, which can be accomplished by varying one of its parameter such as the range and/or the sill.

## 2.6 Geological Characteristics Revealed by Variograms:

In most cases the experimental directional variograms would reveal major changes in the sill or the range as the direction changes. The rate at which the variogram rises toward the sill is a function of a continuity of the property under study. When this rate changes with direction while the sill remains relatively constant, then this phenomena is called Geometric Anisotropy. Another type of anisotropy is called Zonal Anisotropy where the sill changes with direction while the range remains relatively constant. However, the anisotropy found in real life is a mixture of the two types.

Once the axes of a geometric anisotropy have been identified, the theoretical model chosen needs to be adjusted so that it describes how the experimental variogram changes with distance and direction. This is accomplished by first modeling the directional variogram and then defining a transformation that reduces these models into one common model given that they belong to the same type of theoretical variogram.

## 2.7 Experimental Variogram of Safaniya Field:

### SFNC Top Variogram

The directional variograms of the SFNC Top show a trend exists for the depth of the SFNC Top. It shows that SFNC has less continuity from northwest to southeast and a long continuity in the northeast and southwest directions. Figure 2-18 shows an ellipse drawn from the two main directions showing a longer range in the northeast direction of about 4000 meters and a smaller range of 2000 meter in the northwest direction.

### SFNC Base Variogram

Directional variograms of SFNC Base have been calculated in two different directions (Figure 2-19). They show almost the same ranges as those of SFNC Top.

Directional variograms have been calculated for the rest of the variables of rock facies and their properties. Unfortunately, they did not show any directional trend. An example of directional variogram for one of the properties (porosity) is shown in the next section.

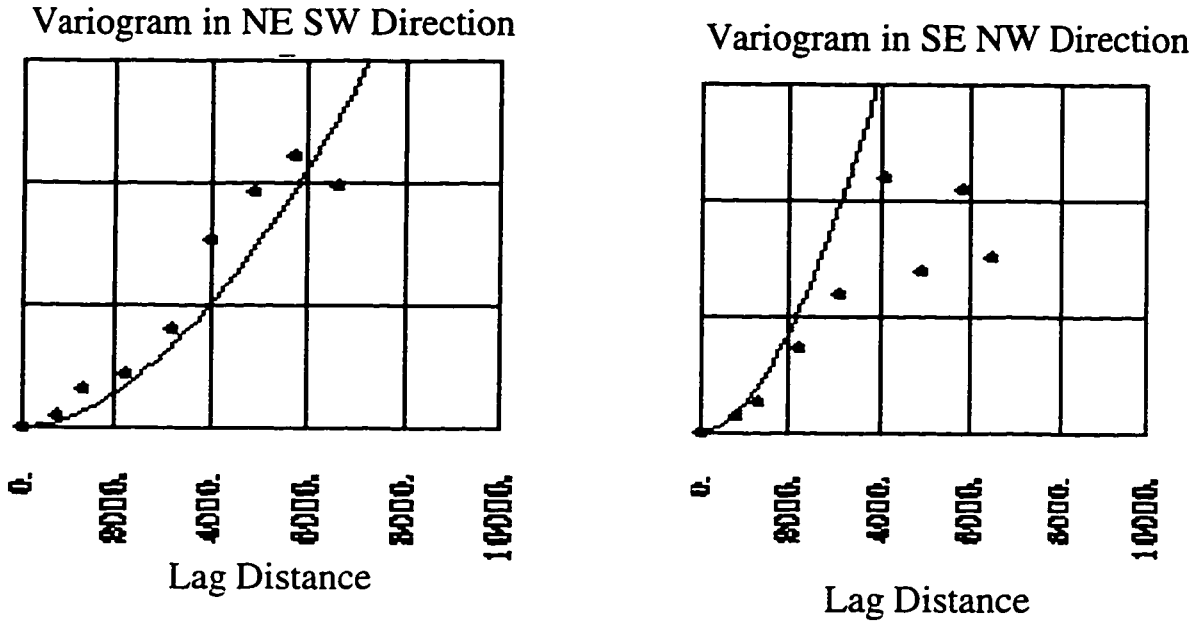


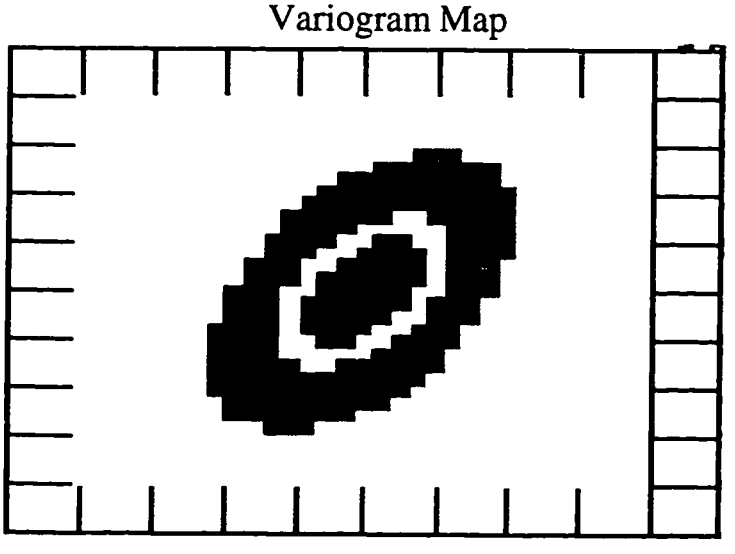


Figure 2-18: Directional variogram of top SFNC.

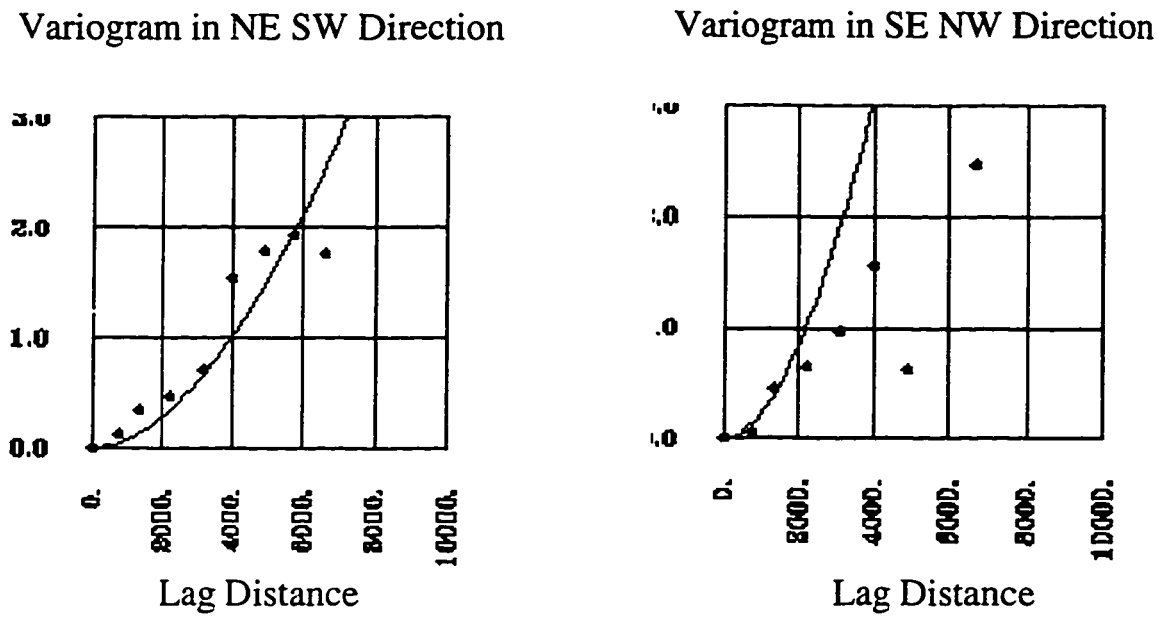


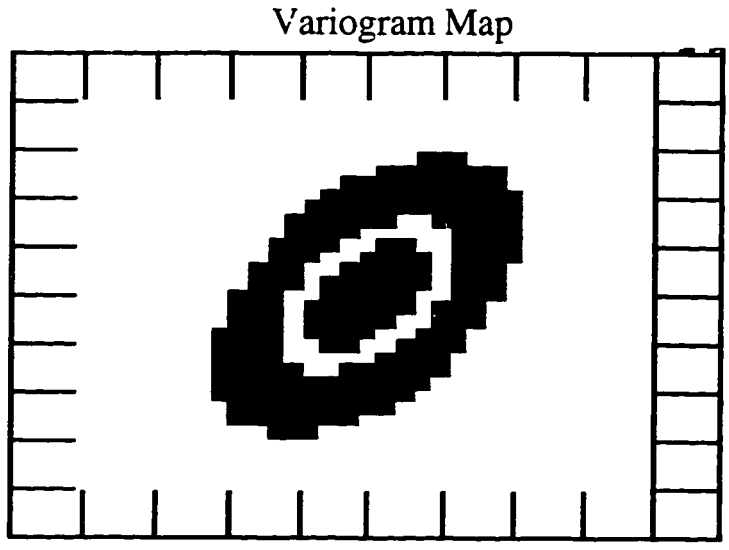


Figure 2-19: Directional variogram of base SFNC.

One can justify the presence of a directional trend for the structures of both the top and base of SFNC Sequence and the absence of a directional trend for the properties by the following:

1- Deposition of SFNC Sequence occurred before any structural reactivation of SFNC Sequence producing the current structural configuration of SFNC Sequence.

2- The forty five wells available to this study is not enough to capture a directional trend if any of SFNC Sequence.

3- The area of interest for this study is not large enough to capture directional trends of the large features of the depositional environment of this sequence.

**Porosity Variogram**

Horizontal directional variograms of porosity have been calculated in eight different directions (Figure 2-20). No directional trend seems to exists. However, Figure 2-21 shows an isotropic variogram of porosity with a range of 1500 meters. It can be concluded that this property has no directional trend at least with the number of wells which are available. However, Figure 2-22 shows a bell shaped vertical variogram of porosity. This bell shaped is due to

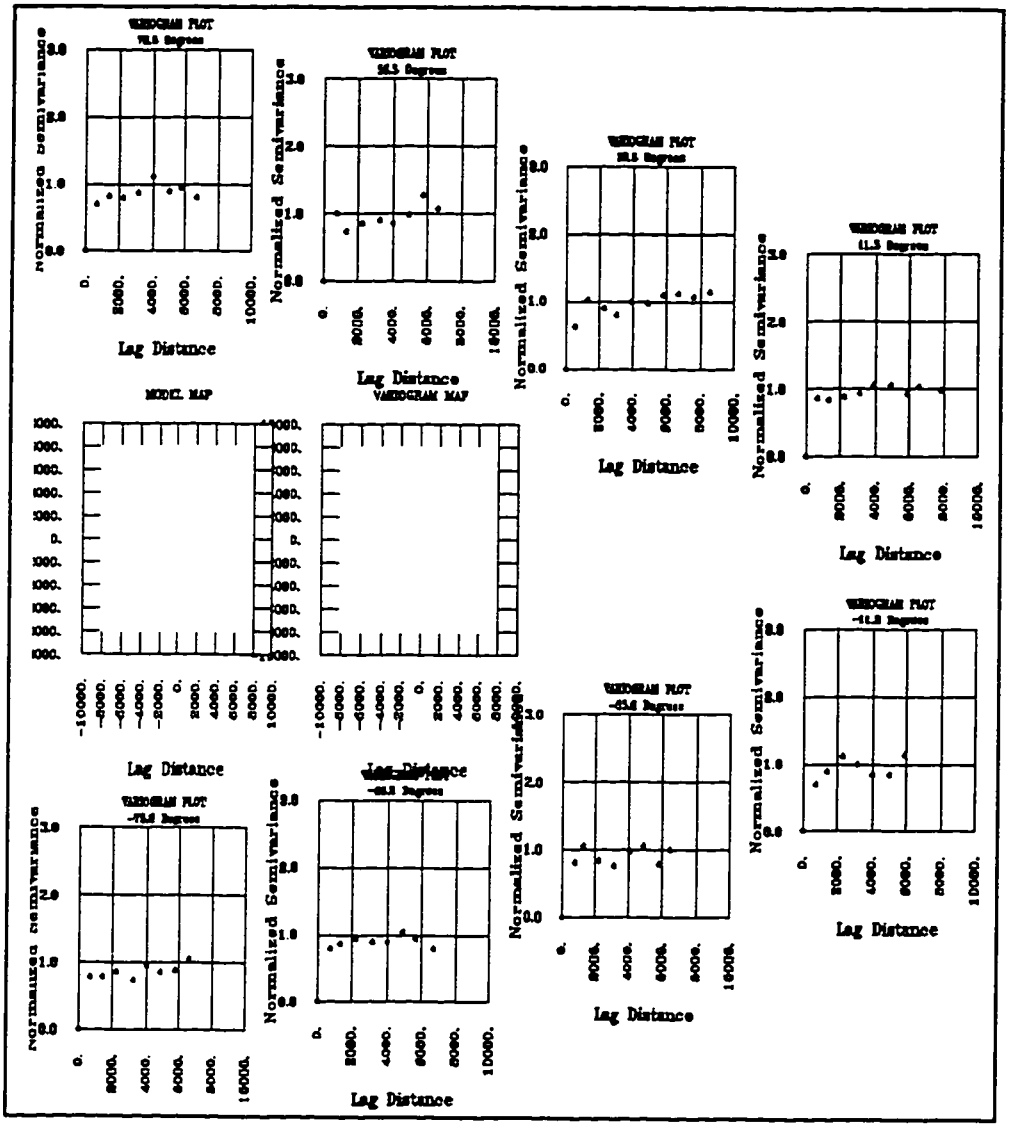


Figure 2-20:Dircetional variogram of porosity.

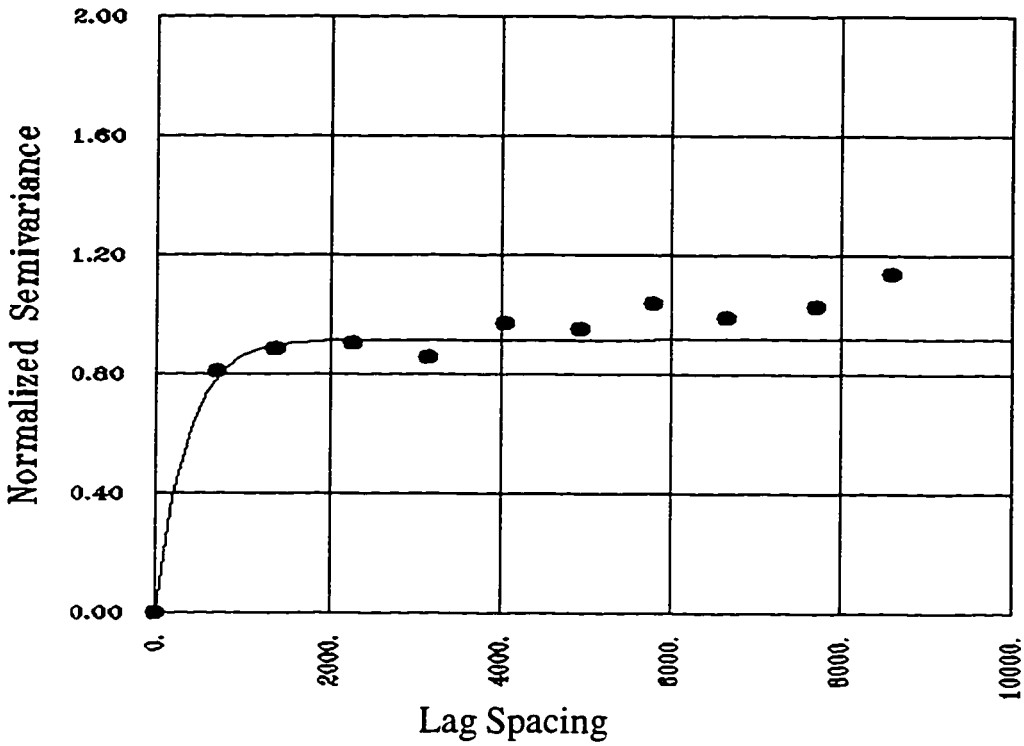


Figure 2-21: Isotopic variogram of porosity

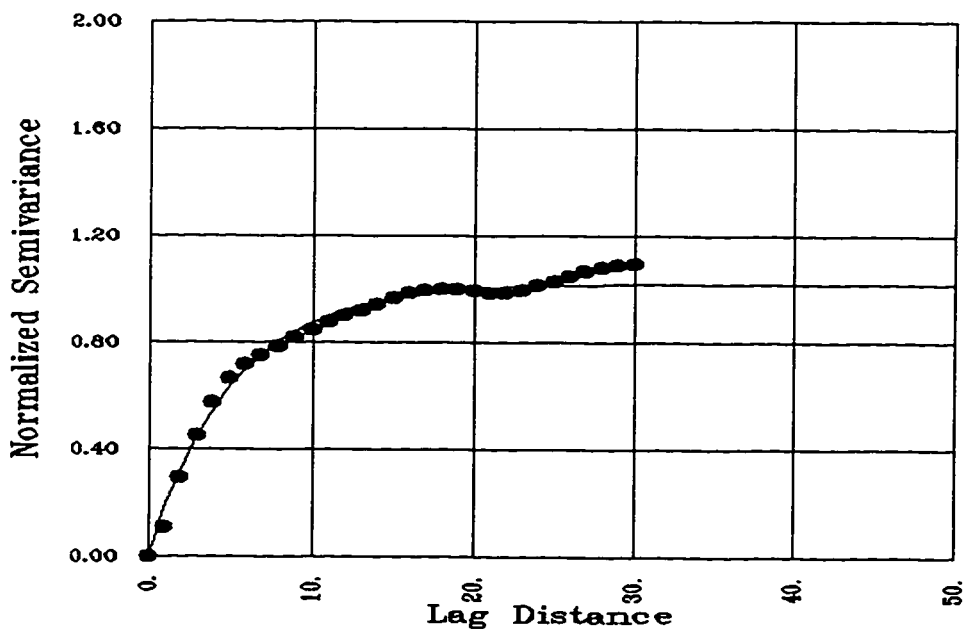


Figure 2-22: Vertical variogram of porosity

the well aligned and regular sampling of the data. The vertical range of the porosity does not exceed 10 ft.

### Volume of Shale (Vsh) Variogram

Traditional isotropic horizontal variogram of the volume of shale data (Figure 2-23) indicates that there is no horizontal correlation for volume of shale values beyond 1238 meters. Vertical variogram shows a continuity of about 20 ft. in the vertical direction as shown on Figure 2-24.

### Water Saturation (Sw) Variogram

Isotropic variogram in the horizontal direction of Swi has been calculated (Figure 2-25). The experimental variogram has been fitted with an exponential variogram with a range of about 2000 meters. Figure 2-26 shows a vertical variogram of the Sw with a range of about 19 ft.

## Indicator Variograms

So far, variograms have been calculated and modeled for continuous variables such as porosity and Vsh. However, variograms can also be calculated for categorical variables such as those of rock facies types. This is basically done by transforming the categorical data into binaries of 0's and 1's

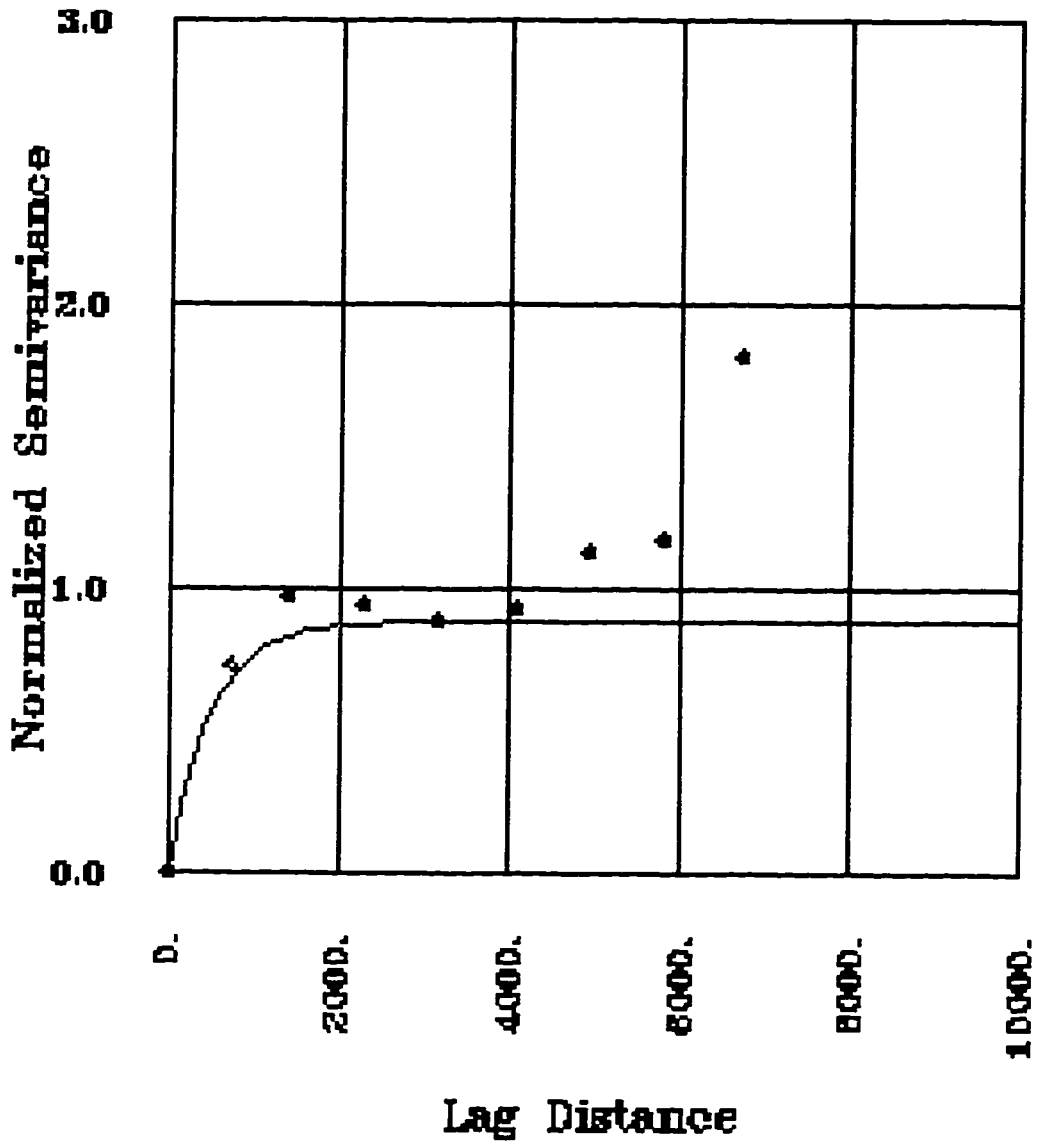


Figure 2-23:Isotropic variogram of vsh

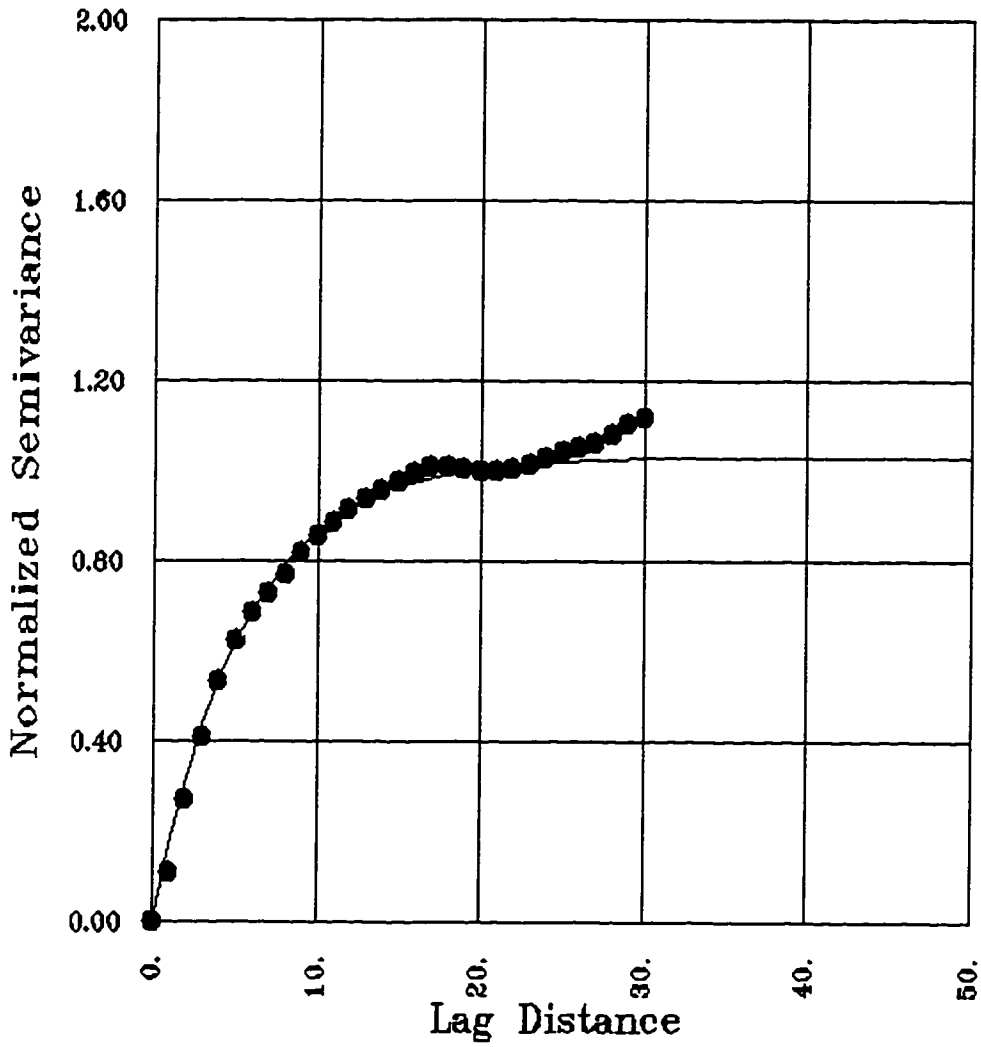


Figure 2-24: Vertical variogram of vsh

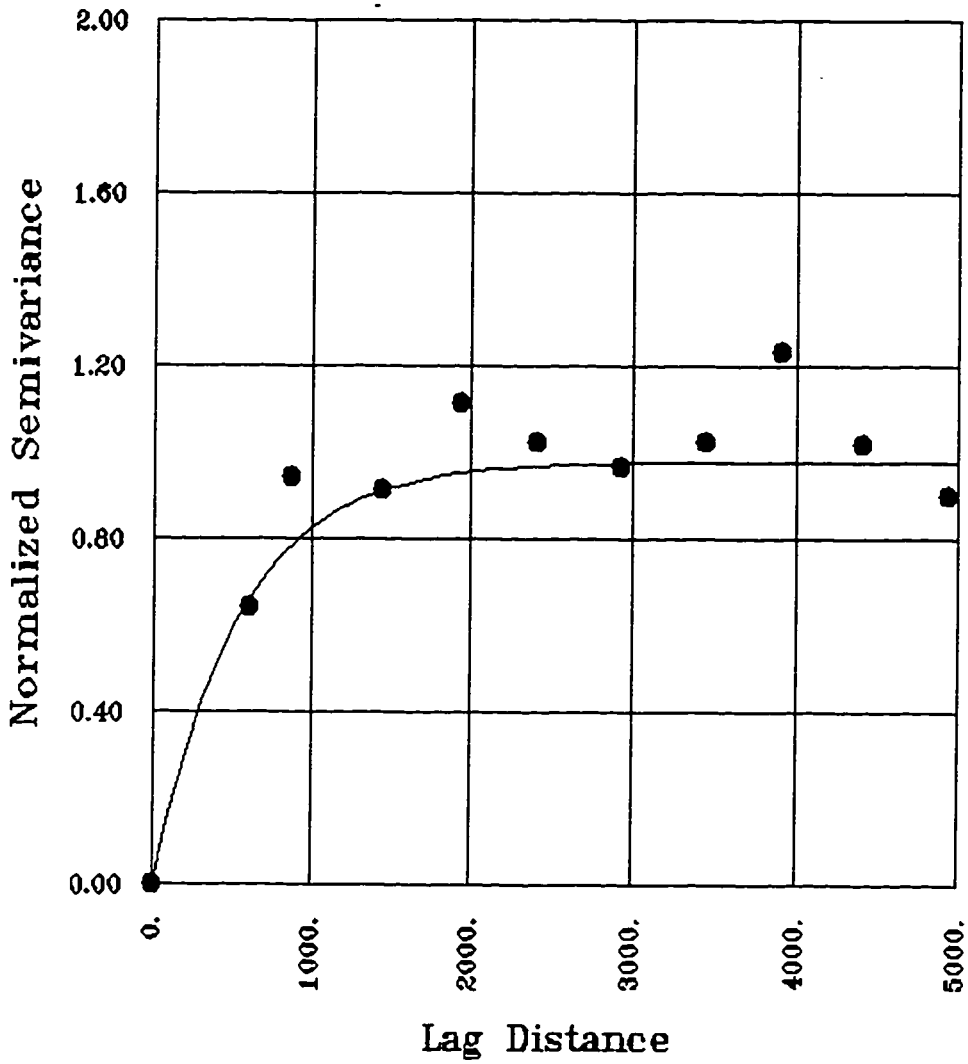


Figure 2-25: Isotropic variogram of Sw.

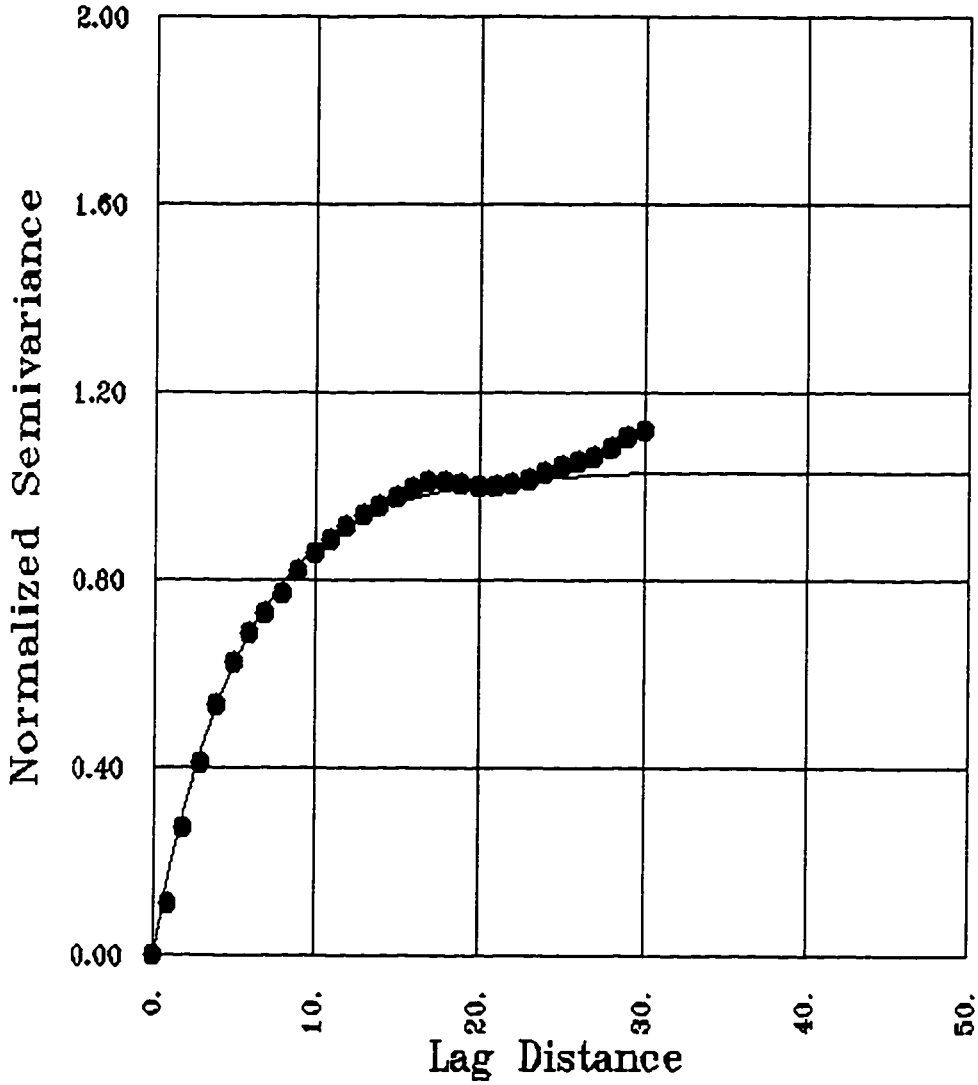


Figure 2-26:Vertical variogram of Sw.

for each category (or a particular rock facies). An indicator variogram is then calculated for each category or a particular facies. A one would be assigned to a sample location if its value is similar to that of the predefined facies or category otherwise the sample location is assigned to zero. Therefore, if there are eight different facies to be modeled, then eight indicator variograms are required. Indicators will be more thoroughly explained in the next chapter.

**Indicator Variograms of Lithofacies**

**Shale Facies Variogram**

An isotropic horizontal variogram has been calculated for the shale facies (Figure 2-27). The experimental variogram has been fitted with a spherical model showing a range of about 1700 meters. A vertical variogram calculated for the shale shows a range of about 4 ft. (Figure 2-28). From both horizontal and vertical variograms, it can be concluded that the shale look like three dimensional bodies which have 1700 meters in length and width and a thickness of about 4 ft. This information about the size of these facies would help in later stages when we start distributing the facies spatially in the modeling process.

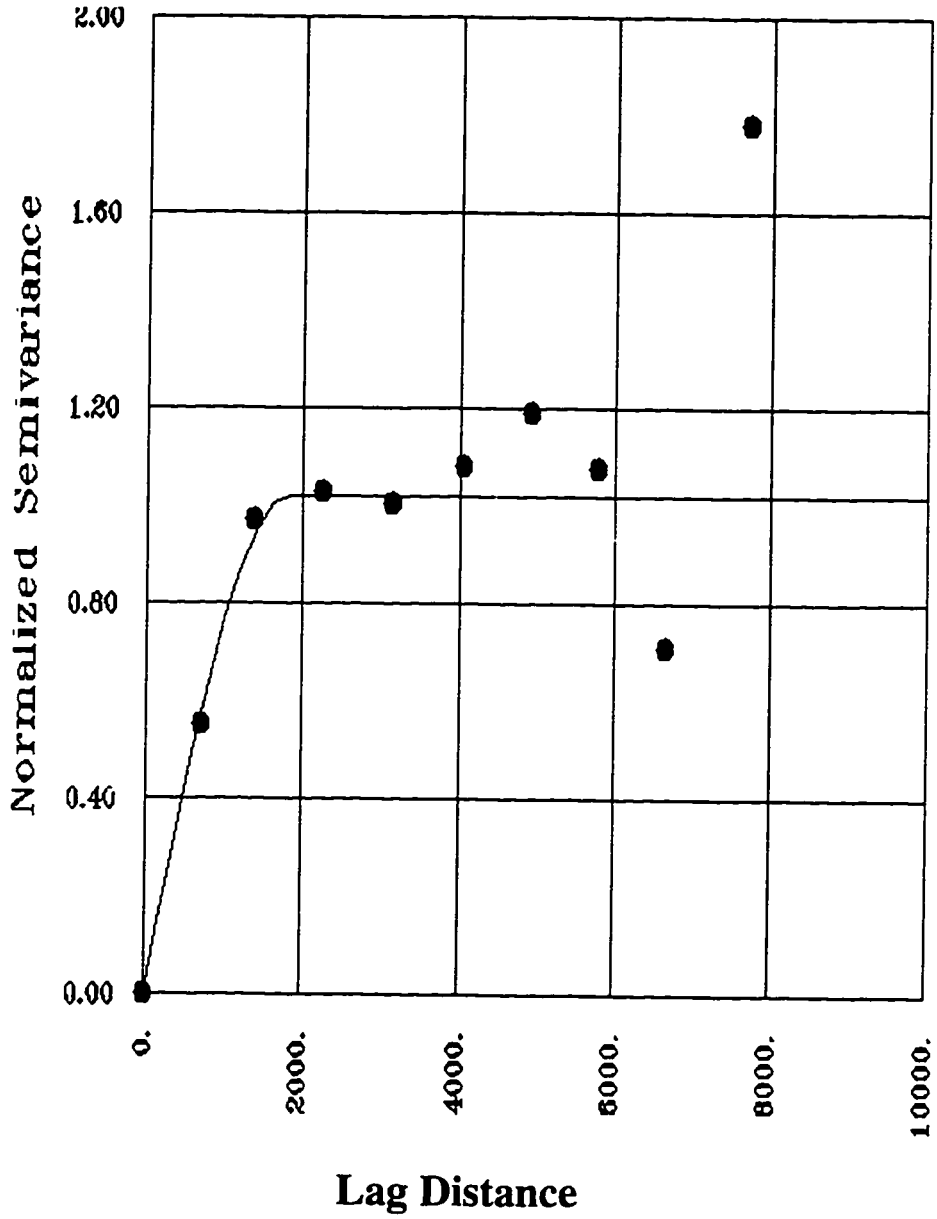


Figure 2-27: An isotropic variogram of shale facies.

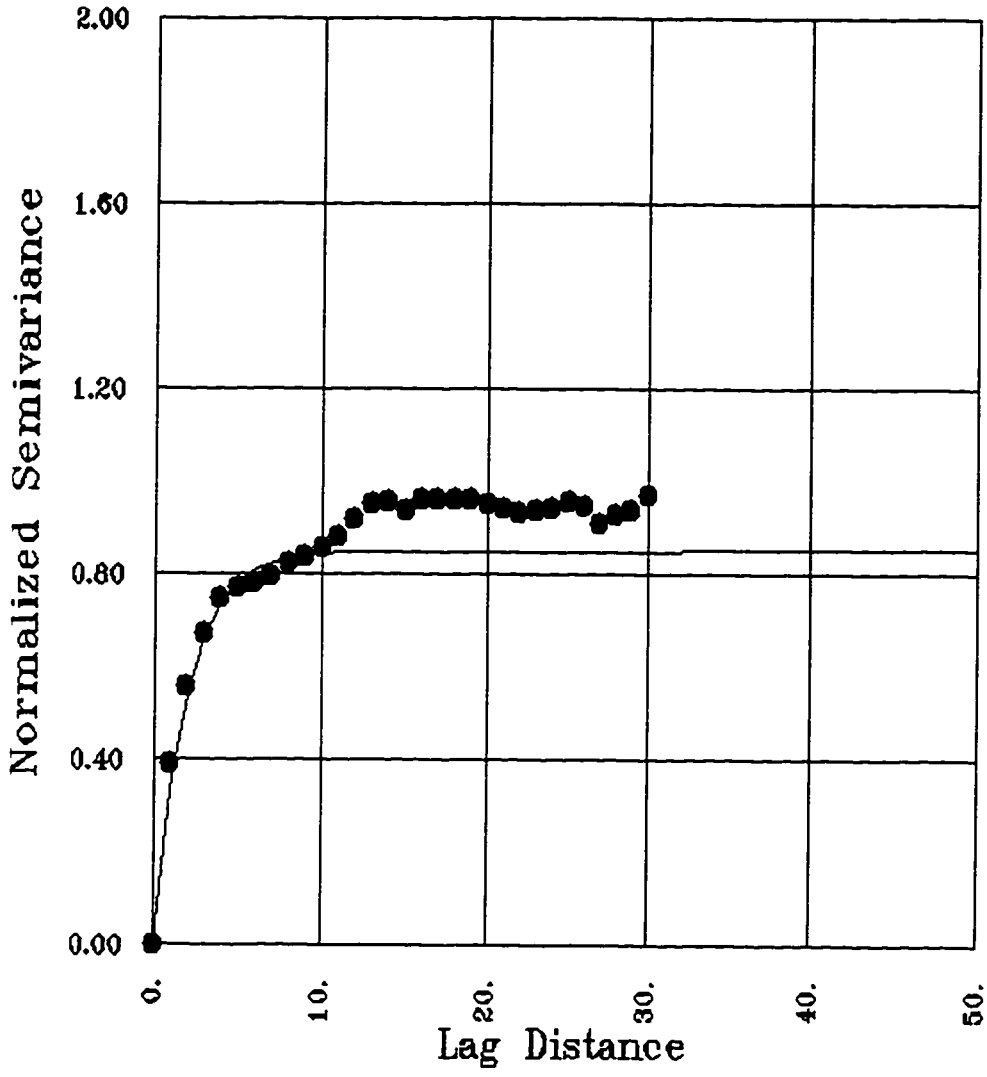


Figure 2-28: Vertical variogram of shale facies

### Very Shaly Sandstone Facies Variogram

Figure 2-29 shows a horizontal variogram of this facies. It shows a similar range as the one for shale facies of about 1600 meters. The vertical variogram shows a vertical range of about 4 ft. as shown on Figure 2-30.

### Shaly Sandstone Facies Variogram

A bell shaped isotropic variogram is shown on Figure 2-31 for the shaly sandstone facies. It shows that it has a relatively longer horizontal range than the previous facies of about 2000 meters. The vertical variogram shows a range of about 3 ft. (Figure 2-32).

### Iron Rich Sandstone Facies Variogram

The horizontal variogram (Figure 2-33) of this facies shows a relatively small horizontal range of about 1067 meters. The vertical variogram shows a range of about 3 ft. as shown on Figure 2-34.

### Clean Sandstone Facies Variogram

An isotropic horizontal variogram of this facies (Figure 2-35) shows that the clean sandstone facies has long horizontal range of about 2100 meters.

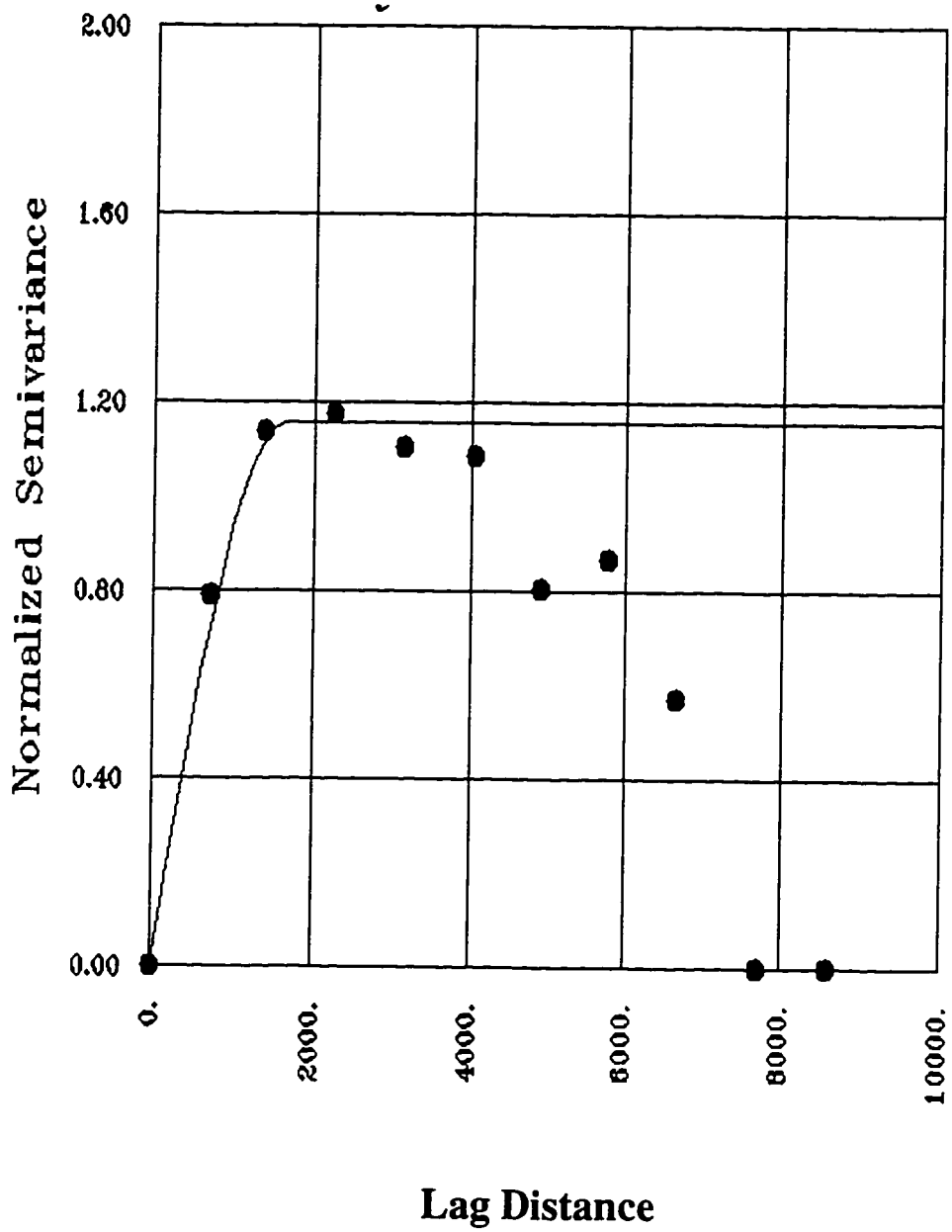


Figure 2-29: An isotropic variogram of very shaly sandStone facies.

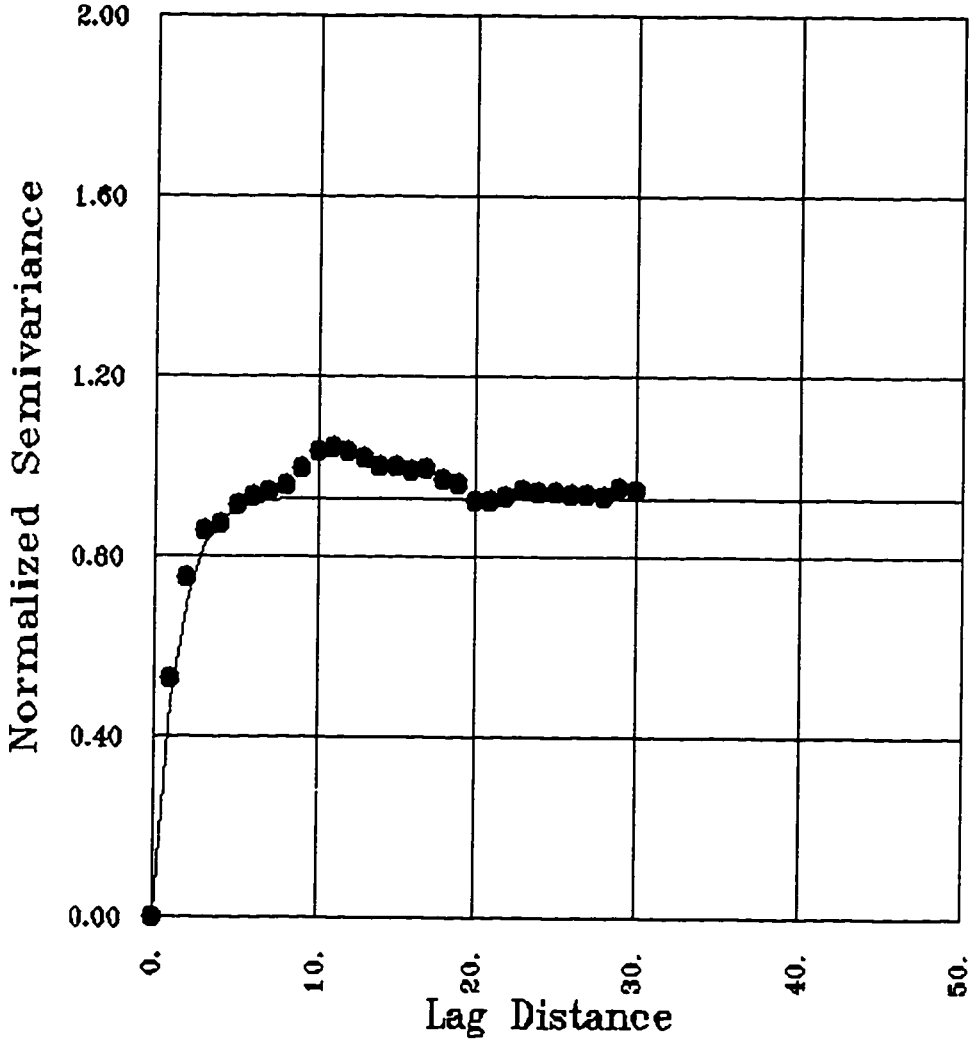


Figure 2-30: Vertical Variogram of Very Shaly Sandstone Facies

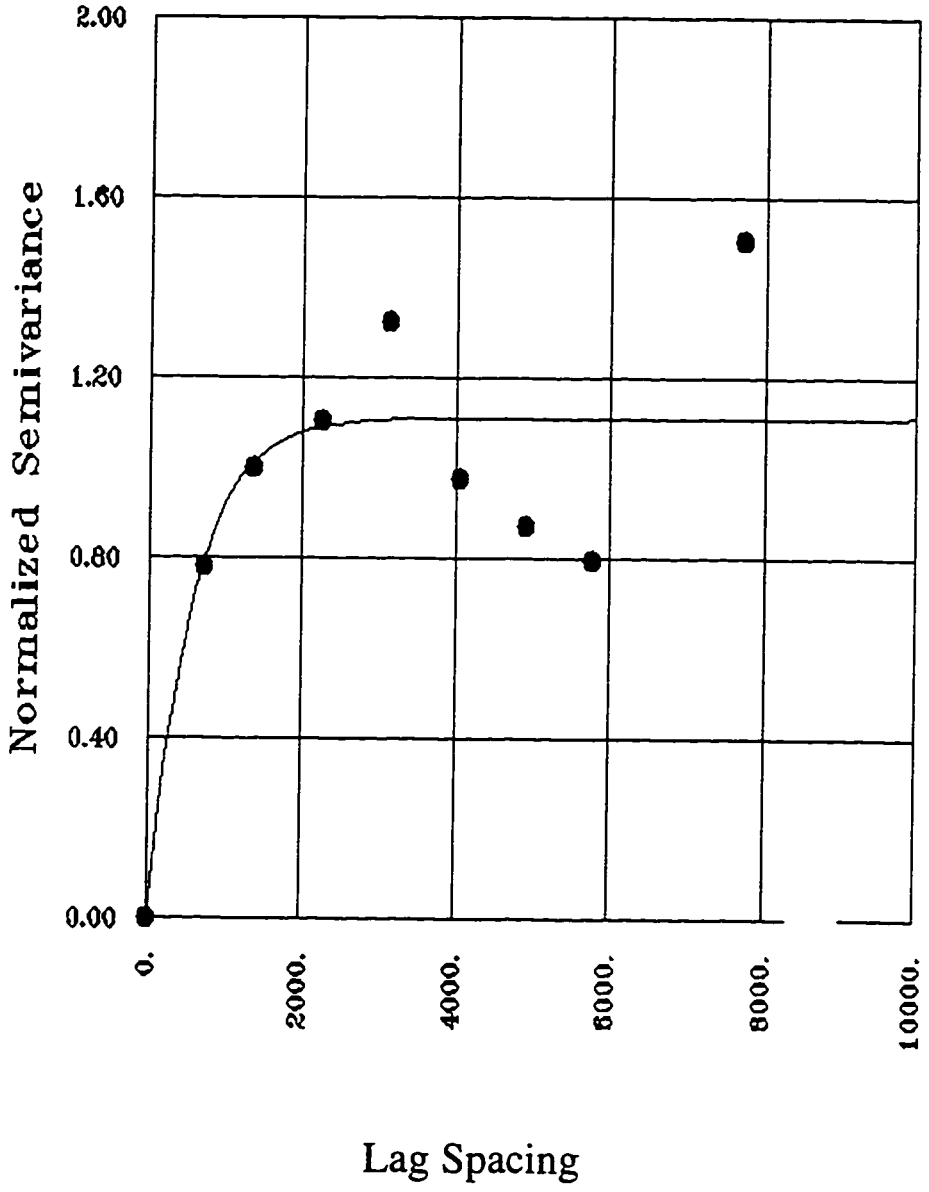


Figure 2-31: An isotropic horizontal variogram of shaly sandstone facies

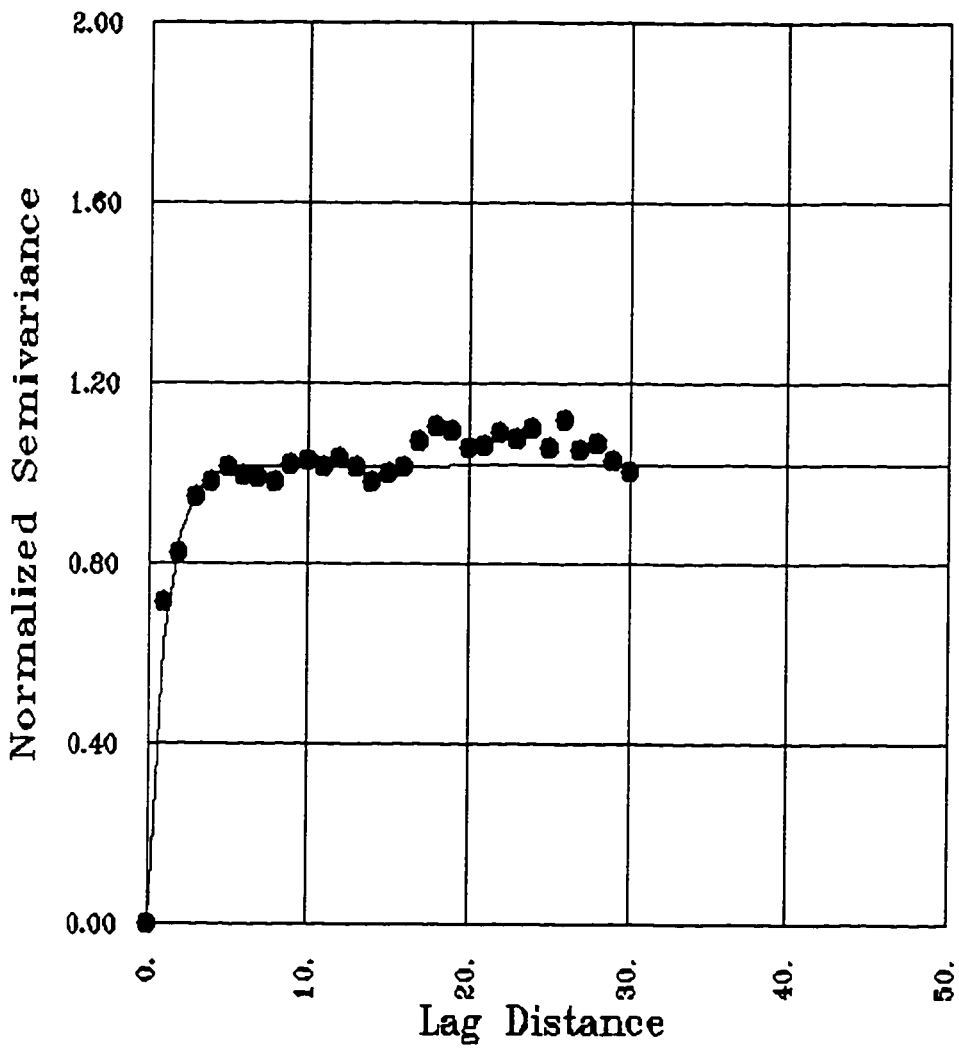


Figure 2-32: Vertical variogram of shaly sandstone facies

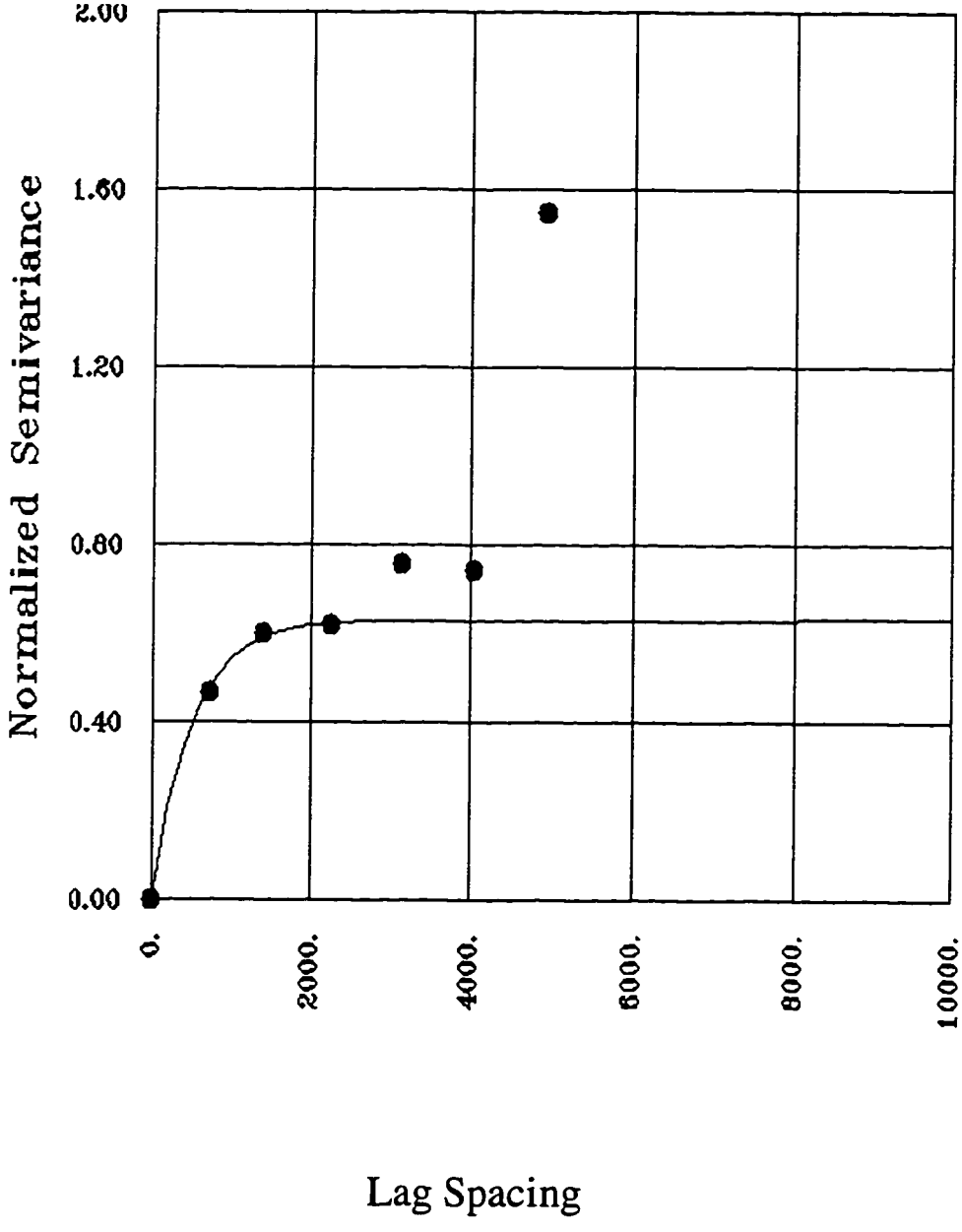


Figure 2-33: Isotropic variogram of iron rich sandstone facies

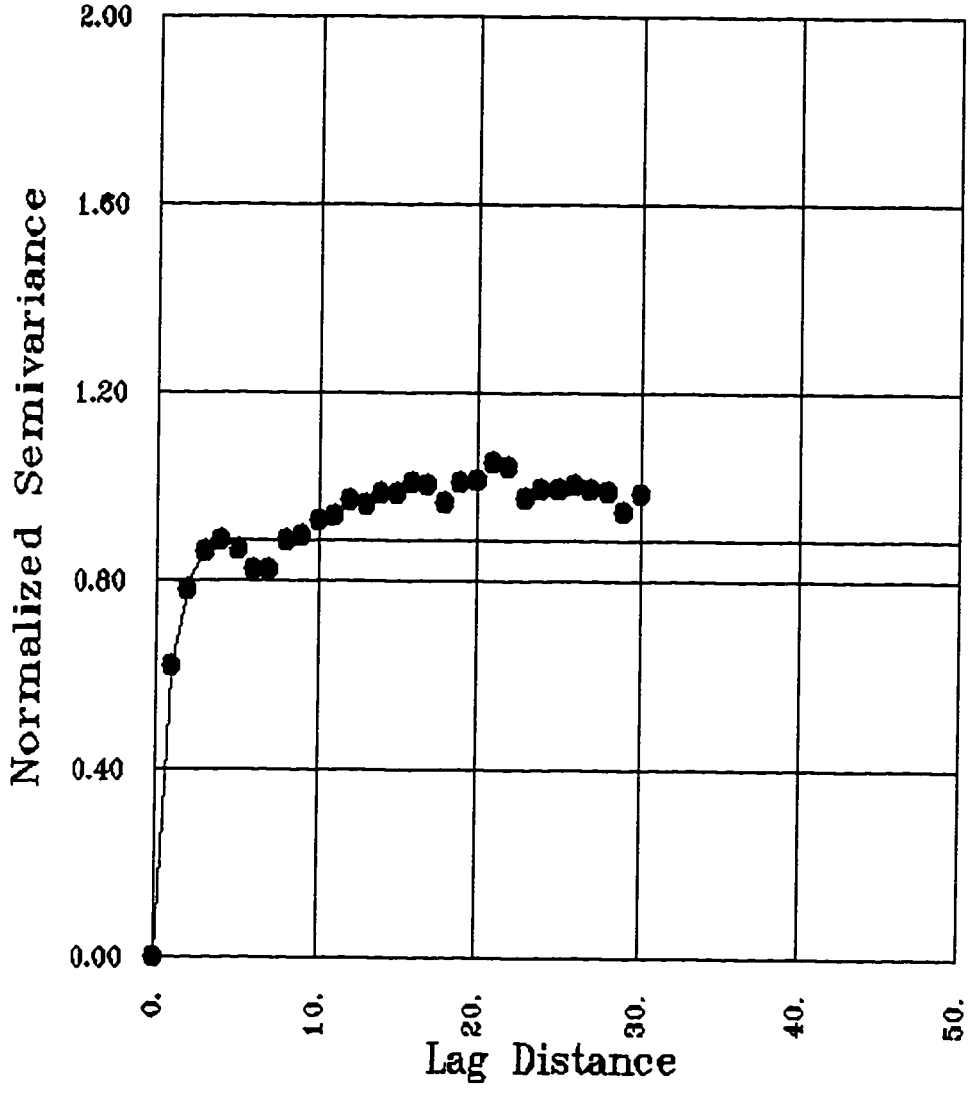


Figure 2-34: Vertical variogram of iron rich sandstone.

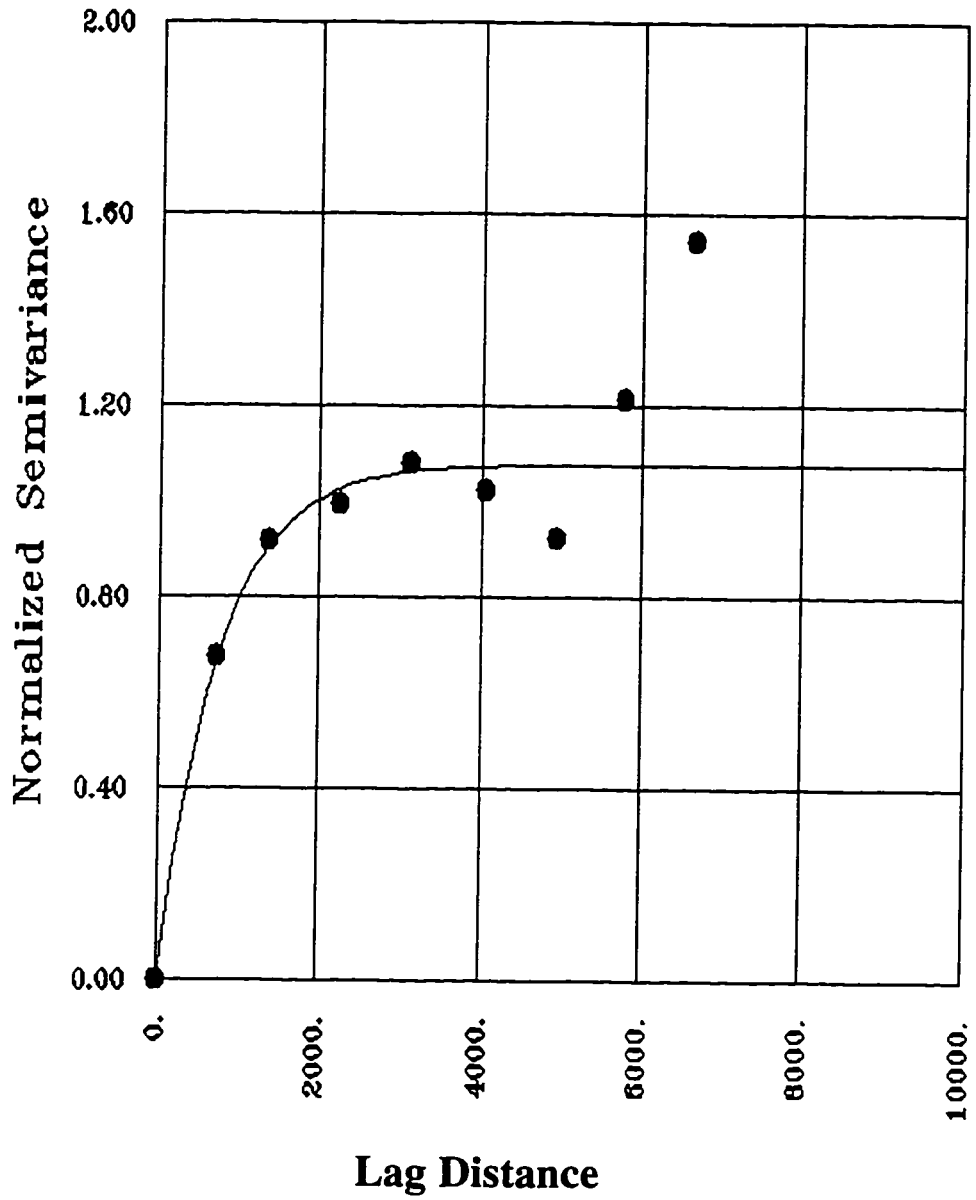


Figure 2-35: An isotropic variogram of clean sandstone facies.

The vertical variogram of this facies shows a range of about 8 ft. (Figure 2-36).

**Very Clean Sandstone Facies**

The variogram of this facies (Figure 2-37) shows a horizontal range of about 1400 meters. The vertical range is about 7 ft. as shown on Figure 2-38.

**Lithoporosity Variograms**

Similar to previous analysis in the univariate statistics section, variograms can be calculated for porosity associated with a specific facies (i.e. conditional distribution). This would help in later stages when porosity is distributed by facies (i.e. distribution of porosity in a predefined facies). This facies dependent porosity distribution will be discussed more thoroughly in the next chapter.

Only reservoir facies will be analyzed here, since all the non-reservoir facies are considered as non porous units.

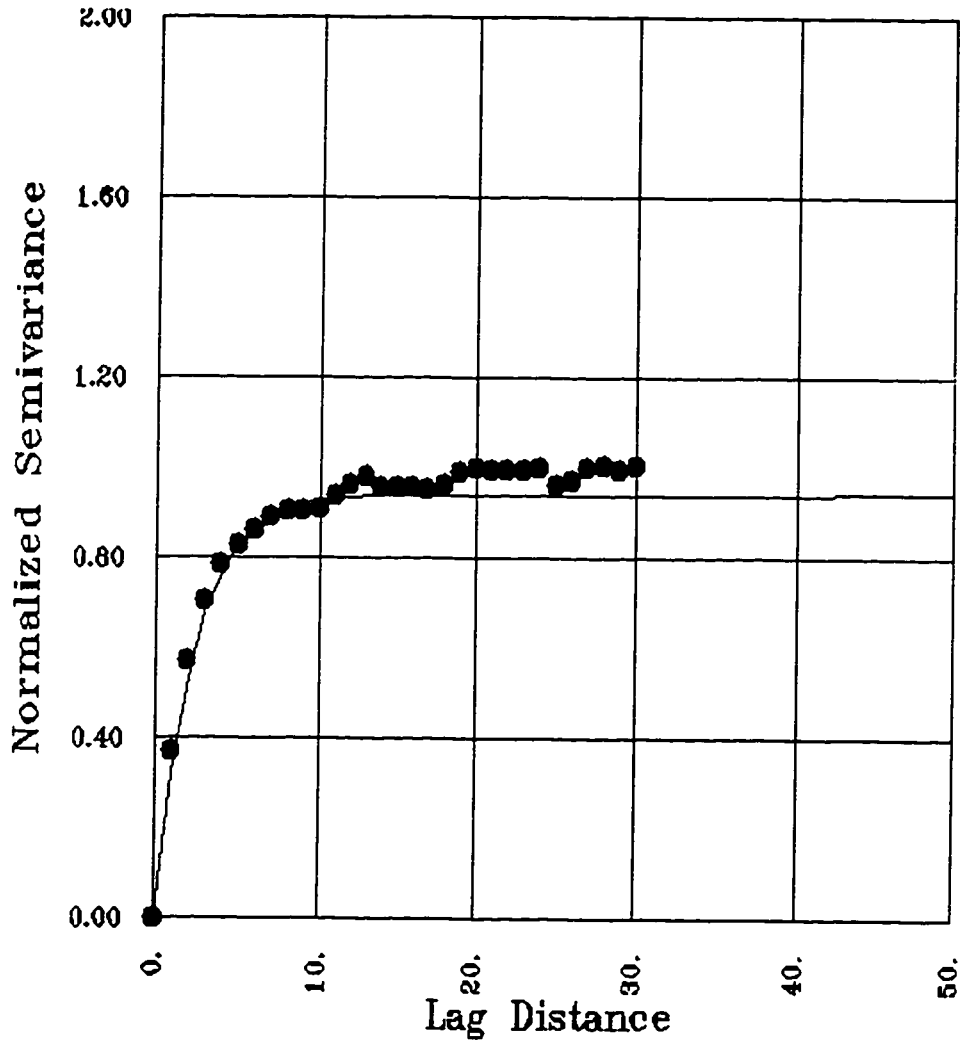


Figure 2-36: Vertical variogram of clean sandstone facies

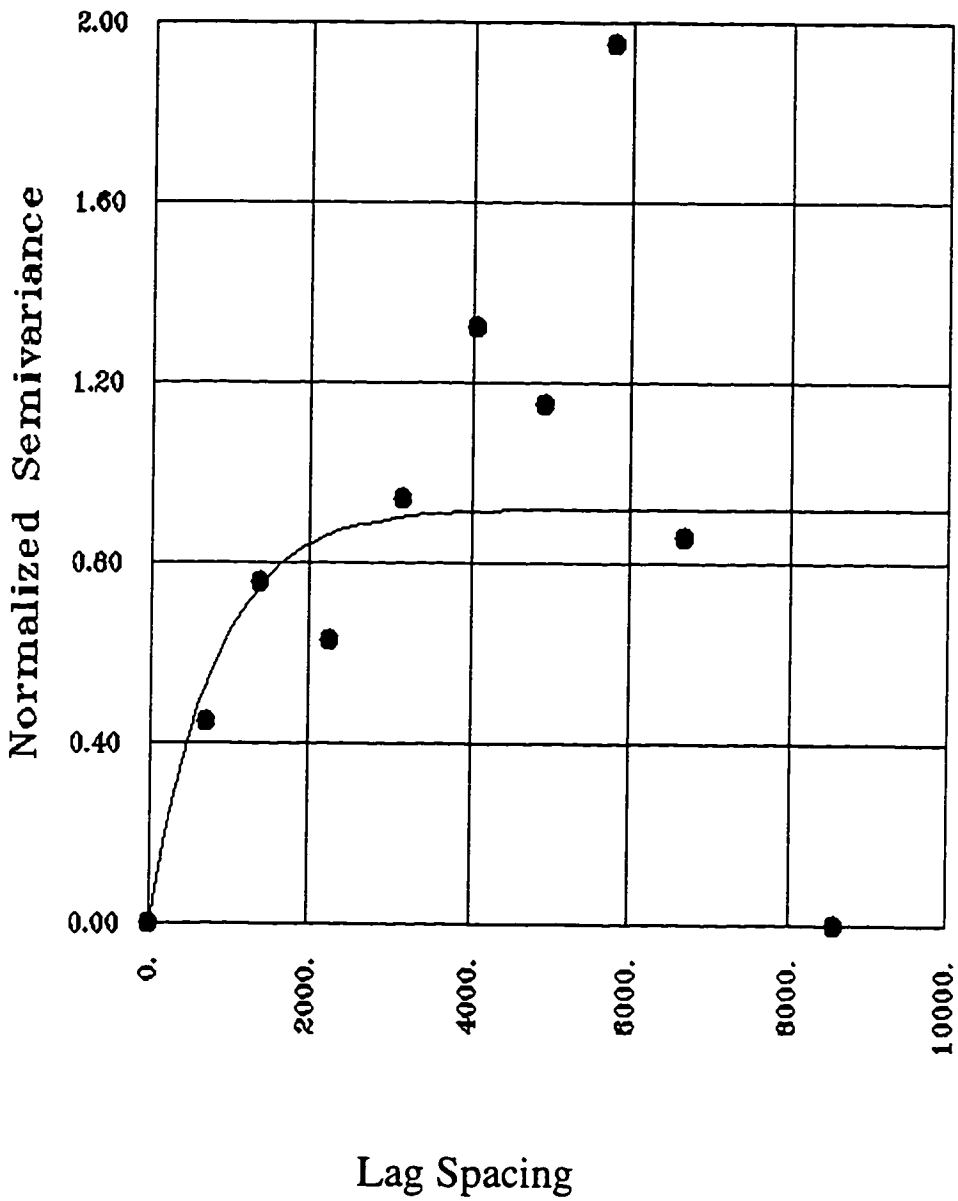


Figure 2-37:An isotropic horizontal variogram of very clean sandstone facies. Note that more than one variogram structure can be fitted.

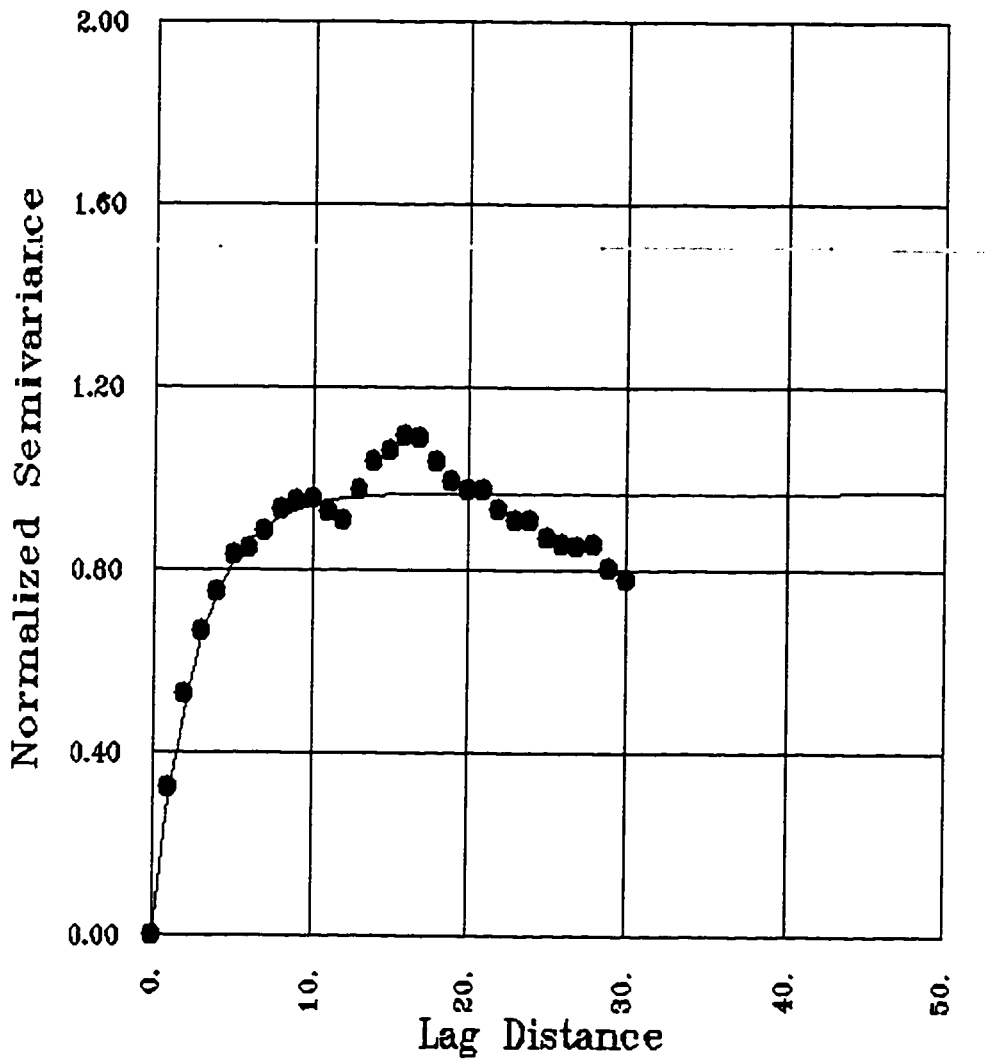


Figure 2-38: Vertical variogram of very clean sandstone facies

**Porosity Variogram of Very Clean Sandstone**

Figure 2-39 shows a horizontal variogram of this facies. The horizontal range of this facies is about 1400 meters. The vertical range is about 3 ft. for this facies as shown on Figure 2-40.

**Porosity Variogram of Clean Sandstone**

Figure 2-41 shows an isotropic horizontal porosity variogram of this facies. It shows that porosity has a range of about 1700 meters. Another porosity variogram is calculated for this facies but in the vertical direction. The variogram shows a vertical range of about 3 ft. as shown on Figure 2-42.

**Porosity Variogram of Shaly Sandstone**

An isotropic horizontal variogram of this facies shows a range in the horizontal direction of about 2000 meters as shown on Figure 2-43. The vertical variogram of this facies shows a range of about 3 ft. (Figure 2-44).

**Porosity Variogram of Very Shaly Sandstone**

The horizontal variogram of porosity of this facies shows a range of about 1600 meters (Figure 2-45). The vertical range of porosity is about 3 ft. as shown on the vertical variogram on Figure 2-46.

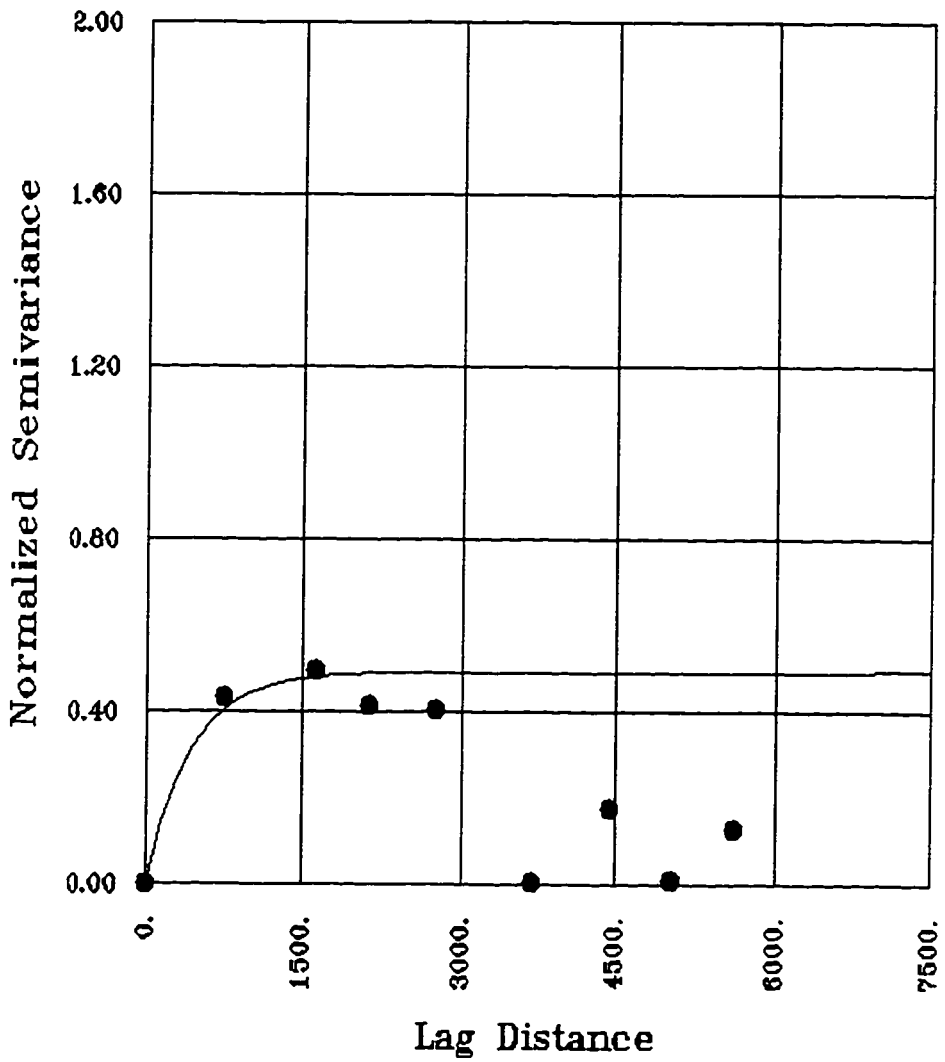


Figure 2-39: Porosity variogram of very clean sandstone facies

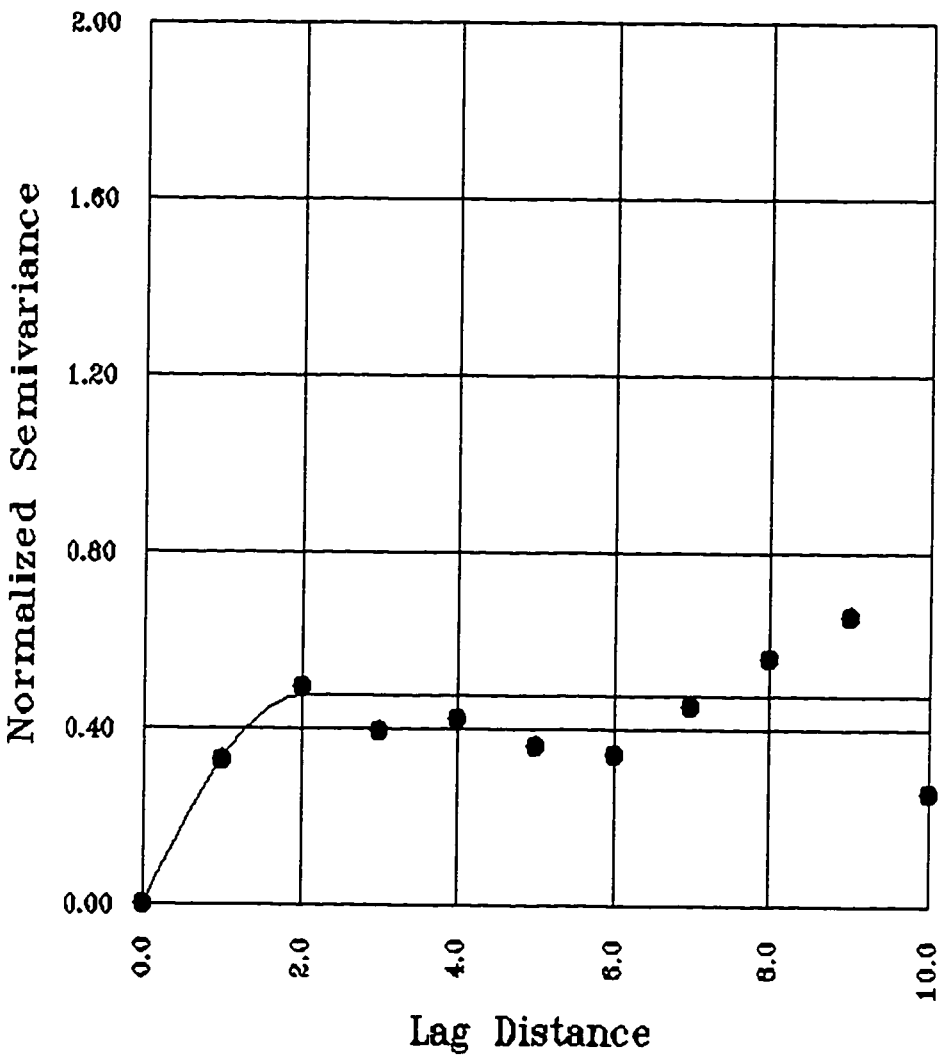


Figure 2-40: Vertical porosity variogram of very clean sandstone facies

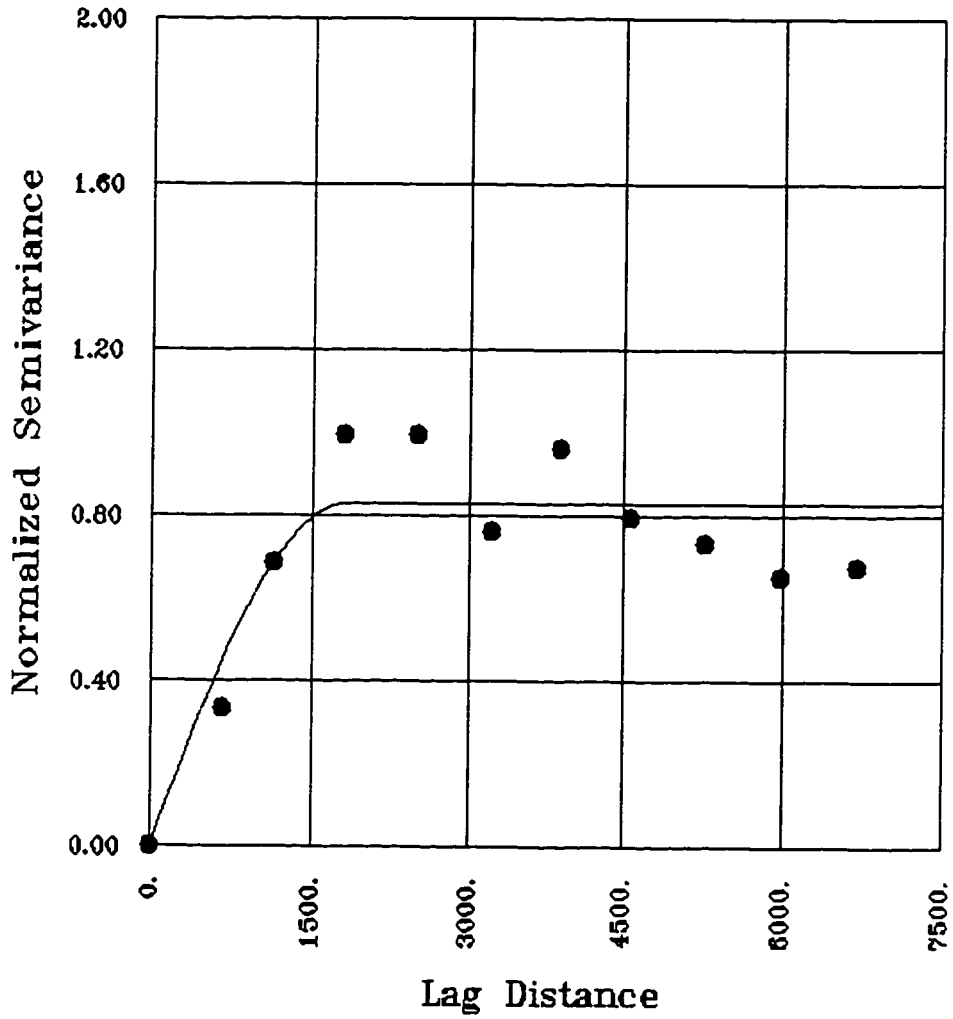


Figure 2-41: Isotropic variogram of porosity in clean sandstone facies

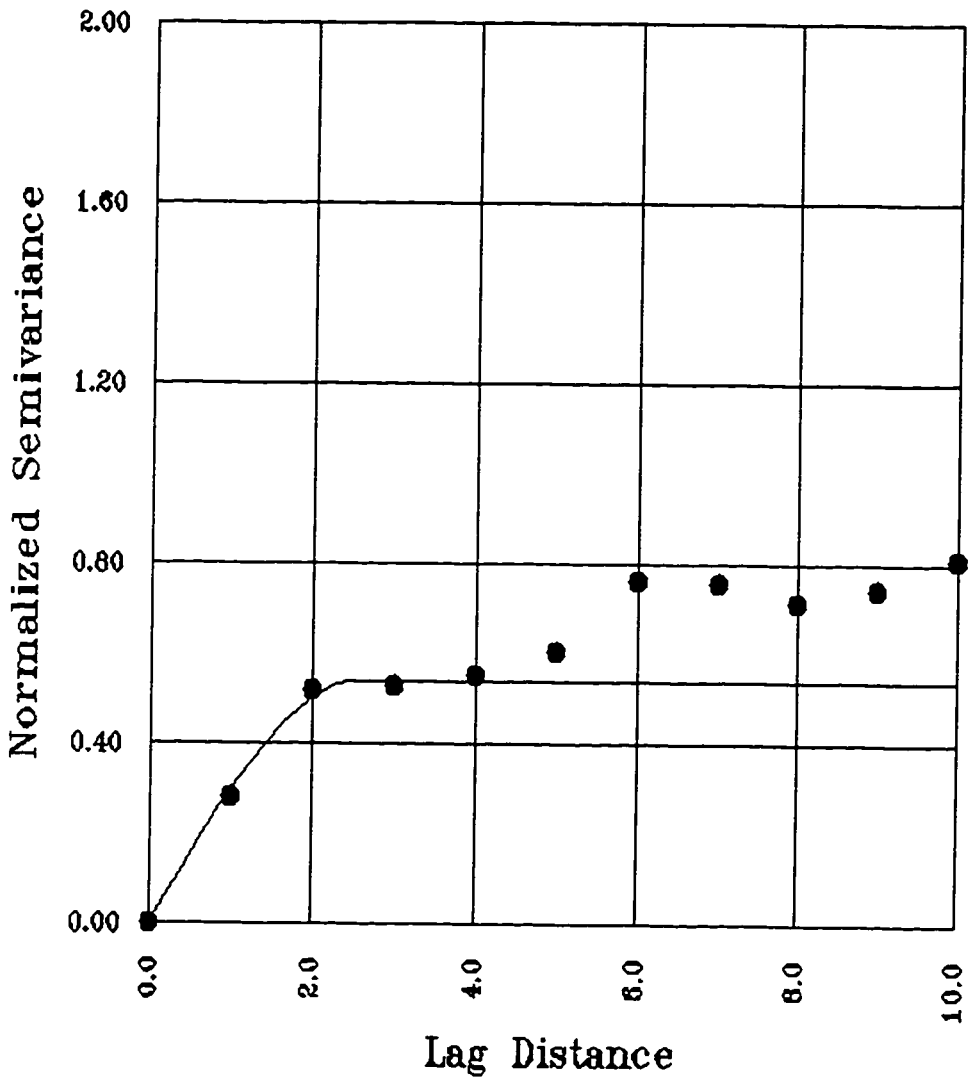


Figure 2-42: Vertical porosity variogram in clean sandstone facies

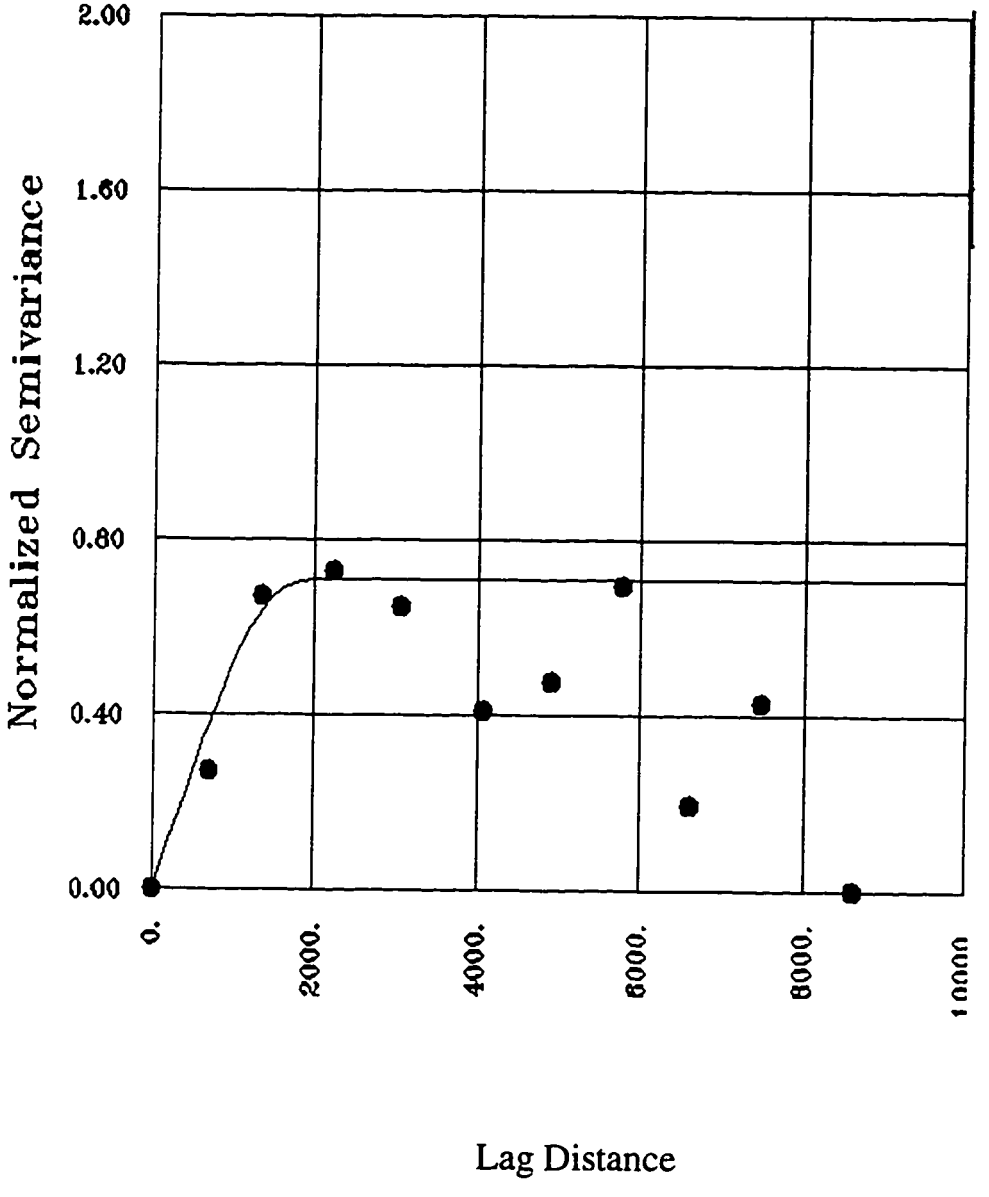


Figure 2-43: Isotropic variogram of porosity in shaly sandstone facies. Notice the periodicity of the variogram indicating more than one structure present.

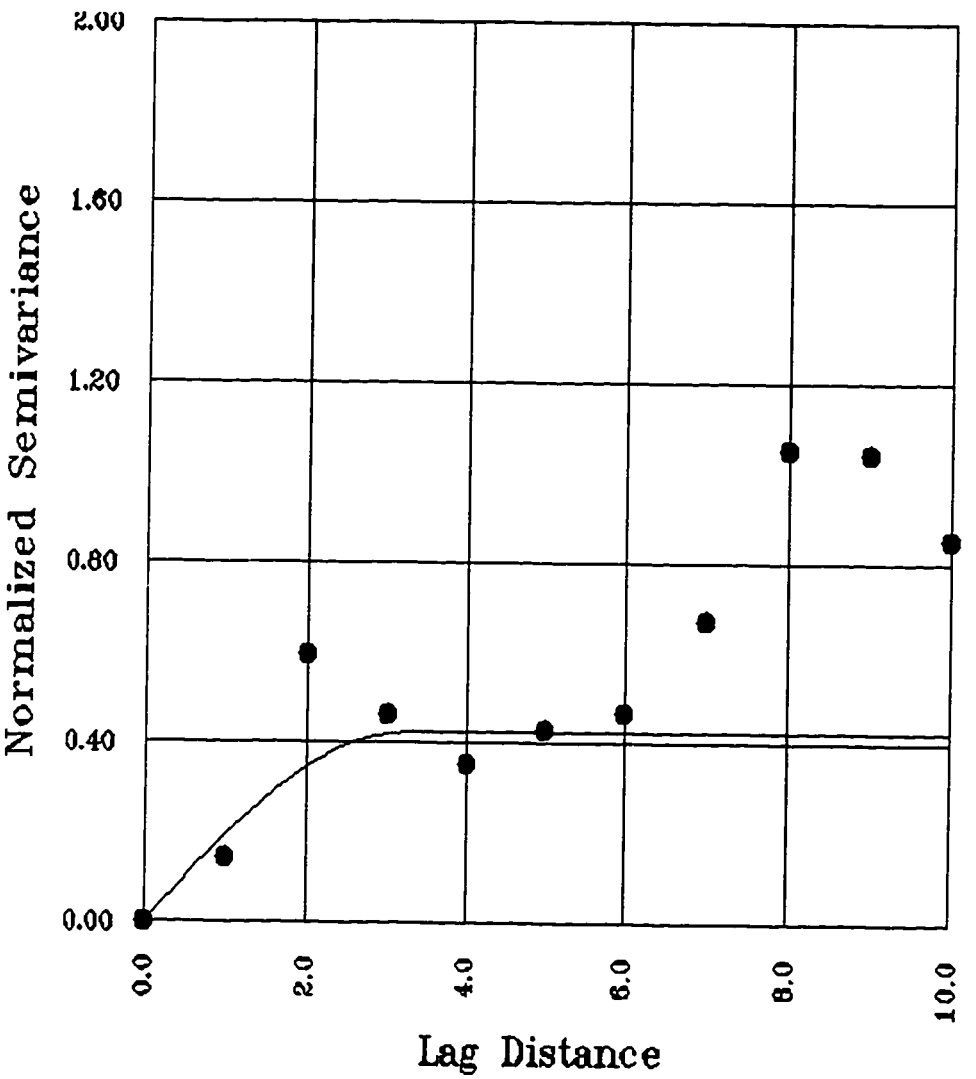


Figure 2-44:Vertical porosity variogram in shaly sandstone facies. Notice the periodicity of the variogram indicating more than one structure present.

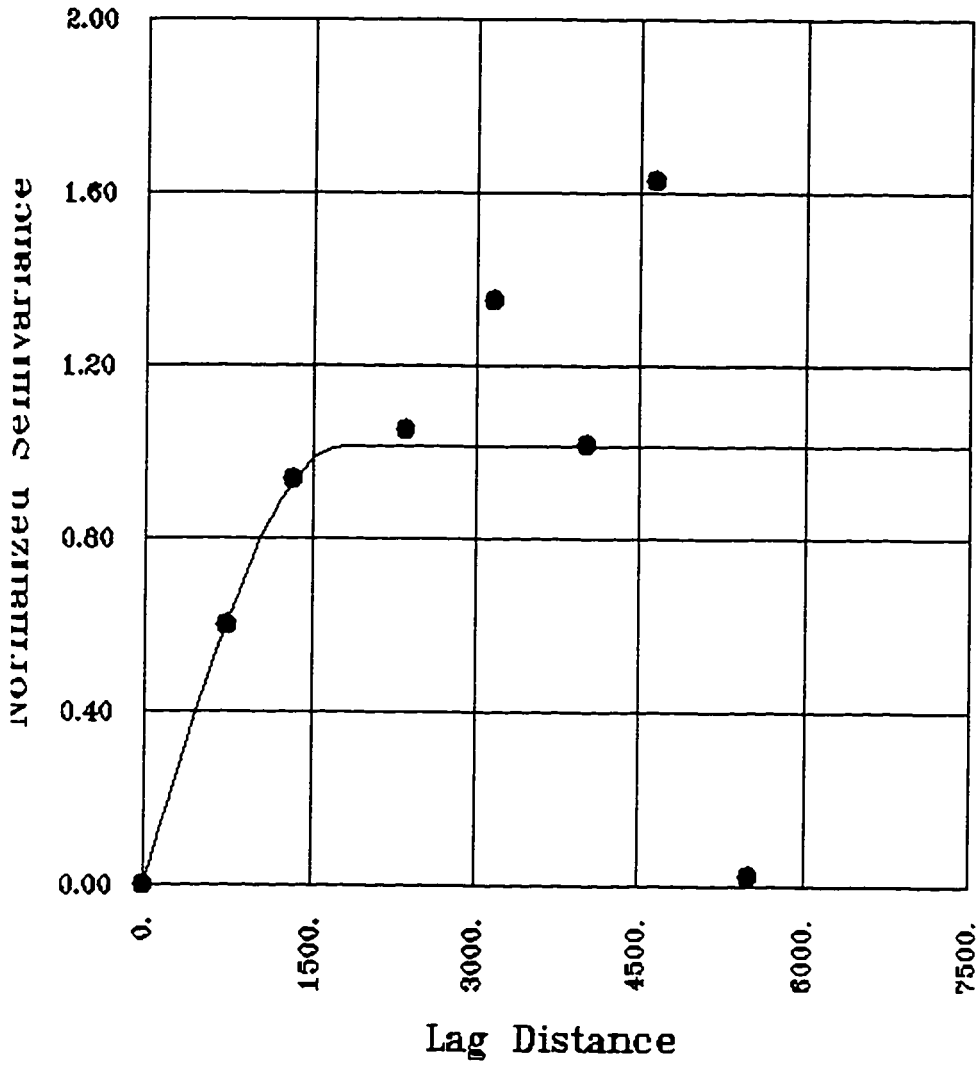


Figure 2-45: Isotropic variogram of porosity in very shaly sandstone facies. It shows more than one variogram structures can be fitted.

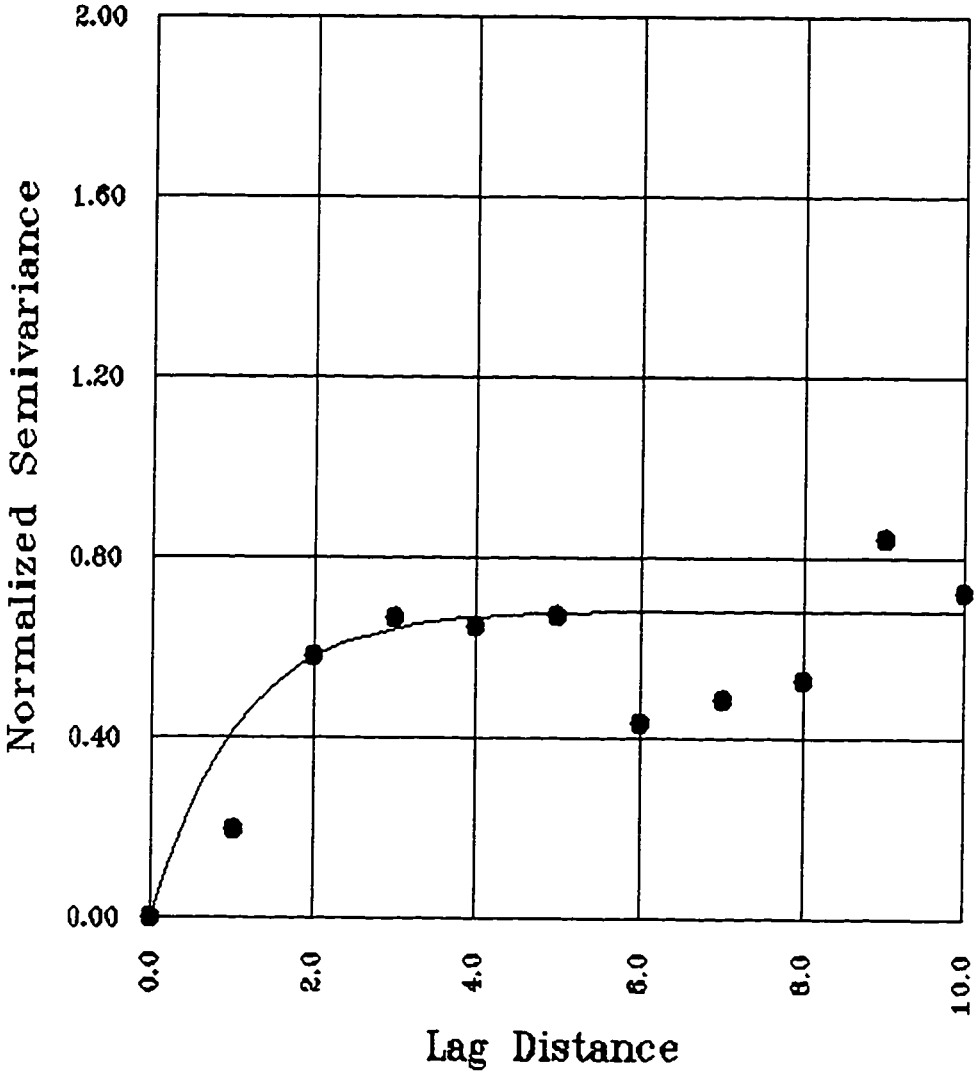


Figure 2-46: Vertical porosity variogram in very shaly sandstone facies

### Porosity Variogram of Iron Rich Sandstone

A relatively shorter porosity range in the horizontal direction of about 1500 meters for this facies is shown on Figure 2-47. The vertical range is about 3 ft. (Figure 2-48).

## 2.8 SFNC Geological Interpretation Obtained From Classical and Spatial Analysis

Classical and spatial statistics can aid in the geological interpretations such as the environment of deposition. This can be demonstrated in the case of SFNC Sequence.

Classical statistics has shown that SFNC Sequence is quite heterogeneous interval as can be clearly seen from the Pie diagram on Figure 2-49. The figure shows that the majority (about 67%) of the facies is considered as reservoir rocks. However, a closer look to the diagram shows that a large percentage of the reservoir facies is occupied by Very Shaly Sandstone which is considered as a very low quality type of reservoir.

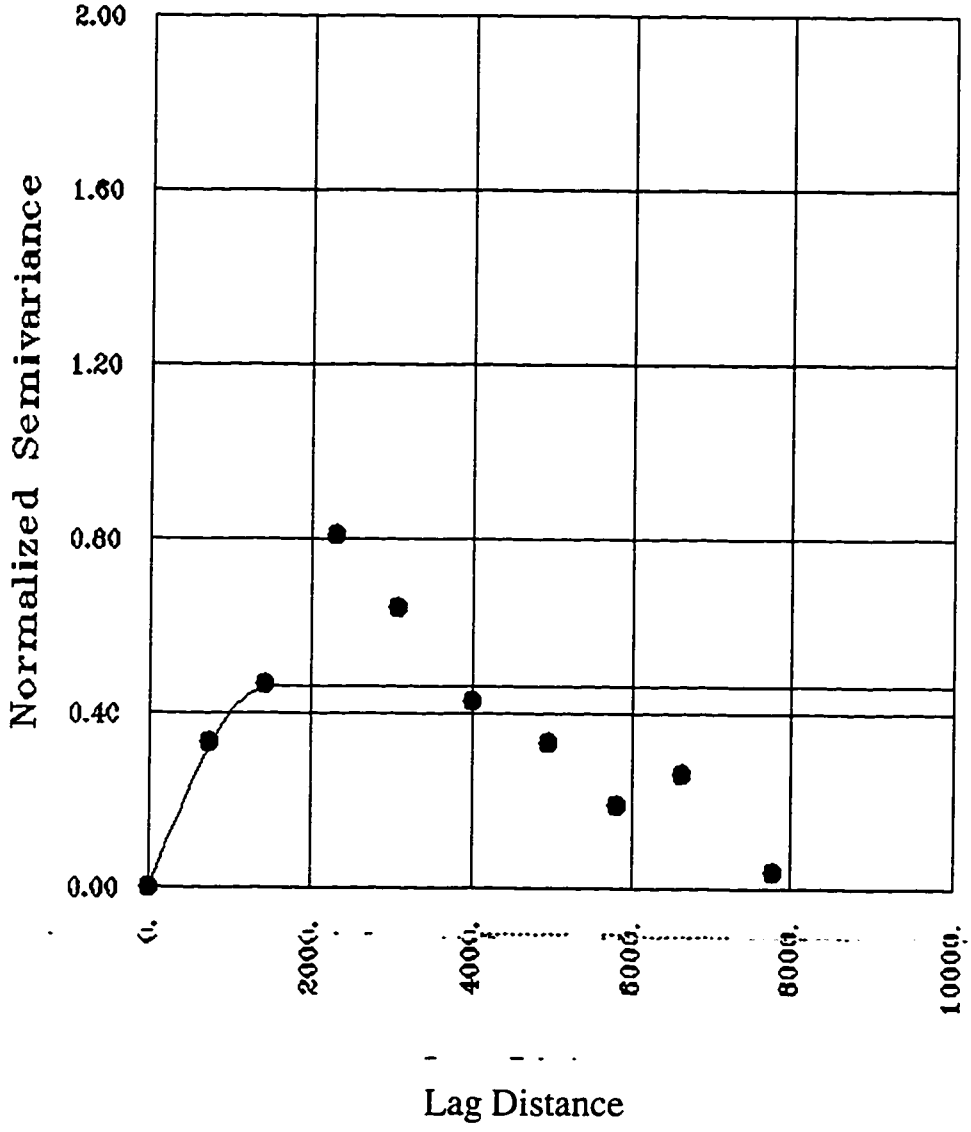


Figure 2-47: Isotropic variogram of porosity in iron rich sanstone facies. Notice the periodicity of the variogram.

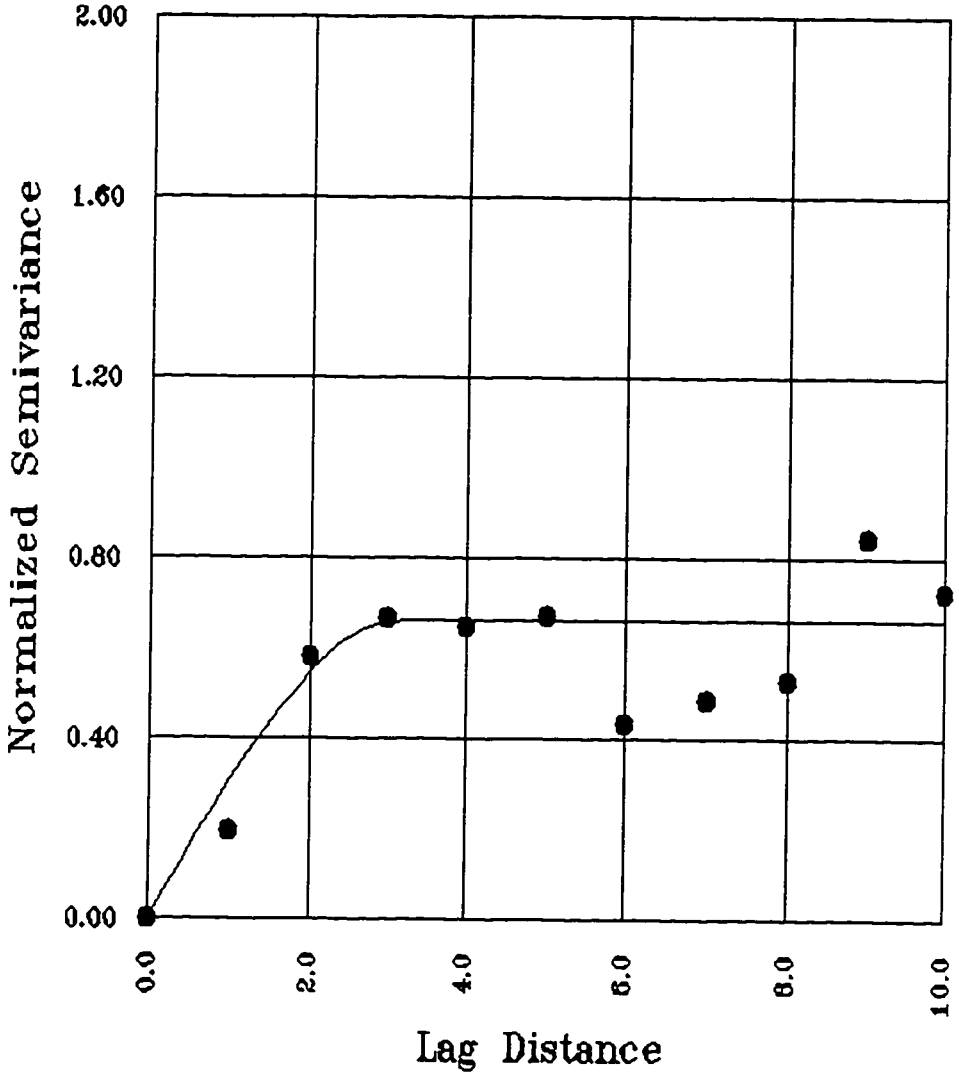


Figure 2-48: Vertical porosity variogram in iron rich sandstone

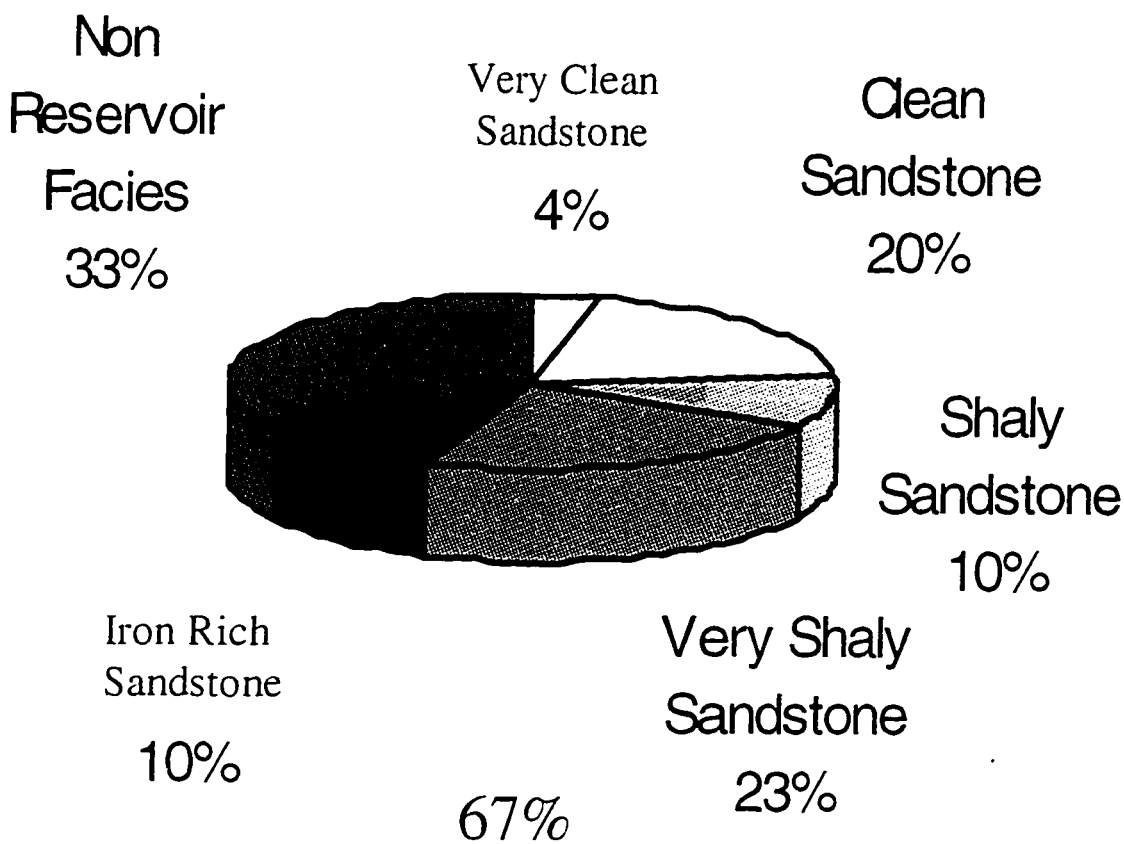


Figure 2-49:A pie diagram showing the percentages of each facies; reservoir facies constitute about 67% of the SFNC sequence

This suggests that the SFNC Sequence was deposited in an environment away from the source of the sand toward the basin. This environment could be interpreted as either distal mouth bar at the delta front or shallow-marginal environment in front of the non-marine facies of fluvial dominated delta systems

This interpretation is also supported by the spatial behavior or continuity of the facies as shown on the summary table of the variograms of SFNC Sequence on Table2. The table shows a summary of both the vertical and horizontal continuity of each facies as thin sheets in space. These sheets are on average of 1.5Km in diameter suggesting an earlier interpretation as a distal mouth bar type of an environment. This environment is located at the front of the delta near the prodelta facies.

| Facies | Vertical Range (Ft.) | Horizontal Range (Meters) |
|---|---|---|
| Very Clean Sandstone | 8 | 1400 |
| Clean Sandstone | 8 | 2100 |
| Shaly Sandstone | 3 | 2000 |
| Very Shaly Sandstone | 4 | 1600 |
| Fe Sandstone | 3 | 1067 |
| Shale | 4 | 1700 |
| Fe Shale | 3 | 1067 |

Table 2-1: Summary table of facies variograms

# CHAPTER 3

# GEOSTATISTICAL MODELING

## 3.1 Introduction

Once the spatial continuity of the variable under study has been modeled, an estimate of the variable can be calculated at unsampled locations from neighboring data values. In addition to providing a single-value estimate of the unknown, the estimation technique should also provide a model of the uncertainty associated to that unknown, this uncertainty is dependent on the information available, the data values and the particular model of the spatial

dependence being used; i.e. the variogram model type. This dependence should always be clearly documented.

Any algorithm used to estimate some unknown quality is called an estimator. The estimation can be empirical such as the one done by an experienced geologist who manually connects pairs of neighboring points and then draws contours using some model of spatial continuity derived from experience about the area under study. Furthermore, estimators can be based on objective optimization, as in the maximum likelihood estimator technique, or least square estimators, or kriging.

Even though for a given task there are many types of estimators and each would give different results, the most commonly desired features of an estimator are that it should give unbiased results and have minimum error variance. This means that the expected value of the error is zero, and on the average the estimator predicts the correct value in the overall areal sense. This can be expressed as

$$E(Z^*-Z)=0,$$

where $Z^*$ is the estimate, Z is the true value of the variable being estimated, and E denotes expected value. This means again that the expected value of the error ("the bias") should be zero.

Another criterium, mentioned earlier, of the best estimator is that the variance of the error should be minimal:

$$Var(Z^*-Z)=E[(Z^*-Z)^2]= \text{Minimum},$$

where $Var(Z^*-Z)$ is the variance of the difference $(Z^*- Z)$.

Thus, the error distribution should have a small spread.

## 3.2 Kriging

Kriging is a generic name of a group of unbiased, minimum error variance estimation techniques discussed in the Introduction.

At each unsampled location, the unknown value can be estimated by a weighted linear combination of the data at sampled locations:

$$Z^*(X_0)= \sum_{1}^{N} \lambda_\alpha \{Z(X_\alpha)\},$$

where $Z^*(X_0)$ is the estimate desired at the unsampled location $(X_0)$; $Z(X_\alpha)$ denotes the data points available at location $X_\alpha$, $\alpha$ goes from 1 to N, the number of sampled locations. $\{\lambda_\alpha\}$ is the set of weights applied to the data locations.

Kriging has two properties. The first property is that the expected estimated value should be equal to the true value, or in other words, that the expected value of the estimation error is zero. This property is the condition of unbiasedness.

However, even though it is called a "minimum error variance" this does not mean that the kriging estimate $Z^*(x_0)$ provided by solving the kriging system will necessarily be closer to the true value $Z(x_0)$ than any other unbiased linear estimate. It will only be so on the average over the area of interest, with an additional restriction that the variogram model calculated from the available data is representative for the whole area and not only for the limited amount of data available.

A striking advantage of kriging not available in traditional estimation methods is that the kriging algorithm honors the data at sampled locations. If a location corresponding to any one of the N sample locations is estimated by

kriging, the kriging system returns the datum value exactly (Journel 1989). This is not the case with other estimators such as the least square algorithm which does not honor data at the sampled locations.

The ability to model anisotropy is another major advantage of the geostatistical estimation over the traditional techniques, including the inverse distance and inverse distance squared methods. A good example of this anisotropy is given on Figure 3-1. The figure shows that if there is a meandering channel in the northeast direction then the porosity values at locations northeast or southwest would be more biased or have more influence than data points located to the northwest or southeast. The classical inverse distance methods would assign equal weights to all the data points.

A further benefit of kriging, which is a major advantage over the traditional inverse distance type of estimation, is its declustering ability. This is illustrated on Figure 3- 2 which shows a cluster of wells at an area which could be a platform of five to six wells in an offshore field. As seen, in the inverse distance methods the weights given to the sampled data locations are solely dependent on the distance to the point to be estimated. This results in weighting the sampled points which are closer to the point to be estimated more heavily.

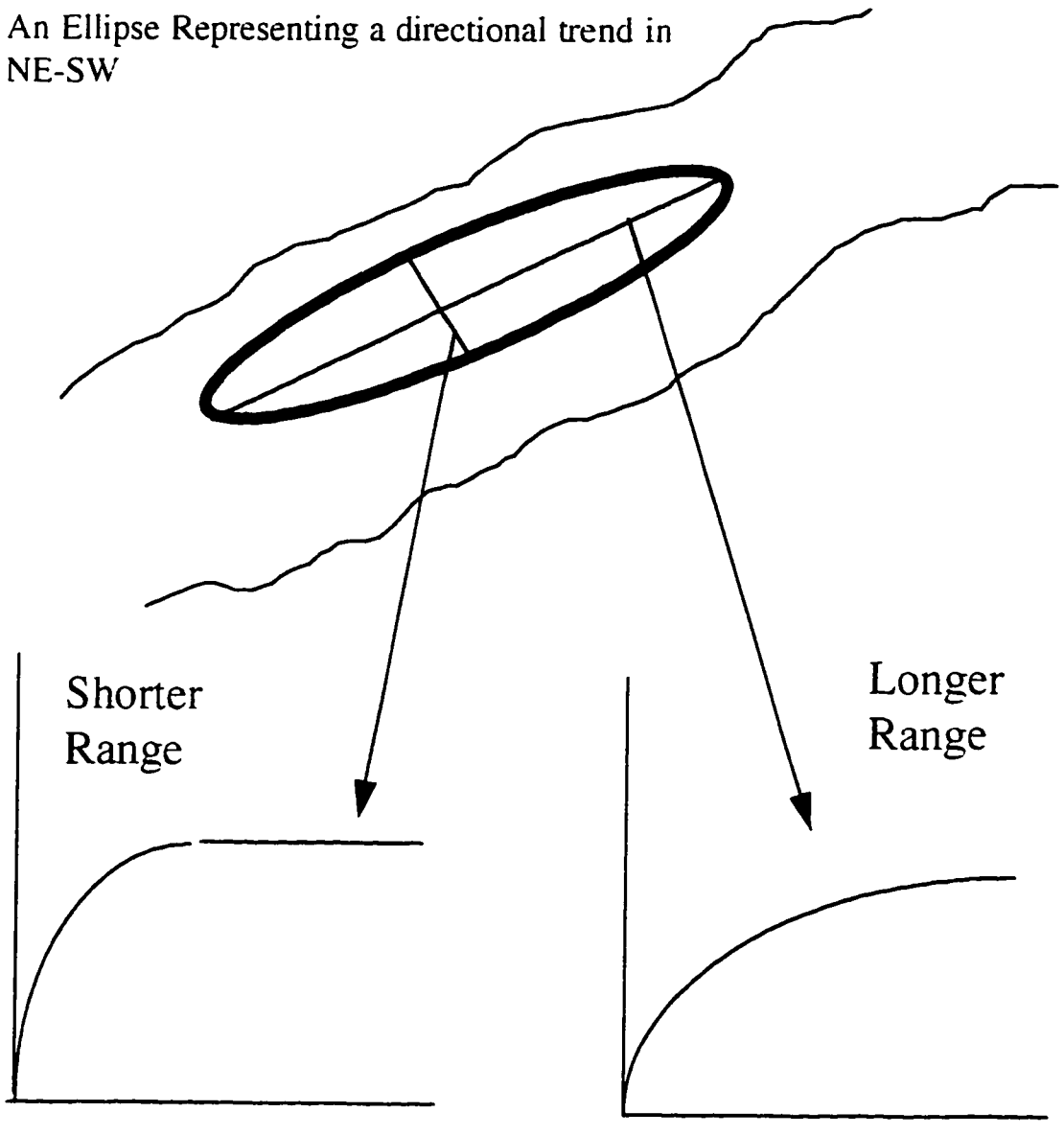


Figure 3-1: Illustration of an anisotropic variogram for a meandering channel which has a NE-SW direction

However, if the distances of the sampled points to the point to be estimated were equal, as shown on Figure 3- 2, then the sampled points would be given the same weights. This would give, as in the case of Figure 3- 2, more influence to the points at the crest than to the point at the flank which, therefore, would make the resulting estimated value look very similar to that of the crest.

However, if kriging is used then the weights assigned to the data points are not only determined by the distance between the data and the point to be estimated, but also on the data configuration or in other words the distances between the sampled data points themselves. This advantage ensures that the kriging weights are adjusted for any clustering of the data. In the case of Figure 3-2, for example, the three points at the crest will be given almost the same weights, since they are very close to each other. However, the flank well will have more influence since it is the only point which represents the flank area. This advantage would ensure that the estimate would not only be governed by the three crestal points.

Another feature of kriging is that it gives a quantitative measure of uncertainty associated with the estimate at each unsampled location. This

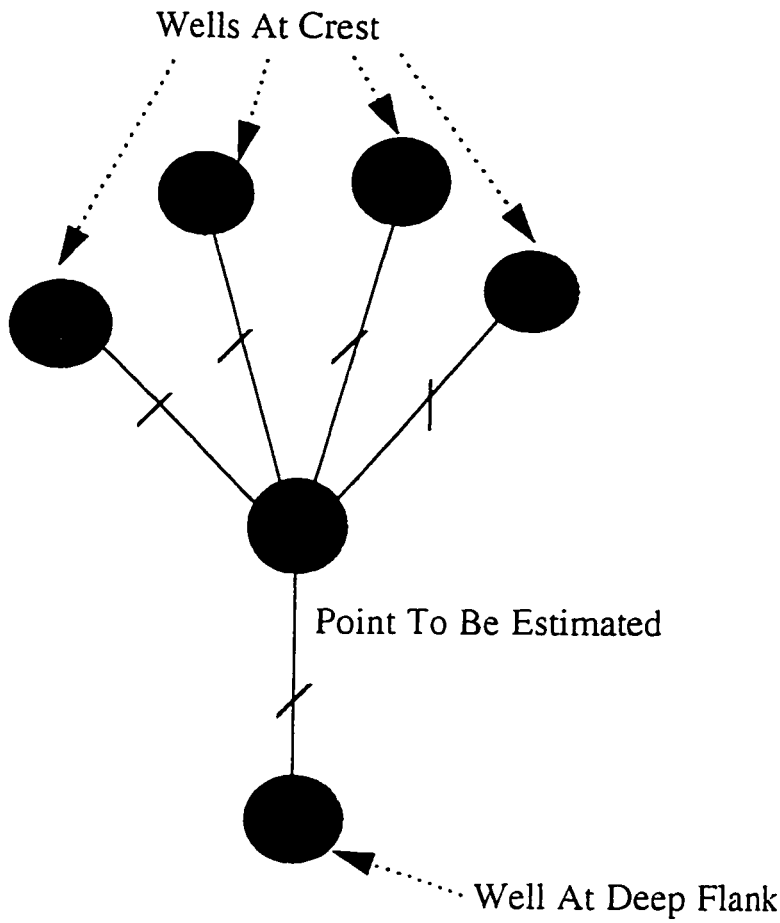


Figure 3-2: A point to be estimated between a cluster of wells at the crest and an opposing flank well.

measure is derived from the kriging variance, under the assumption that the errors are normally distributed and the variance associated with kriging estimate does not depend on the data values at the sampled location. If these conditions are met, it is possible to construct confidence intervals around the estimate, i.e. we shall have a kriging estimate plus/minus the kriging standard deviation.

## SFNC Porosity Kriging

Using the variogram which was calculated in the previous chapter for the porosity of the SFNC sequence, the average porosity was kriged between the wells as shown on Figure 3-3. It is noticed that the porosity distribution is smoothed spatially as a result of kriging. Figure 3-4 shows two slices of a kriged porosity volume. The variogram used for kriging this volume was the same as used to krige the average porosity. Even though the variogram used was isotropic, the two slices show a trend toward the north-south direction.

## Kriging Variance

The kriging variance on Figure 3- 5 of porosity, as provided by the kriging systems, are useful to characterize data configuration, but without

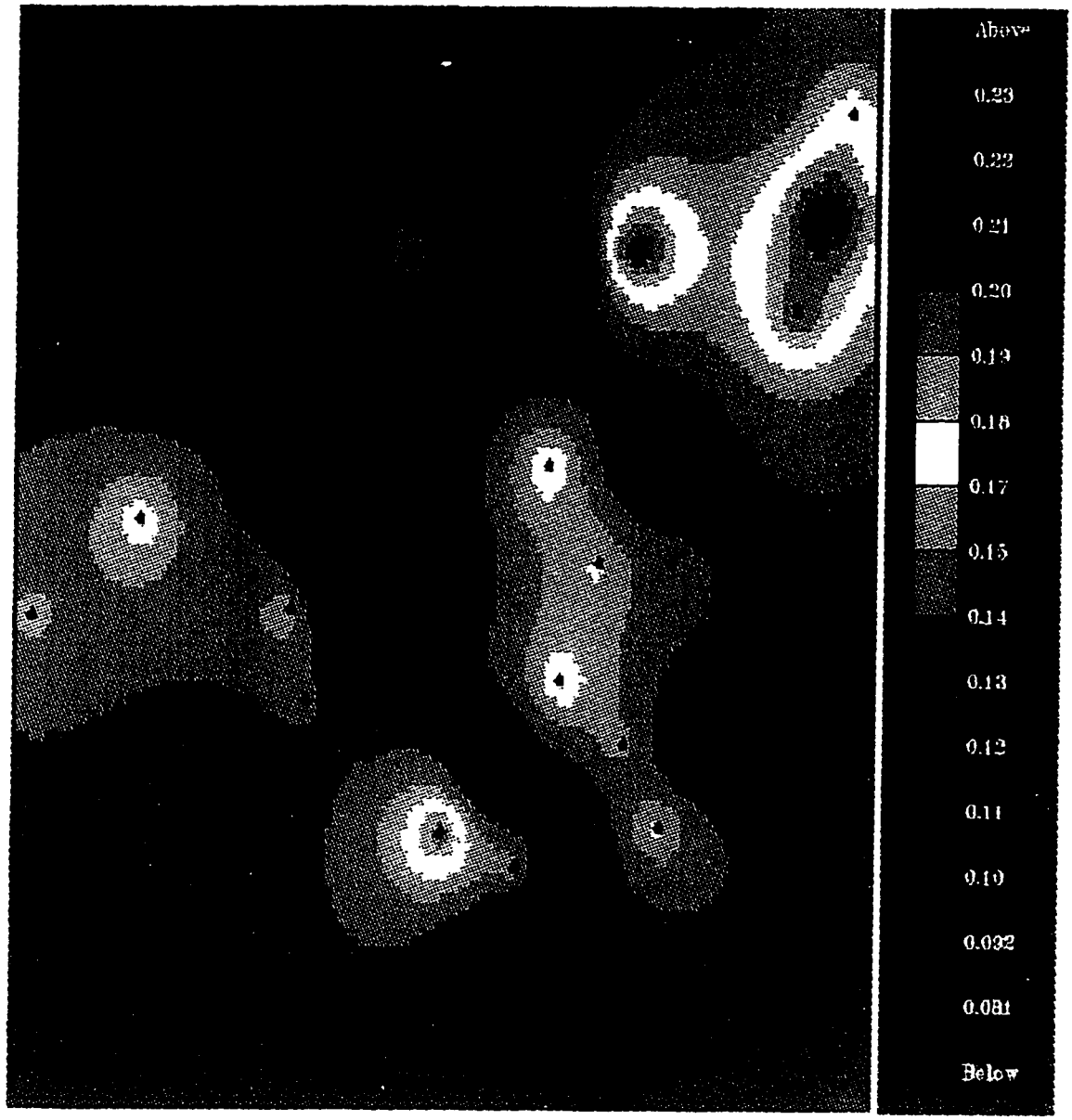


Figure 3-3: Kriged average porosity map of the SFNC Sequence

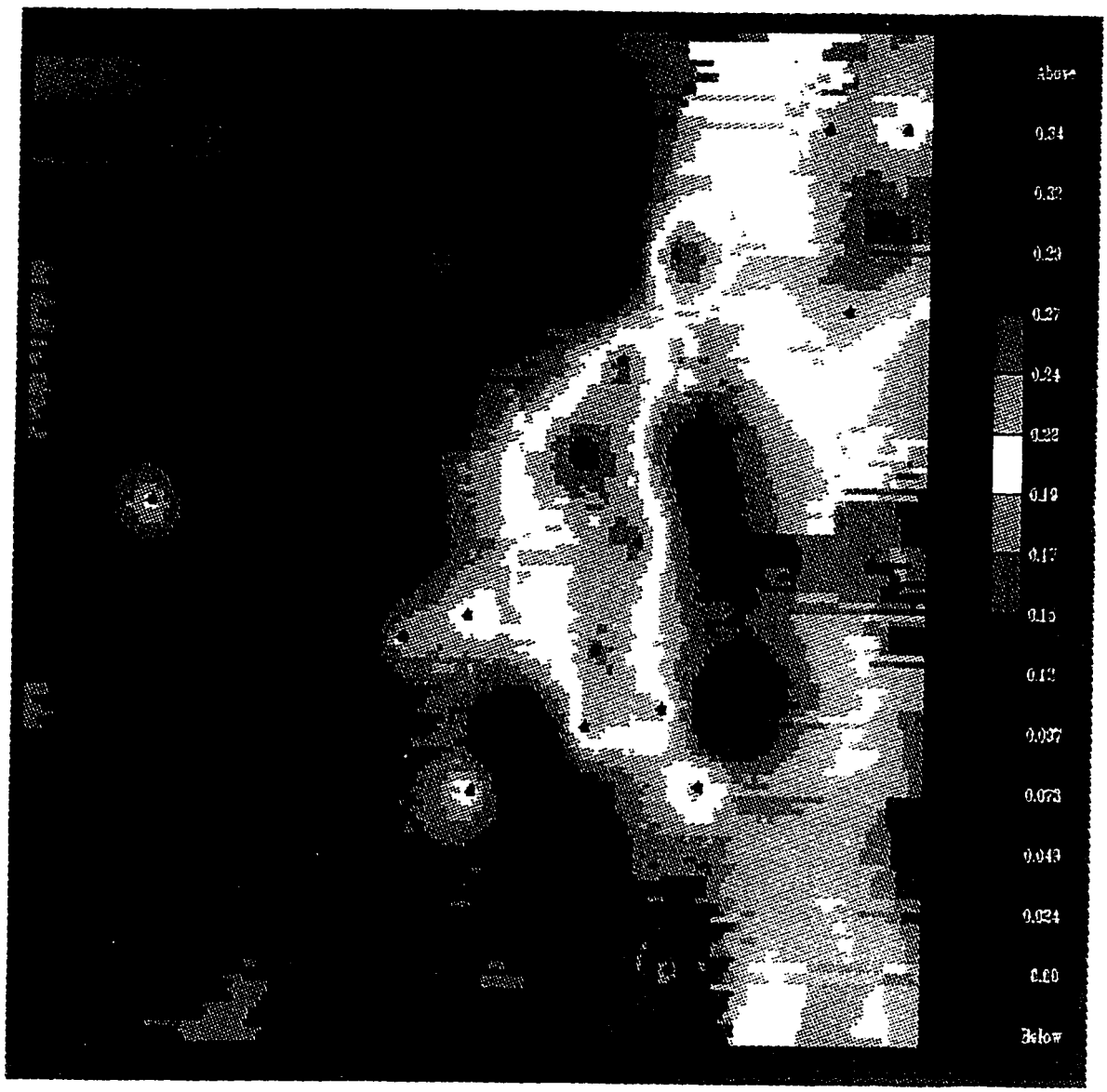


Porosity Scale

Figure 3-4: Slice of a kriged porosity volume

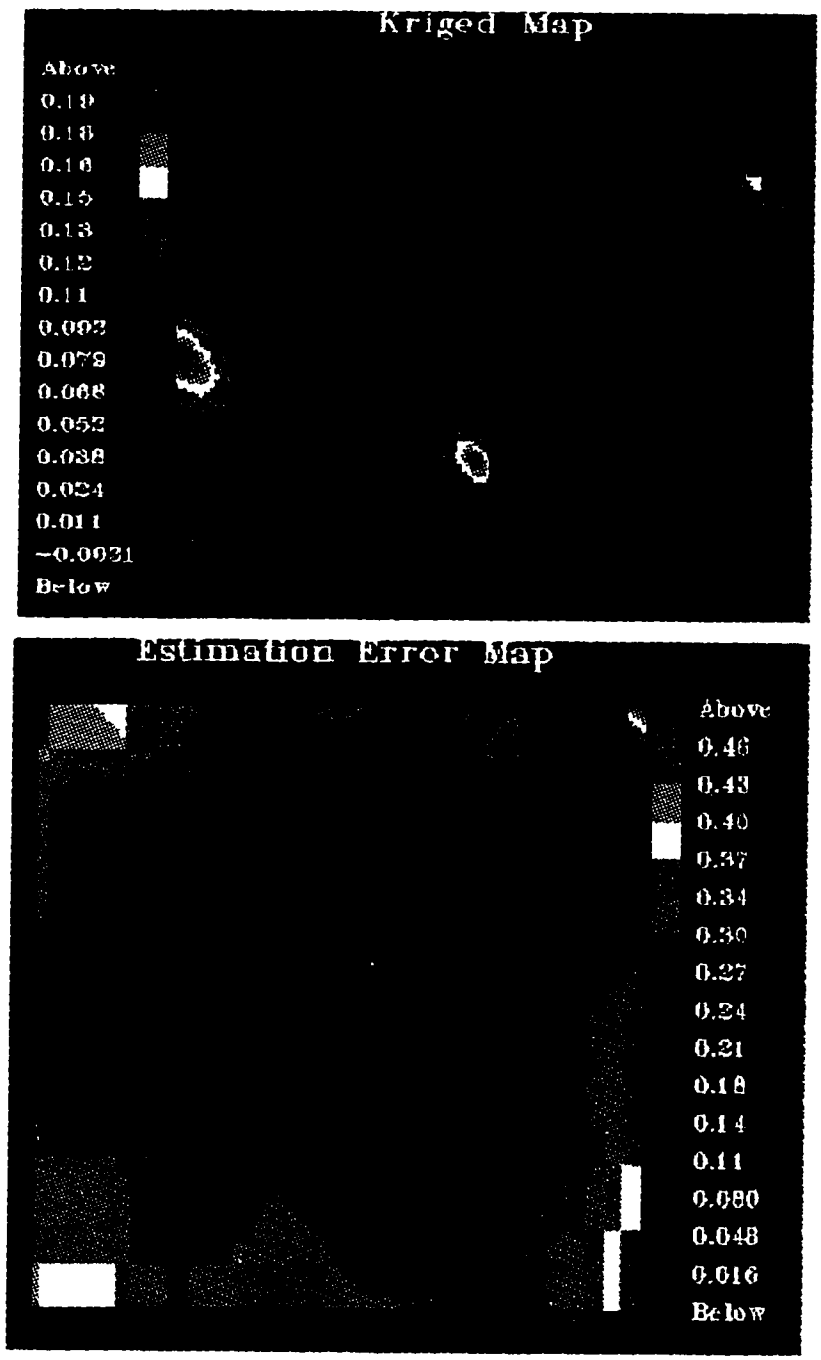


Figure 3-5: Kriging variance in the lower graph associated with the kriging estimates shown in the upper graph.

further assumptions it is not a measure of accuracy (Journel 1989). Therefore it can not be used as a measure of uncertainty or reliability and hence of limited practical utility.

### 3.4 The Non Parametric Alternative

Traditional deterministic interpolation techniques, including inverse distance methods, do not yield any information about the reliability of the estimates or the probability of that estimate to be true. As mentioned earlier, the main advantage of probabilistic interpolation techniques such as kriging is that an error variance is attached to each estimate. Unfortunately, unless a parametric distribution of the spatial errors is assumed (such as a normal distribution), the error variance can not be used to construct confidence intervals. Most of the time symmetric (such as normal) distribution models are assumed for the errors; these models are fully characterized by two parameters, the error mean and the error variance. Such an assumption, however, is only reasonable for the distribution of, for example, measurement errors in the highly sampled and well-controlled environment of a laboratory (Journel, 1989). However, such Gaussian (normal) models are questionable when

applied to describe the spatial estimation errors, the kind considered in this study (Isaaks and Srivastava,1989). Indicator geostatistics, also called non-parametric geostatistics, provides an alternative to the parametric methods discussed earlier. It allows a direct estimation of the cumulative distribution function of the random variable being studied at each unsampled location, without assuming any parametric shape (such as Gaussian) for that distribution.

### 3.4 Indicator Kriging

Indicator kriging (Journel, 1989, Deutsch and Journel, 1992) is based on a non parametric model of the cumulative distribution function (cdf). The data is first non linearly transformed to a set of ones and zeroes. Figure 3- 6 shows this on the case of a continuous variable. The variable at a sampled location is set to one if it is less than or equal to a predifined cutoff, otherwise it is set to zero.

$$i(Z_0; Z_j) = \begin{cases} 1 \text{ , if } Z_0 <= Z_j \\ 0 \text{ , if } Z_0 > Z_j \end{cases}$$

where $Z_0$ is the value at location (0) and $Z_j$ is the cutoff value.

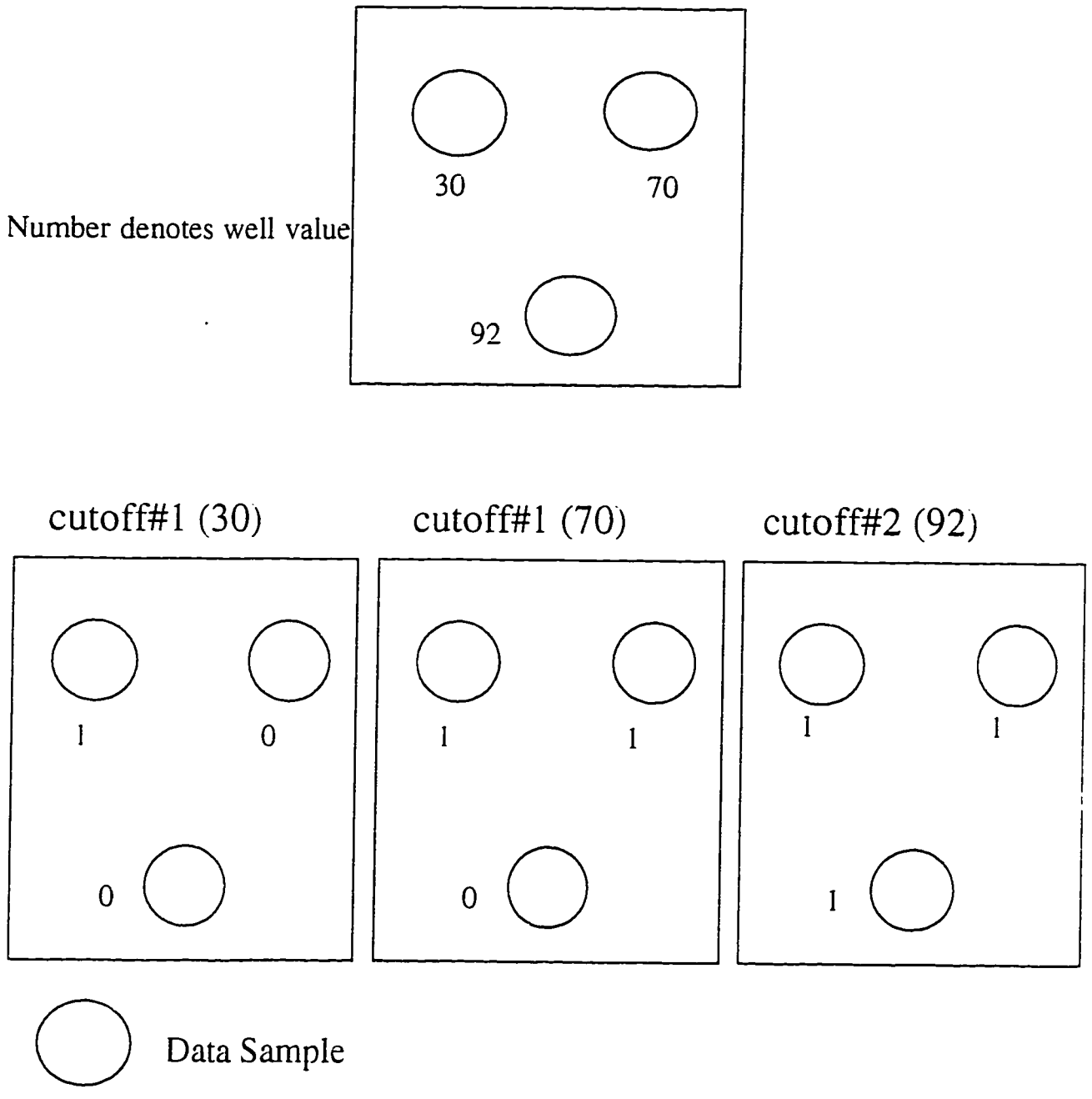


Figure 3-6: A schematic example of indicator kriging of a continuous variable. Three cutoff values are defined.

In the case of a categorical data set such as facies, the data at a sampled location is set to one if this facies is present, otherwise it is set to zero. An example of a categorical variable is shown on Figure 3- 7.

In case of a continuous variable, the number of cutoffs can be set to any value, but most often between 3 to 10 or the nine deciles of the sampled data. In case of categorical variables the number of cutoffs is equal to the number of categories.

Once the data have been transformed into a number of indicators (0's and 1's) for each cutoff, the second step is to calculate the experimental indicator variogram for each cutoff value, and model these variograms as discussed in Chapter Two. This gives a unique flexibility of modeling each facies individually (in case of categories), or a specific high or low value in case of continuous variables. When doing the modeling, the anisotropy and the range can be different for each indicator cutoff. This advantage is far beyond anything available with traditional techniques, even with ordinary kriging. This flexibility is very important in the spatial modeling, for example, of facies (and other geologically defined variables), and it often helps to identify different anisotropies for sand and shale respectively. This geologically makes sense as

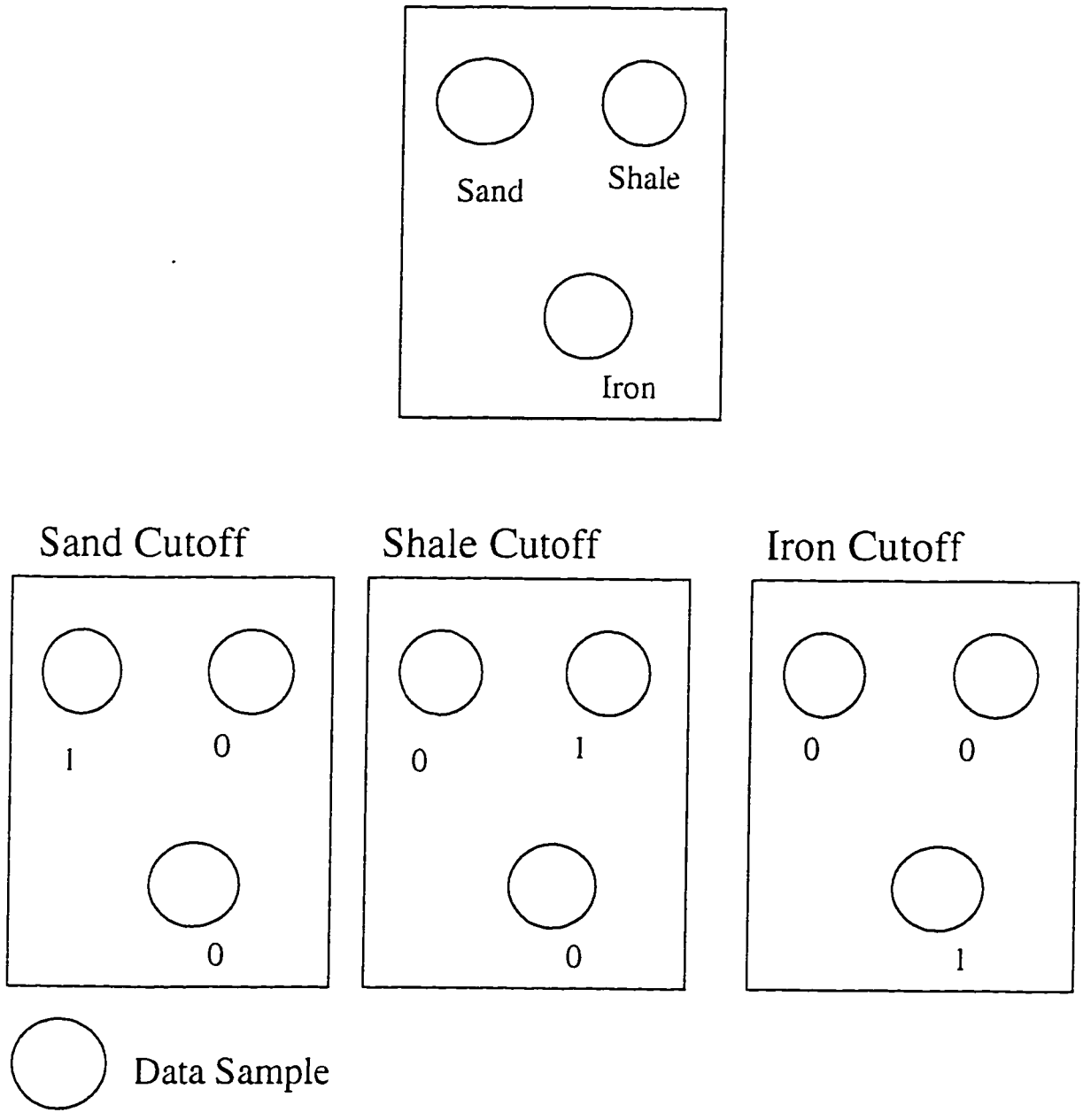


Figure 3-7: An example of indicator kriging of a categorical variable.

sand could be associated with point bars which has a certain directionality, while the shale could be associated with an older abandoned channel. The advantage is also obvious in case of continuous variables. For example, the high permeability values associated with fractures which might have a totally different directional anisotropy than the low or non-permeable zones.

The last step is to do kriging for each of the cutoff. Note that the weights given to data points will be generally different from cutoff to cutoff. The result of kriging each cutoff will be the probability that the value at the given location is below, or equal, to a specific cutoff in case of continuos variables; or the probability of occurrence of a given facies in case of categorical variable (Deutsch, 1992; Isaaks & Srivastava, 1989). After estimating the probability for the cutoffs, a complete cdf estimate at each location can be built up conditional to data (Deutsch, 1992; Journel, 1989; Haldorsen, 1990, Yarus, 1994).

**Indicator Kriging of Facies (A Categorical Example)**

Eight different facies are present in SFNC in varying proportion. Table 1 shows that the very shaly sandstone facies has the highest proportion and iron

| | Proportion |
|---|---|
| [illegible] | 3.6% |
| [illegible] | 20% |
| [illegible] | 9.1% |
| [illegible] | 22.4% |
| [illegible] | 19% |
| [illegible] | 2.9% |
| [illegible] | 10% |
| [illegible] | 13% |

Table 3-1: Proportion of each facies within SFNC Sequence

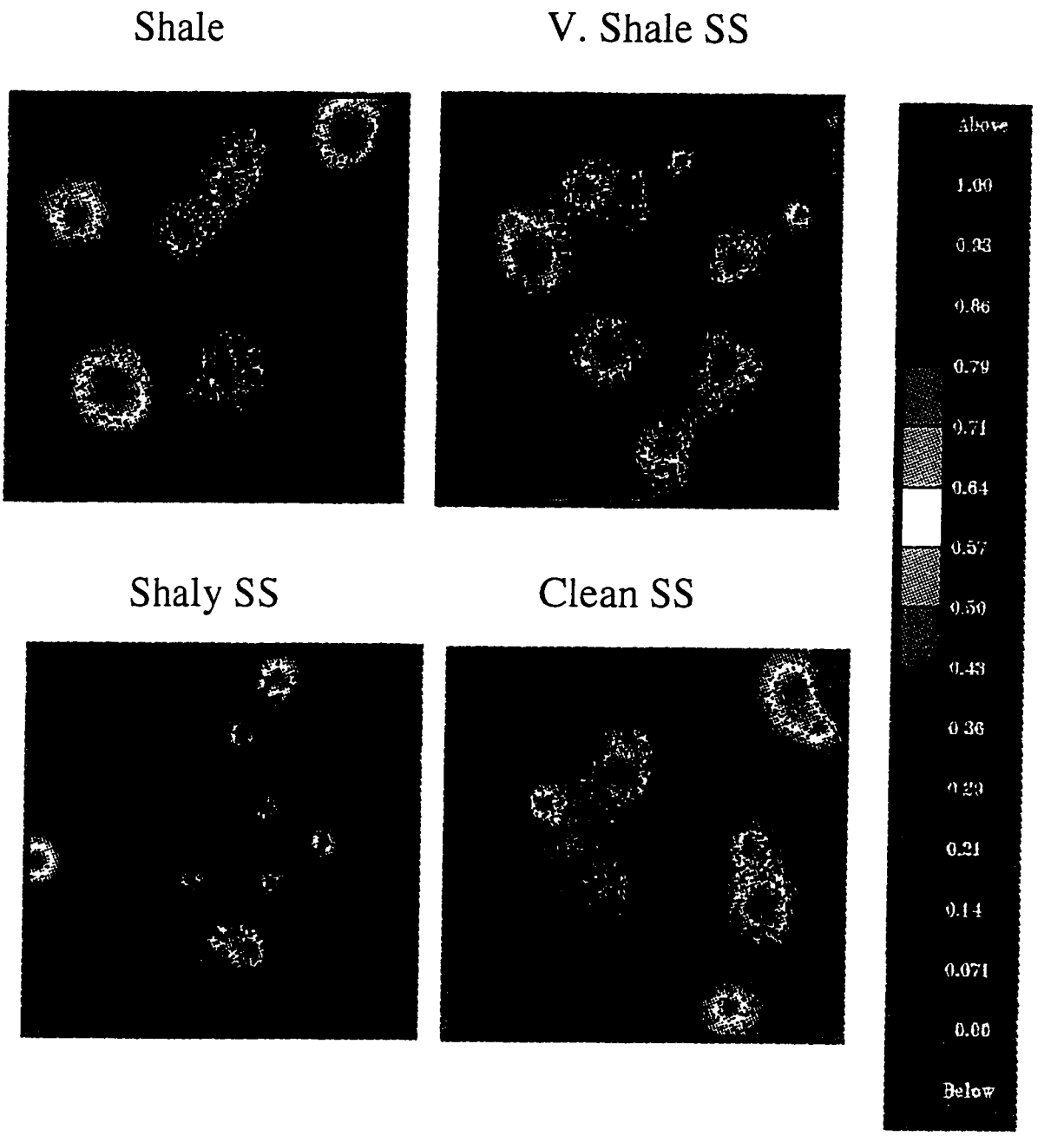


Figure 3-8: Four kriged maps of the individual facies. Each map shows the probability of that facies to be at the given location.

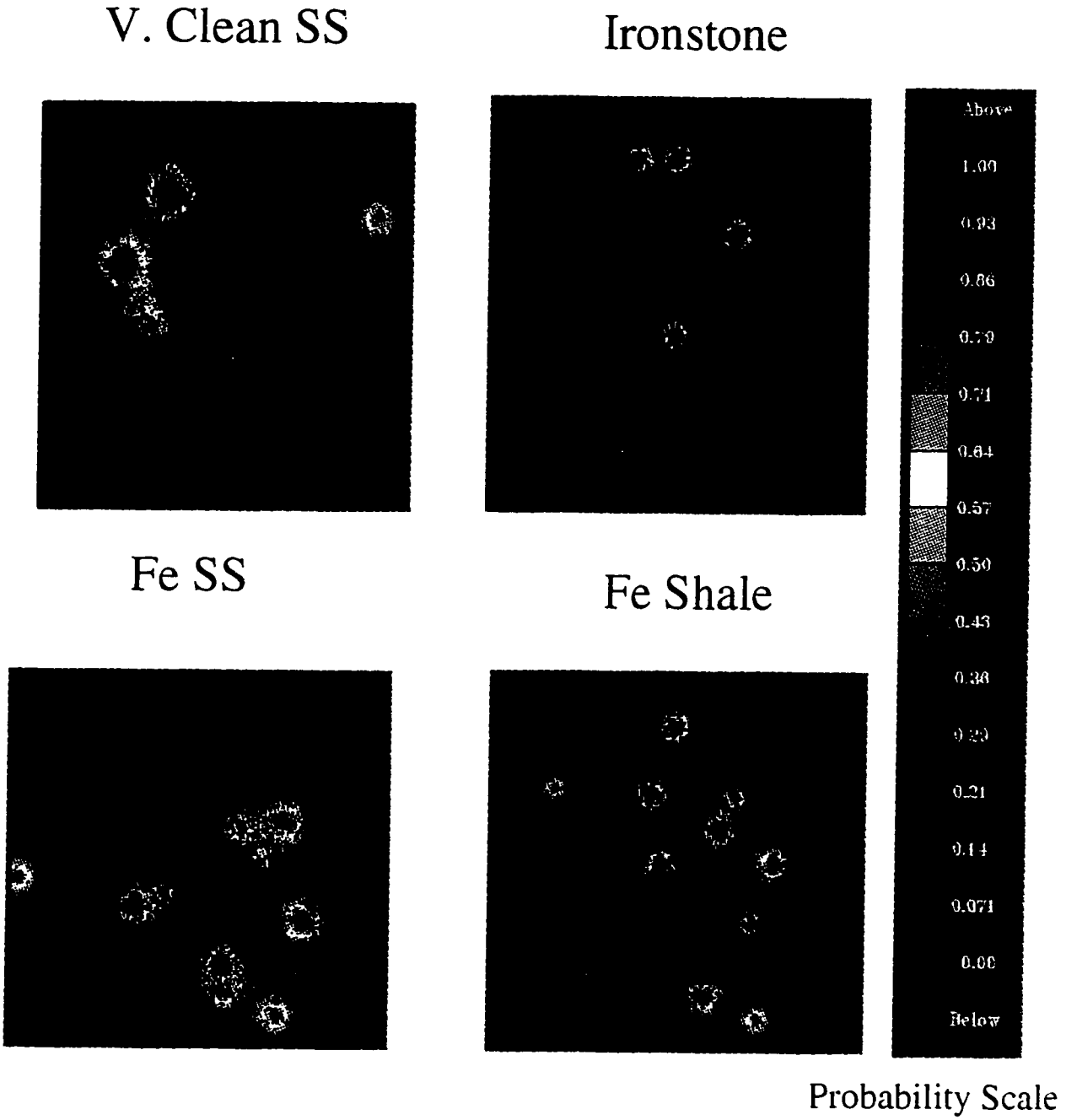


Figure 3-9: The other four facies kriged between the wells using indicator kriging.

rich shale has the lowest. The indicator variogram of each facies has been calculated in Chapter Two. Figure 3- 8 and Figure 3-9 display eight indicator kriging maps which show the probability of the occurrence for each facies using their proper indicator variogram.

## 3.5 Simulation

The goal of most interpolation methods including the ones that have been discussed here such as kriging is to give the best unbiased estimate $Z^*(x)$ at each unsampled location without special concern about the resulting spatial statistics of the estimates $Z^*(u)$. Furthermore, in the case of using kriging or any other estimation method as e.g. some interpolation algorithms, it can only give a single numerical model (the best local estimate) without giving any alternative answers. Also, most of the estimation algorithms including kriging give smooth estimates of the variables being studied which is not similar to what is observed in reality. This is not considered a problem for some applications such as resources estimation (calculating oil reserves for example) but, is definitely a problem for the spatial distribution of properties in reservoir modeling. The presence of extreme high and low flow zones can be very

critical in controlling fluid flow within the reservoir. Kriged maps tend to smooth such extremes by averaging them.

As an alternative, conditional simulation is the process of building alternative, equally probable, high resolution models of the spatial distribution of the variable Z(x). The variable Z(x) can be continuous such as porosity and permeability, or can be categorical such as the presence or absence of a specific facies. Unlike traditional estimators, simulation produces a large number of realizations which have equal probability of being true. This can be illustrated by a simple example. Suppose we give one hundred geologists the same data such as porosity at well locations, and then ask them to map the porosity between well locations. Each geologist will have his/her own interpretation and therefore will come up with different maps and each of these maps will be equally probable of being true since they all honor the information at the well locations. At each estimated location, there are one hundred potential answers.

Conditional simulation is a form of stochastic simulation that can produce equi-probable realizations of the geological phenomena under study. Each of the realizations honors all the conditioning data available, the global

distribution (histogram from the data available at sampled locations) of the variable, and the spatial correlation (variogram) of the variable under study.

There are many kinds of conditional simulations. Each has its own advantages and disadvantages and of course one could be more appropriate for some problems than others. Only the most common simulations will be briefly outlined here, and one among them, the sequential type, will be discussed in more details.

### A-Fractal Simulation

This type of simulation is based on creating an estimation of the actual data (by kriging for example) producing the known smooth model. A random fractal function is then used to construct an unconditional simulation which is based on the fractal variogram (Fractal Brownian Motion). This unconditional simulation model (which is some type of noise) is added to the smoothed model created earlier by kriging. The final model honors the data and also has the appropriate pattern of spatial variability.

### B-Object Based Simulation

This type of simulation is based on creating objects that have some generic significance rather than being built up one node or pixel a time for a reservoir model. Such objects could be meandering sand channels or sand channels in a turbidite system. In addition to selecting a basic shape for these objects, we need to describe how the final overall proportion of this shape by providing parameters like the size of the object, anisotropy ratio, and orientation of the long axis of the channels. More importantly, all these shapes need to honor the information at the well locations. Once the parameters and positioning rules are satisfied, then the reservoir model is filled with some lithofacies background.

### C-The Sequential Way

The sequential type of simulation works by randomly sampling an available cumulative distribution function (cdf), which could be perhaps created earlier from a previous indicator kriging, producing a simulated value at unsampled grid nodes of the variable under study. Having this done at each unsampled location, it would produce values at all unsampled grid nodes.

These values would be independent of one another yet the histogram of the random variable under study would be honored. This would be geologically unsatisfactory, because the geological variables are spatially dependent on one another.

Nonetheless, this is overcomed by randomly selecting a pre-existing local cumulative distribution function and then including the newly simulated value to the rest of the sampled data and treating it just like a sampled data as well as updating all the local cumulative distribution functions. Then the same procedure is repeated by visiting another unsampled grid node randomly and drawing from the updated local cumulative distribution function another simulated value and then including it to the conditioning data. This procedure (sampling and updating local cdf's) is repeated until all the grid nodes are full with values. Thus, each grid node is simulated conditionally to the available data plus all the previously generated data. The whole trick here is how to choose the path of visiting unsampled grid nodes randomly. Thus an unlimited number of maps or volumes can be generated by choosing different random paths covering the grid.

In terms of practice however, various types of sequential procedures can be obtained by only changing the way the local cumulative distribution function (cdf) is estimated. Furthermore, there are many different ways to produce this local cdf. One of these ways, already introduced in a previous section, is indicator kriging.

**Sequential Gaussian Simulation (SGS)**

This type of simulation is the most commonly used and most straightforward type of simulation for generating images of the variable under study. The basic concept of the sequential Gaussian simulation method is the assumption that the variable under study has a multivariate Gaussian distribution. Once this is assumed then the rest takes the following steps:

1- Construct a representative global cumulative distribution function of the variable under study. Caution must be taken to produce a global cdf which is not only representative of the sampled data but also of the whole population of the variable under study.

2-Transform the original sampled data of the variable into a normal (Gaussian) variable. This is easily done by graphically transforming the

original sampled data cdf into a normal distribution function as shown on Figure 3- 10. Once this step is completed, the transformed data has a univariate standard normal distribution with a mean and a standard deviation of Kriging according to the Central Limit Theorem (David, 1987; Deutsch, 1992; Yarus, 1994.

3-Perform a kriging on each grid node. The result of kriging will be a kriging estimate and variance.

4-Define a random path to visit the unsampled grid node.

5-Draw a value of the randomly visited grid node from the Gaussian distribution which has the same mean and a variance as those of the kriging.

6-Include the simulated value to the conditioning data.

7-Repeat step 3 to 6 until all the grid nodes are simulated.

8-Back-transform all the simulated values at each grid node; i.e. reverse step 2.

It should be noticed that the major drawback of this type of simulation is that the transformation to Gaussian distribution and the inverse transformation are dependent on how representative is the global cumulative distribution

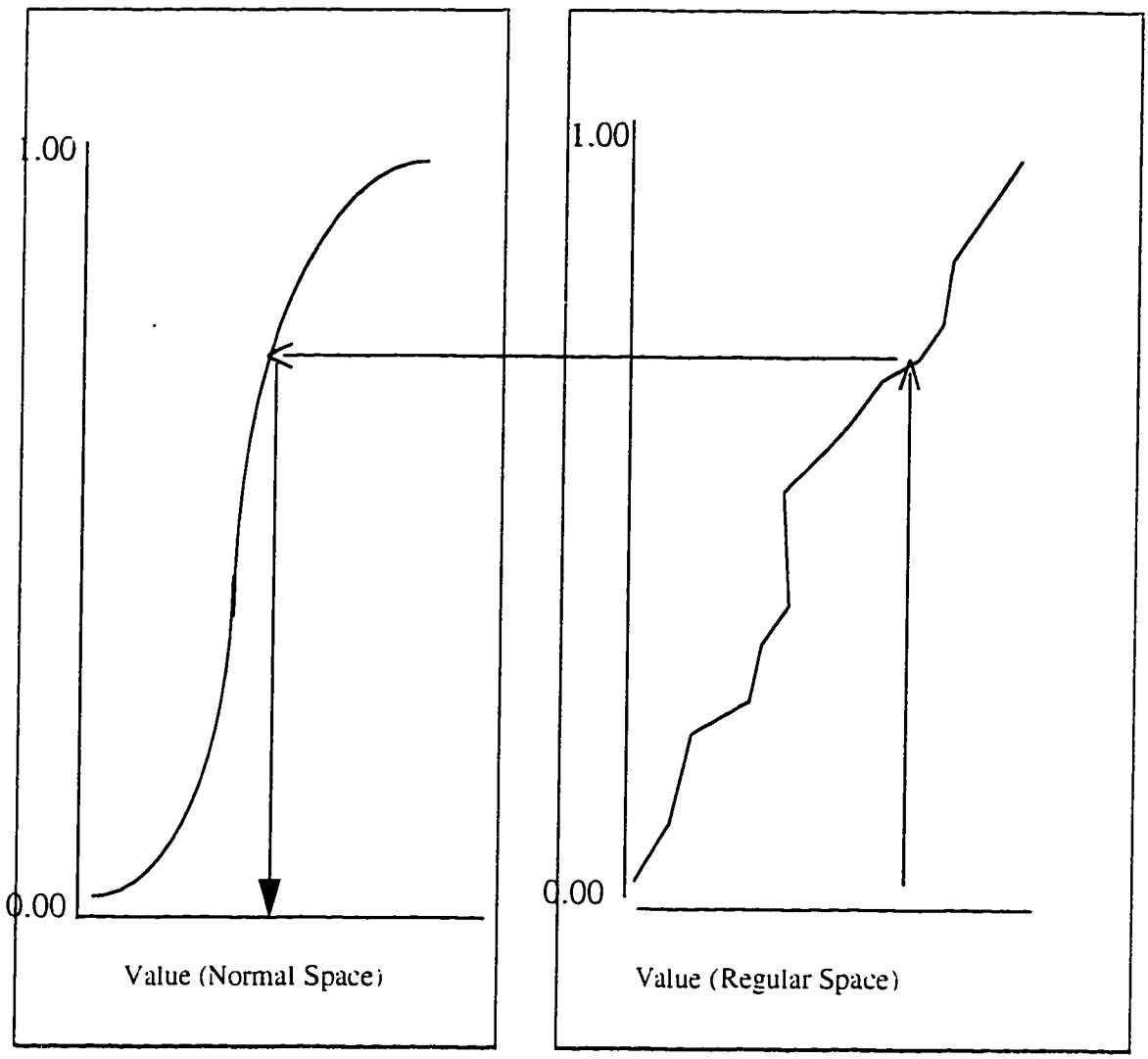


Figure 3-10: A graphical explanation of the normal score transform

function of the variable under study. Sometimes a representative cdf from all the available data looks inferior to the cumulative distribution function taken from a cluster of data sampled at one particular area of a population. Using a cdf from a clustered data, however, would produce results which are more biased to that area of the population. Another disadvantage of the Sequential Gaussian Simulation algorithm is that it obviously can not be used when the variable under study is categorical as it only works for continuous variables.

Another important disadvantage of this type of simulation is the assumption about the multinormality of the variable under study. This is due to the fact that the univariate normal distribution of the set of all sampled data does not mean that the regionalized variable under study is normal. The next necessary condition is to check for binormality of any pair of data points of the transformed variable. However, even if binormality holds this does not necessarily implies multinormality.

### Sequential Gaussian Simulation of Porosity

Figure 3- 11 shows a volume of simulated porosity using the same variogram as used for the kriging of porosity. Normal score transform was

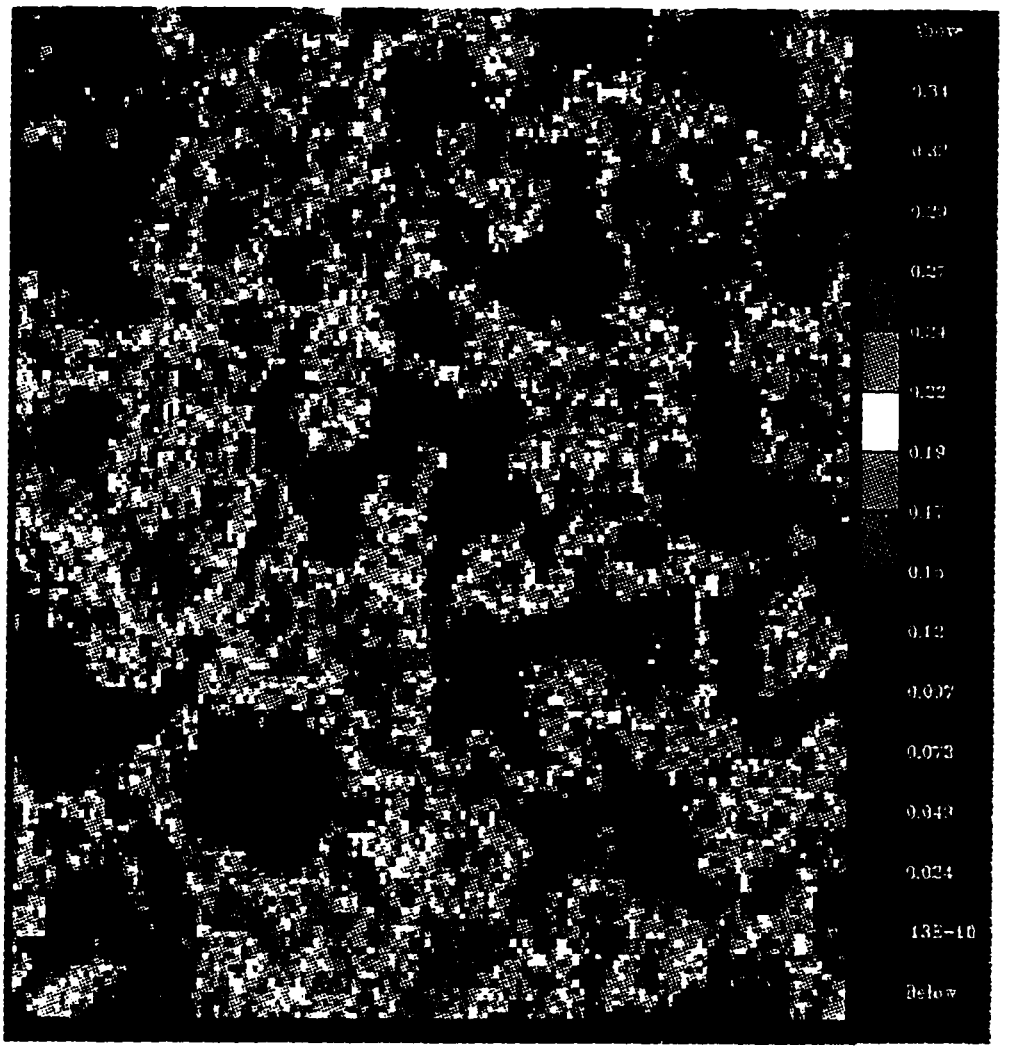


Porosity Scale

Figure 3-11: A slice through a volume of a sequential Gaussian simulation of porosity in the SFNC Sequence.

done using the cdf of the porosity data available from the well information. Unlike the volume resulted from kriging (Figure 3-4), the simulated porosity does not show any smoothing effect between wells. This is closer to reality as we know that porosity is not a smoothly distributed property.

**Sequential Indicator Simulation (SIS)**

As the name suggests, sequential indicator simulation is based on non-parametric indicator kriging. The local cumulative distribution function produced from kriging is adopted in the simulation part. The major requirement needed beside the local cumulative distribution function is a model for the spatial dependence (spatial correlation) of the variable under study. This could be obtained by modeling the experimental indicator variograms calculated for each cutoff.

The major improvement of this type of simulation as compared with the sequential Gaussian simulation is that it does not require any assumption of multinormality of the variable under study. Furthermore, it is also not required that the data be transformed to any particular distribution. Moreover, similar to the advantages of indicator kriging over ordinary kriging, sequential

indicator simulation shares the same advantage over other conditional simulations (Journel, 1989; Yarus, 1994). Such advantages include the flexibility to model each cutoff separately which is very important if we do reservoir modeling for the purpose of fluid flow simulation. Unlike sequential Gaussian simulation, sequential indicator simulation can be done for both continuous and categorical variables.

The sequential indicator simulation works by first randomly visiting unsampled grid nodes. At a particular grid node a simulated value is produced by randomly drawing a value from a preexisting local cumulative distribution function produced from indicator kriging. In the case of categorical variables, the probability distribution function is randomly sampled. The new simulated value is then included to the rest of the sampled conditional data. Then the process is repeated by randomly visiting another grid node until all the grid nodes have been visited and simulated. The local cumulative or probability distribution function (which is estimated by weighted linear combination of the indicator data) is conditional to the sampled grid nodes which are considered as part of the sampled data. Of course, very large number of images can be produced by varying the path of visiting the grid nodes. Note that all these

images are conditioned to the same sampled data and are equiprobable of being true.

The sequential indicator simulation technique also has its limitations. One of these is that it is computationally intricated. For example, to do a volume of sequential indicator simulation of a variable with nine cutoffs would require eighteen indicator variograms; nine for horizontal and nine for vertical directions. Nine indicator kriging is then required, one for each cutoff. A random path should next be chosen to visit each grid node to produce simulated values. In comparison, if sequential Gaussian simulation is used, only two variograms are required: one horizontal and one vertical, to produce a volume of the same variable.

### Sequential Indicator Simulation of Facies

The indicator kriging of the eight facies produced earlier does not produce a cube of facies distribution but rather it gives a cube of the probability of occurrence for a predifined facies. When all the eight indicators are summed up, a probability distribution function (local) at each location is produced. By randomly drawing from this summed local probability

distribution function (pdf) at each location as discussed earlier, a cube of the eight facies distribution is produced as shown on Figure 3- 12. All what remains to be done is to distribute the reservoir properties, such as porosity and permeability, among these facies which will be discussed next.

**Facies Dependent Reservoir Properties**

The distribution of reservoir properties such as permeability and porosity can be quite different depending on which rock or facies types they belong to. For example, the spatial distribution of high porosity values associated with the very clean sandstone facies can be different from the distribution of the same class of high porosity values associated with an iron-rich sandstone facies. As a result, the reservoir architecture which includes the reservoir facies should be first constructed spatially and then filled with the reservoir properties such as porosity or permeability. The reservoir architecture of geological facies could be built up with most of the previous algorithms including the most information-demanding Object Based method. However, there are simpler ones which require minimal information such as the range and/or directionality of

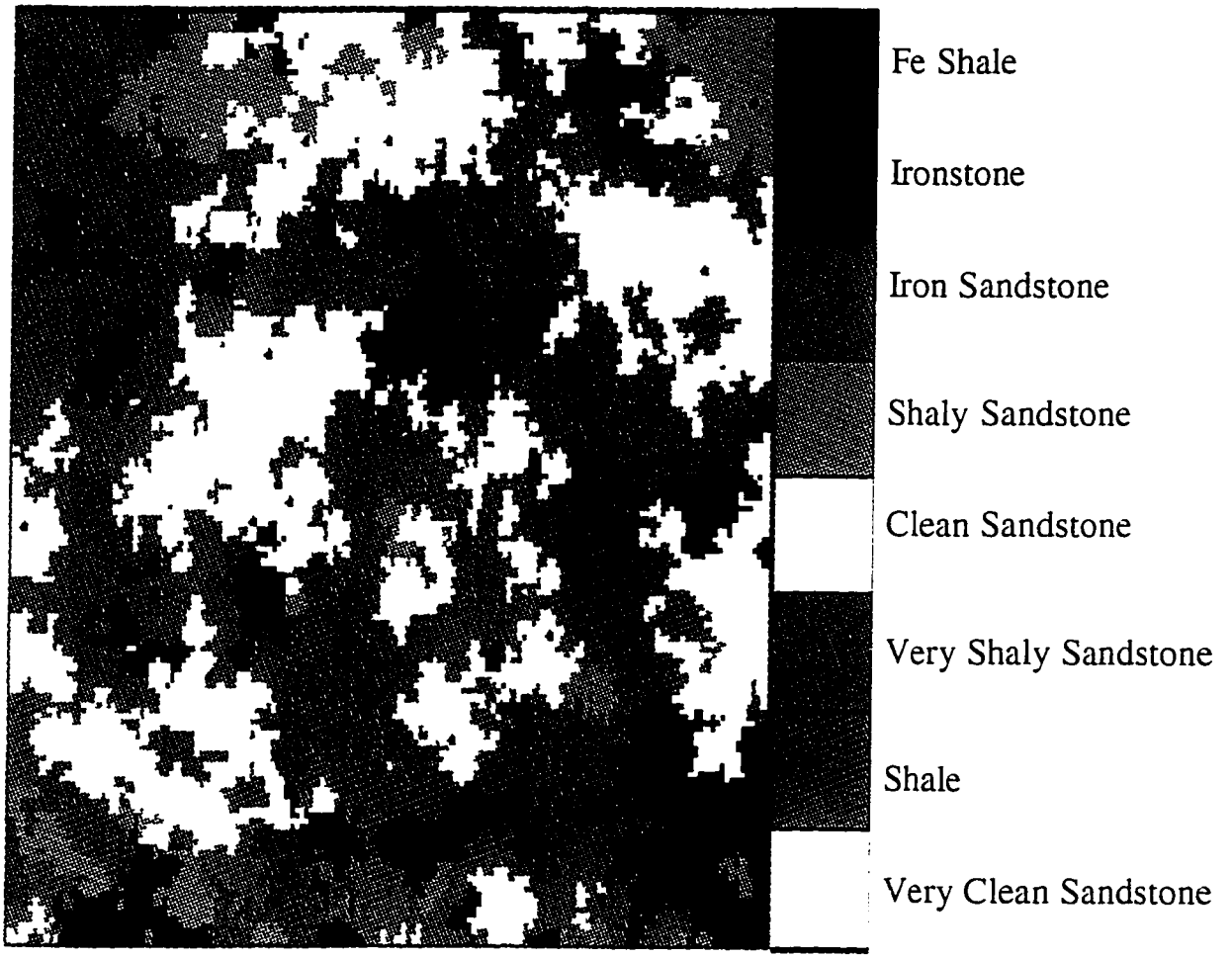


Figure 3-12: Facies distribution done by using sequential indicator simulation of the SFNC Sequence facies

the geological facies. These methods include, for example, sequential indicator simulation.

Once the architecture of the reservoir facies has been built up, we have to spatially distribute the corresponding reservoir properties. This is easily done by using various forms of simulations, including sequential Gaussian simulation and sequential indicator simulation.

### 3.6 Facies Dependent Porosity Distribution

Reservoir flow simulation requires complete grids of certain reservoir properties including porosity. Since the geological architecture of the facies has already been built up for the eight facies, the reservoir properties can now be distributed among them. Figure 3- 13 shows the porosity distribution of the eight facies by using the variograms calculated earlier in Chapter 2 for the facies-specific porosity. For these non-reservoir facies such as shales and ironstone the range has been selected as a very small value. Figure 3- 14 shows the striking similarities between the facies model and the porosity model. This is very important because instead of just connecting similar porosities between

wells as done in ordinary kriging or SGS, the porosities here are connected depending on which facies they occupy.

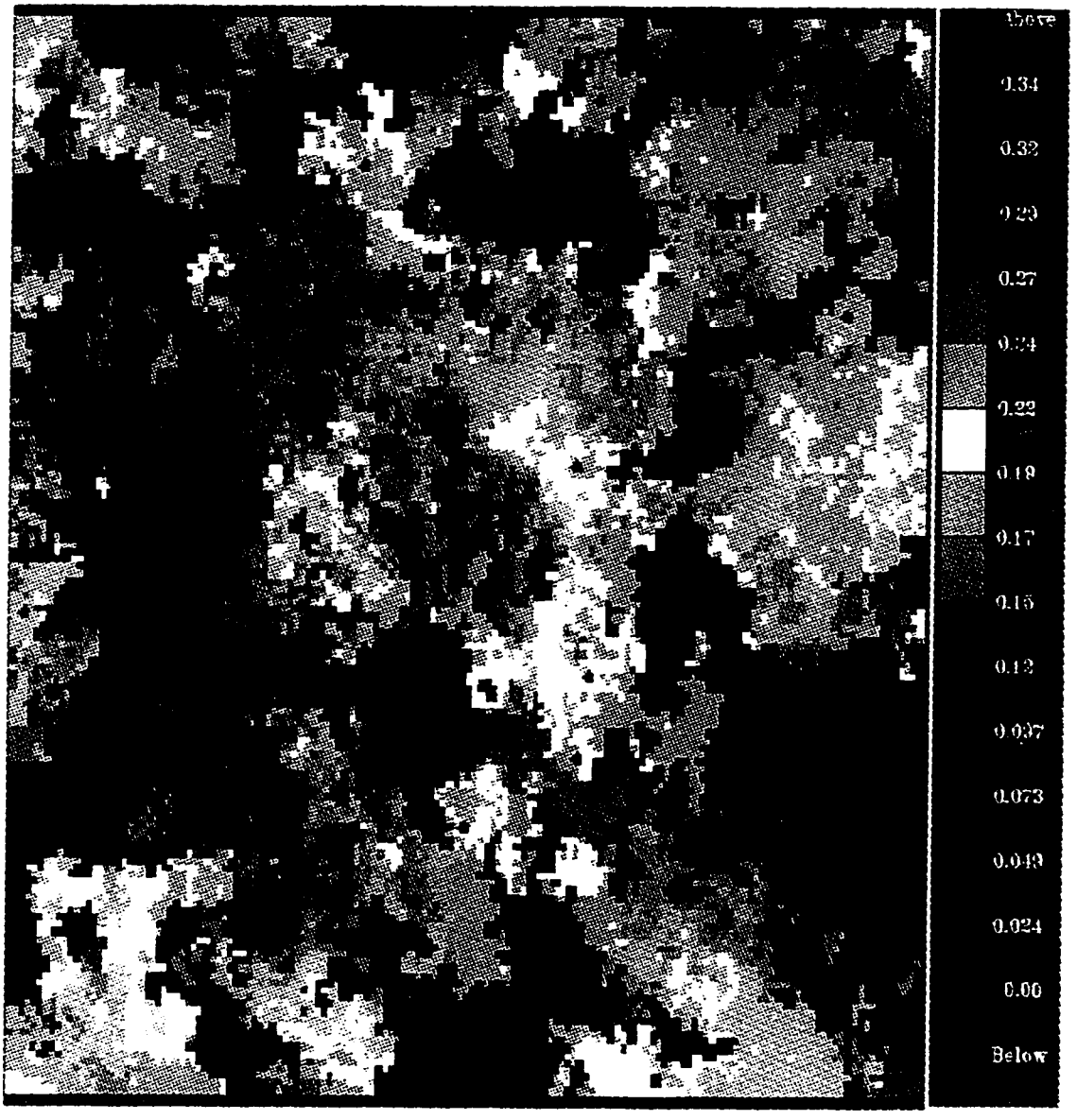


Figure 3-13: Porosity distribution within each of the SFNC Sequence facies.

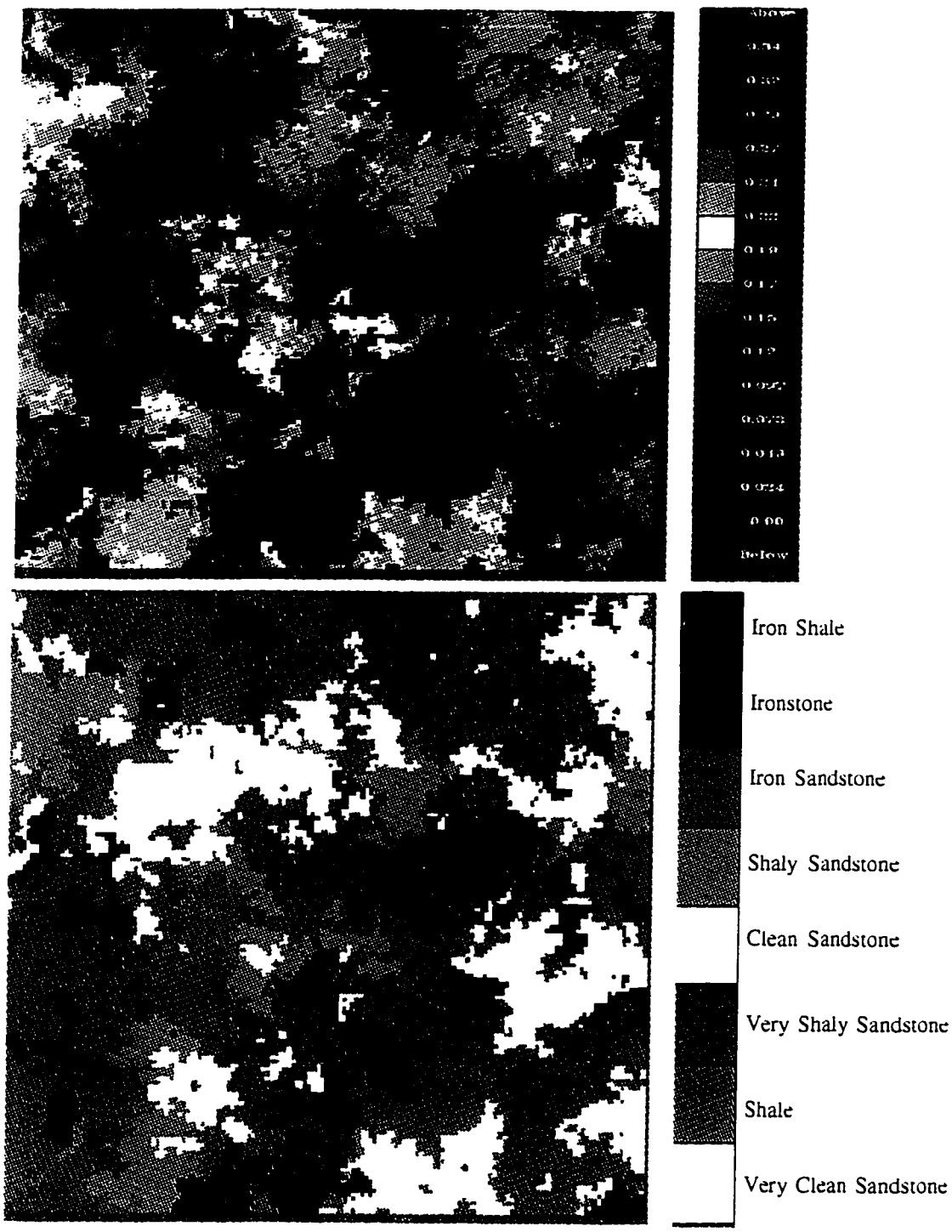


Figure 3-14: Comparison of a lithofacies model (lower graph) and its corresponding porosity model (upper graph).

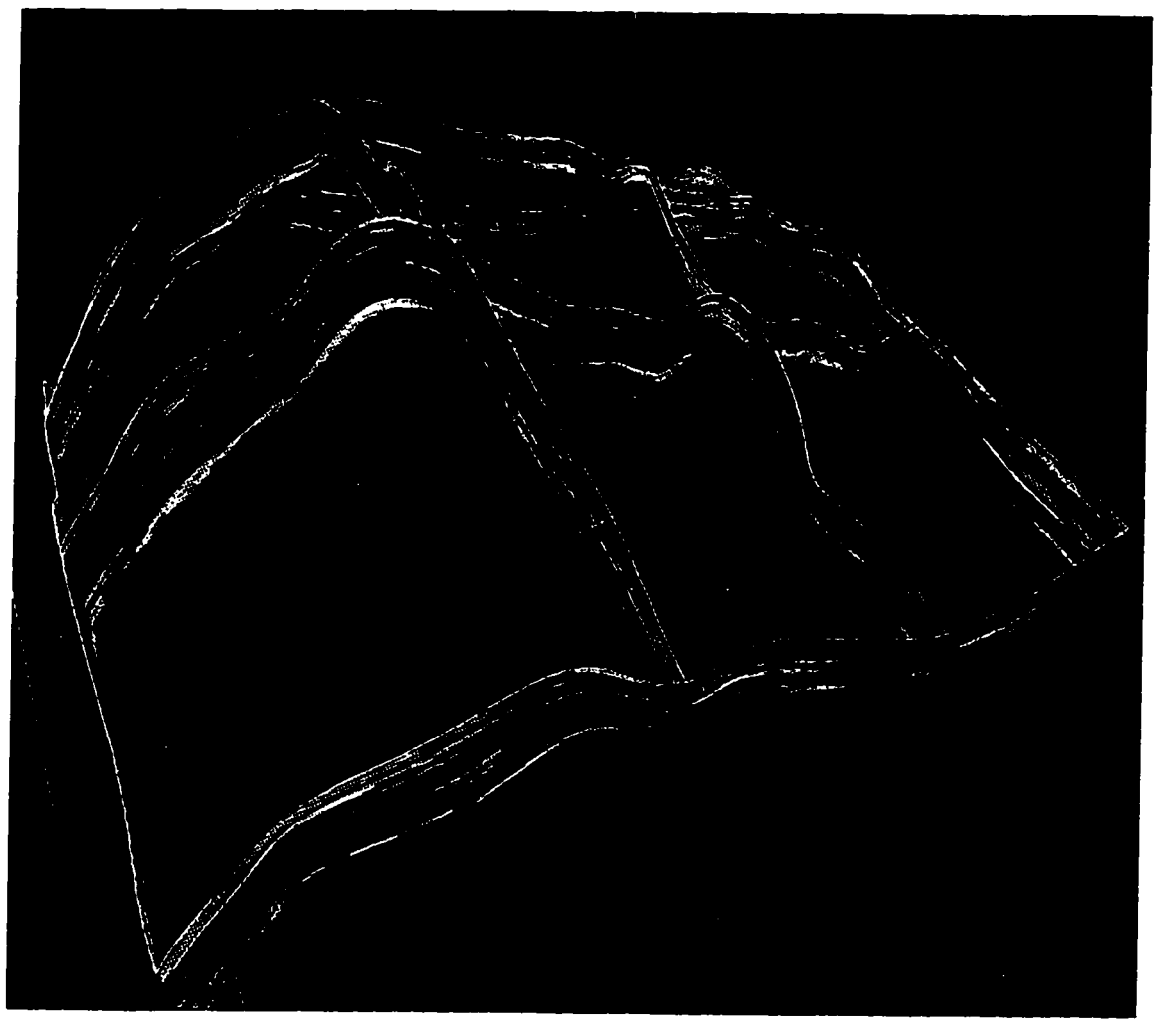

Figure 3-15: A fence diagram of porosity condition to lithology

# CHAPTER 4

# SUMMARY AND CONCLUSION

One of the main objectives of this study was to investigate the use of geostatistics in reservoir characterization using Safaniya Reservoir in Safaniya Field as an example.

Geology of the Safaniya Reservoir was first introduced. Stratigraphy and structural configuration of the Safaniya Member were analyzed. A brief discussion of both reservoir zonation and deposition of environment of Safaniya Member was then given. This (First Chapter) helped in giving the first pace of understanding the geological processes that led to the deposition of the reservoir which was utilized in the Second and Third Chapters.

In the Second Chapter, a brief discussion was given on the classical statistics of the properties of Safaniya Reservoir. It showed that shape of their distributions are close to normal in most cases. It was shown that the classical statistics are very important to validate the initial data and help in understanding later results. The second part of this Chapter briefly explained the random variable concept. Spatial measures of the geological variables were introduced and thoroughly explained. The geological variables included both rock facies and their corresponding physical properties. It was shown that the variogram is the basic tool for identifying the patterns of spatial continuity of a variable. Indicator variograms, however, provide additional flexibility to examine individual classes of the variables understudy or specific rock facies to find its own spatial pattern. This flexibility includes capturing high permeability zones caused by fracturing which might have a different anisotropy than low permeability zones resulted from shale deposition. After calculating the experimental variograms of the Safaniya Field, these variograms were modeled by the appropriate functions to be used later in the Third Chapter. The Chapter was concluded by showing the power of both classical and spatial statistics in aiding the interpretation of the environment of

deposition of SFNC Sequence. Nested structures, which was not documented, defined as the presence of more than one structures was observed for both the horizontal and vertical directions when modeling the physical properties of SFNC Sequence.

The Third Chapter utilizes results of the Second Chapter with the geological understanding from the First Chapter. Three-dimensional models of rock facies and porosity were generated using various types of geostatistical techniques.

Kriging was first introduced as an example of an estimation method. It was shown that ordinary kriging gives a very smooth, relatively simplistic model of porosity distribution. The non parametric way was then given as an alternative to some of the disadvantages of ordinary kriging. Conditional Simulation was then introduced to give alternative, equally probable, high resolution models of spatial distribution of rock facies or their physical properties. Some of the most used types of conditional simulation were explained and examples were given. Sequential Gaussian Simulation (SGS) was thoroughly explained and a porosity example of SFNC Sequence was given. The non parameric Sequential Indicator Simulation (SIS) was then

explained as an alternative of SGS to eliminate the assumption of normality and to demonstrate the SIS capability of handling both continuos and categorical data type. Examples of SIS was demonstrated using rock facies of SFNC Sequence. Chapter Three concluded by showing that by infilling the simulated rock facies types with reservoir properties including porosity, the simulations could be used as a basis for reservoir fluid flow simulations. Running fluid flow simulations by using several of the generated rock properties simulation models could provide estimates of the uncertainly concerning important output variables such as breakthrough times and sweep efficiencies. This could be used in reservoir development, risk assessment, and future economic planning.

# CHAPTER 5

# RECOMMENDATIONS

The following recommendations can be made from this study for future work:

1-Use porosity simulation results as an input for fluid flow simulation models.

2-Model directional variograms to capture anisotropic trends within the reservoir.

3-Model variograms with nested structures to better model local variograms within specific reservoir zones.

4-Model facies with probability field indicators to lower the time it takes to build SIS lithology models.

5-Augment the reservoir models by integrating soft (secondary) data such as engineering and seismic data.

# CHAPTER 6

# REFERENCES

Alabert F. ,1987, The practice of fast conditional simulations through the LU decomposition of the covariance matrix. Math Geology, 19 (5): 369-386.

Al-Sabti, H. and Bassam, K, 1993, 3-D Electrofacies Model, Safaniya Reservoir, Safaniya Field, Saudi Arabia, SPE Middle East Oil Show; Bahrain, April 1993, SPE # 25611.

Atlas Wireline Services, 1987, Fundamental of Diplog Analysis, Western Atlas International, Unpublished Book.

David, M., 1977, Geostatistical Ore Reserve Estimation, Elsevier, Amsterdam, 360p.

Davis, J. C., 1986, Statistics and data analysis in geology, second edition: Jhon Wiley and Sons, New York

Davis. M.,1987, Production of conditional simulations via the LU decomposition of the covariance matrix. Math Geology, 19 (2): 91-98.

Deutsch, C. V. , Journel, A, G., 1992, GSLIB: Geostatistical Software Library and User's Guide. Oxford University Press, new York, NY.

Dubrule O., 1989, A review of stochastic models for petroleum reservoirs. In Armstrong, editor, Geostatistics, pages 493-506.

Hagen, W., 1975, Regional Study of the Wasia & Biydh Sands (Lower Cretaceous) In Northeastern Saudi Arabia & Adjacent Countries.

Haldorsen H. and Damsleth E., April 1990 , Stochastic modeling. J. of Pet. Technology, 404-412, .

Hohn M., 1988, Geostatistics and Petroleum Geology. Van Nostrand. New York, NY.

Isaaks E. and Srivastava R., 1989, An Introduction to Applied Geostatistics. Oxford University Press, new York, NY.

Journel, A. G. & Huijbregts, 1978, Mining Geostatistics, Academic Press, London.

Journel, A. G., 1989, Fundamentals of Geostatistics in Five Lessons. American Geophysical Union.

Journel, A. G., 1994, Conditional Stochastic Simulations to varying local anisotropy directions. Stanford Center for Reservoir Forecasting (SCRF) Report.

Journel, A. G., 1993, Geostatistics and Reservoir Geology. Stanford Center for Reservoir Forecasting (SCRF) Report.

Kashifi, M., 1976, Geology of Persian Gulf, Geological Society of America, Vol. 7, Oct. 1976.

Mahmoud, D., 1979, Wasia Formation Facies Distribution and the Cretaceous-Recent structural Evaluation of the Safaniya-Zuluf-Marjan Area, Unpublished Report.

Powers, R., 1966, Geology of the Arabian Peninsular-sedimentary Geology of Saudi Arabia, 1966.

Sahin, A., 1992, Advanced Geostatistics Course, KFUPM.

Senalp, M., 1993, Khafji Reservoir Geologic and GEOSET Modeling, ZULF Field, Unpublished Report.

Senalp, M., 1991, Safaniya Reservoir Multi-Layer Geologic Model, Marjan Area, Unpublished Report.

Senalp. M., Al-Keel, S., and F. Jones, 1988, Khafji Reservoir Multi-Layer Geologic and GEOSET Modeling, Marjan Area, Unpublished Report.

Yarus, J. M., 1994, Stochastic Modeling and Geostatistics. AAPG Computer Application in Geology, No. 3.